

---

# Next generation radiation mapping using UAS assisted dynamic monitoring networks

Angelos Plastropoulos

A dissertation submitted in partial fulfillment of the requirements of the University  
of the West of England, Bristol for the Degree of Master of Science

Module Number: UFMED4-60-M

Faculty of Environment and Technology, University of the West of England, Bristol

August 2015

---

---

## Abstract

Nowadays, unmanned aerial systems (UASs) have become increasingly popular in a wide range of applications, from military to recreational. The Interface Analysis Centre (IAC) at the University of Bristol has developed a UAS, called the AARM (Advance Airborne Radiation Monitoring) system, which could be used to provide visual and thermal monitoring of radiation after a release of nuclear material. AARM system has successfully measured radiation in one of the most highly contaminated prefecture areas in the Fukushima Daiichi nuclear power plant after the disaster caused by the earthquake and tsunami in March 2011.

The purpose of this project is to advance the existing capability for radiation surveillance at civil nuclear sites of the first generation AARM system. There are many approaches that can be followed to improve the existing system. In the context of this project the following progressions have been proposed:

- Equipping the UAS with advanced sensors. An extensive testing of proximity sensors has been conducted to identify the strengths and the weaknesses of the existing commercial off-the-self (COTS) sensors.
- Developing a realistic simulation and assisted flight method. It is an imperative requirement to evaluate and test UAV in difficult or dangerous

---

scenarios without any harm to real and expensive UAV hardware. Most of the time it is faster to run a simulator instead of starting the whole scenario on a real robot. Because of these reasons, a comprehensive simulation based on ROS and gazebo has been developed. Using that simulation, an assisted teleoperation mode for obstacle avoidance has been implemented.

- Creating advanced human robotic interfaces. The main mission of the UAS is to map the radiation levels. An iOS mobile application for visualising the individual gamma energies and intensities (cps) on a map has been developed. In addition, a second iOS application was implemented which can be utilized to teleoperate a ROS enabled UAV. The operator gets feedback from the onboard devices and sends control commands.
- Designing the next generation AARM system. Having examined a wide range of improvements a specific design is proposed using the computational power of a companion computer onboard.

---

## Acknowledgements

(It will be added)

---

## Supporting Files

All the project's related files, including source code, videos and documentation can be found in the online repository: [github.com/plusangel/radiationUAV](https://github.com/plusangel/radiationUAV)

### Note

The first draft of the dissertation is printed in gray scale. The final submission will be printed in color.

---

## Contents

Part A – Introduction	<b>1</b>
A.1 Unmanned Aerial Vehicles (UAVs)	1
A.1.1 Social impact	2
A.1.2 Ethical impact	5
A.1.3 Legal impact	6
A.1.4 Industrial impact	7
A.1.5 Economic impact	8
A.2 Interface Analysis Centre (IAC)	9
A.3 The project	10
Part B – Literature Review	<b>12</b>
B.1 Radiation mapping	12
B.2 UAV flight	15
B.3 UAV stabilisation	23
B.4 UAV sensors	27
B.5 UAV simulations	29
Part C – Sensors	<b>34</b>
C.1 Ultrasonic sensor	34
C.1.1 Devantech SRF02 Ultrasonic Range Finder	34
C.2 Infrared sensor	40
C.2.1 Sharp GP2Y0A02YK0F	40
C.3 Optical flow sensor	44
C.3.1 Px4flow smart camera	44

---

C.4 Laser sensor	49
C.4.1 LIDAR-Lite	49
C.5 Applications	51
C.5.1 Mapping application	52
C.5.2 Proximity application	56
 Part D – Simulation	 <b>61</b>
D.1 Introduction	61
D.2 UAV package	63
D.3 UAV configuration in simulator	68
D.4 The radiation mapping and simulation requirements	71
D.5 Topics nodes	72
D.6 Actions nodes	74
D.7 Obstacle Avoidance	79
D.8 Testing	84
 Part E – Human robot interface	 <b>87</b>
E.1 UAV teleoperation application	87
E.1.1 Topology	88
E.1.2 Functionality	91
E.2 Radiation mapping application	93
E.2.1 Topology	94
E.2.2 Functionality	96
 Part F – UAV	 -
It will be added	-
 Part G – Conclusions	 -
It will be added	-

---

Appendix A – UAV Configuration	<b>100</b>
A.1 Chassis, brushless motors and Electronic Speed Controllers (ESC)	100
A.1.1 General description	100
A.1.2 Vibration damping	102
A.1.3 Magnetic interference	104
A.1.4 Power module	105
A.2 Flight controller	106
A.3 Telemetry	108
A.4 GPS and compass module	109
A.5 On-board computer	110
Appendix B – Sensors Circuits	<b>112</b>
B.1 Ultrasonic sensor	112
B.2 Infrared sensor	113
B.3 Optical flow sensor	114
B.4 Laser sensor	116
B.5 Applications	118
Appendix C – Simulation Topics	<b>122</b>
C.1 ROS	122
C.2 Gazebo	124
C.3 Terminology	125
C.4 ROS development approach	127
C.5 UAV manipulation input devices	130
C.6 System configuration	131
Appendix D – Mobile Applications Configurations	<b>133</b>
D.1 UAV Teleoperation application	133
D.2 Radiation mapping application	135



## Part A

### Introduction

#### A.1 Unmanned Aerial Vehicles (UAVs)

Over the last few years, one of the fastest growing fields of Robotics and Autonomous Systems is the Unmanned Aerial Vehicles (UAVs). There are also other names that refer to this specific field like drones, Unmanned Aircraft Systems (UAS) or Unpiloted Aerial Vehicles, all having similar meaning and subtle differences. In general, an Unmanned Aerial Vehicle is an aircraft that can be controlled without humans on board, either remotely or autonomously. Unfortunately, UAVs were made popular when they first appeared because they reduce collateral damage in wars and because were convenient seeing as the controller can be thousands of miles away from the UAV itself. However, this is not the whole truth and the UAVs' field has the potential to be exploited in a wide range of non-military activities with impressive outcomes. The development of this technology has a field of great competence of countries around the globe. Nevertheless, the deployments are not solely based on the technological progress but also on the operation framework that will be imposed by national administration aviation authorities like Federal Aviation Administration (FAA) the States and Civil Aviation Authority (CAA) in the UK.

Similar to any other revolutionary technological development, like the Internet for example, UAVs have faced controversial reactions. Many people feel that UAVs threaten their privacy while others look forward to using them to facilitate their business. Furthermore, political and ethical problems pose an issue. The reality is that technologies develop regardless of public issues. It is a question of how they will be used and for what reason. There are cases though, where everyone unambiguously agrees that it is better to use an UAV than the human presence. For example, when the Fukushima Daiichi nuclear

power plant was severely stricken by the tsunami, there was no way to assess the contamination since static radiation monitoring stations around the site were disabled. Because of that, a traditional manned airborne was conducted at the nuclear site. Beside the poor resolution of the measurements due to the unfriendly environment, it is clear that the flight crew was exposed to a significant amount of radiation. Consequently, the exploitation of UAVs in places where humans must not be exposed to dangerous situations is of great interest and therefore deserves further research.

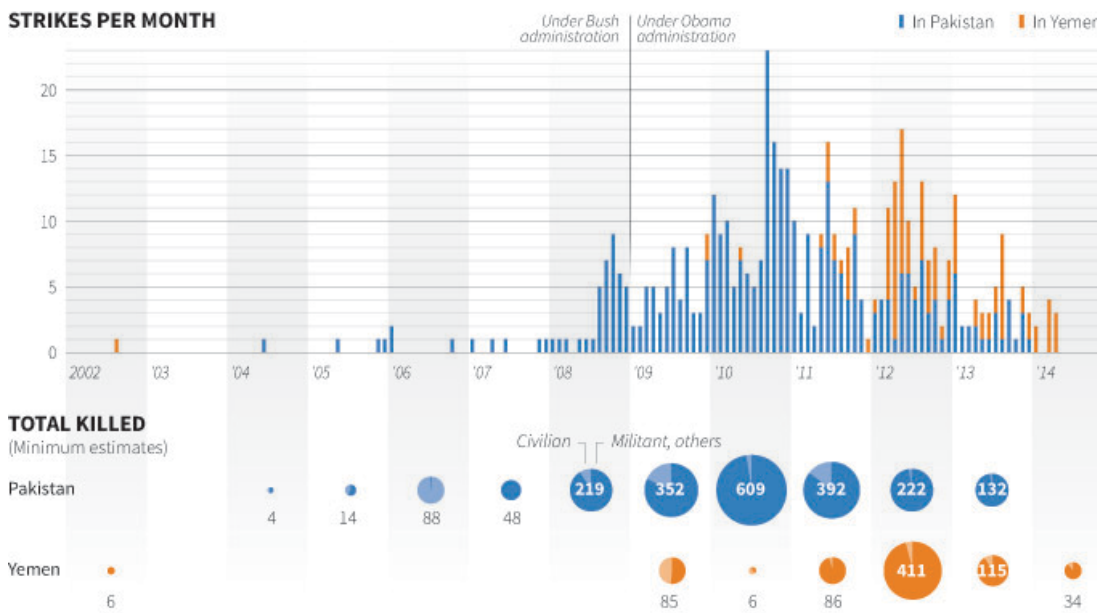
The development of the UAVs has related impacts on the national economies as well. However, because of the current airspace restrictions non-defense use of UAS has been extremely limited. A well-known case is Amazon's prime air concept, a futuristic delivery system for his company's products. The biggest hurdle facing Amazon Prime Air is that commercial use of UAV technology is not yet legal in the United States.

#### A.1.1 Social impact

Unmanned Aerial Vehicles at the early stages of their existence were primarily used for military purposes. UAVs are well suited for long distance missions, reconnaissance, and keeping soldiers safe. They are cheaper than many fighter jets, and their smaller size allows drones. In nine years the Pentagon has raised the drone fleet thirteen times and the military is spending at least \$5 billion a year in addition (The Economist, 2011). Generally speaking, there is a concern that attacks and civilian deaths may increase as drone technology becomes available to many militaries (fig.A.1). There are also concerns about safety. Opponents of the UAVs fear that there will be cases where UAVs crashes, collisions with airplanes, or that remote control over them could be lost. Essentially, the facts related with the military use of drones are so obvious that it is difficult to combat the criticism, although this is definitely not the only way to use UAVs. There are many other applications, which can improve peoples' lives drastically.

## U.S. drone strikes

U.S. drone strikes and casualties in Pakistan and Yemen since 2002.



Source: New America Foundation. \* Includes air, drone and cruise missile strikes. Data through April 20, 2014.

Staff, 21/04/2014

REUT

*Fig.A.1 This figure displays the number of US drone strikes in Pakistan and Yemen from 2002 to 2013, with an upward trend in drone usage. (image from Reuters, 21/4/2014)*

UAVs are increasingly performing civilian tasks as the technology becomes more common (57 countries and 270 companies were producing UAVs in 2013). In the U.S., the Federal Aviation Administration (FAA) predicts that approximately 7,500 commercial small UAVs could be flying in the U.S. within the next five years. Among the wide range of possible applications a general classification of the basic categories is: safety control, scientific research and commercial applications. In order to depict the wide variety of specific areas that will benefit from the UAV usage, I can mention fields like:

- Wildfire mapping
- Agricultural monitoring
- Disaster management
- Thermal infrared power line surveys
- Law enforcement
- Telecommunication

- Weather monitoring
- Aerial imaging/mapping
- Television news coverage, sporting events, movie-making
- Environmental monitoring
- Oil and gas exploration and
- Freight transport.

One additional social dimension of using UAVs is in humanitarian applications. Humanitarian organizations have started to use UAVs for data collection and information tasks that include real time information and situation monitoring, public information and advocacy, search and rescue, and mapping (fig.A.2). Furthermore, they can be used in the area of delivery and logistics for the transportation of small medical supplies, such as vaccines. To address the good practices and guidance related to this approach, the United Nations Office for the Coordination of Humanitarian Affairs (OCHA) has published a pivotal policy document on the use of civilian UAVs in humanitarian settings (Unmanned Aerial Vehicles in Humanitarian Response, 2014).



*Fig.A.2 A Sky-Watch Huginn X1 supports the humanitarian response in Tacloban, Philippines after Typhoon Haiyan in 2014 (image from [www.irevolution.net](http://www.irevolution.net))*

### A.1.2 Ethical impact

It is helpful before analyzing the ethical impacts of UAVs to gain some understanding of the notion of ethics. Ethics in a basic definition relates to agents who execute actions which are then deemed ethical or unethical. As Dwight Furrow states (Wilson, 2014), ethics are related to appraising actions and actions are performed by those capable of being moral agents. Continuing Furrow says, "When we evaluate an action, we can focus on various dimensions of the action. We can evaluate the person who is acting, the intention or motive of the person acting, the nature of the act itself, or the consequences." Consequently, the actions of UAVs are only capable of being assessed based upon the actions of the person controlling them. The ethical issues emerge as the result of the interaction of how the UAV is operated by an operator in contrast with those who experience the UAV's function. There is the controller of the UAV, the UAV, and those who are affected by the activities of the UAV.

One of the simplest applications of an UAV is to use it for aerial photographs. Even an inexperienced hobbyist can buy a ready-to-use kit (UAV equipped with cam) and use it straight away in a park. If the user wants to take photographs for artistic purposes there is no problem. On the other hand, if the picture contains inadvertently other people, this could be considered as an invasion of privacy. It can be made even clearer in a case where someone who wants to follow or stalk another person controls the UAV. It is clear that even the simplest case of using drones for recreational purposes raise ethical problems. Essentially, the great mobility and capabilities of UAVs combined with their wide availability can lead to serious problems. The situation can get even more serious when the operators are experienced and can use special devices to spy on communications. One is for sure, the debate has just started and that it is only going to increase in intensity as the numbers of drones used increase in the near future.

There are many organizations related to civil rights, which already have published recommendations for the civil use of UAVs. For example in the States, the American Civil Liberties Union (ACLU) (Protecting Privacy From Aerial Surveillance, 2011) fears that UAVs' deployment has been held up by the Federal Aviation Administration (FAA) over safety concerns, but the agency is under strong industry and Congressional pressure to pave the way for domestic deployment. It refers to the increasing interest by police to deploy drones for various surveillance tasks but there is a lack of privacy laws strong enough to ensure that the new technology will be used responsibly and in consistence with democratic values. Consequently, they believe that we will end up being a "surveillance society" in which our every move will be monitored, an unfortunate development that would profoundly change the character of public life.

#### A.1.3 Legal impact

Up to this point I have referred to the numerous concerns about the safety, ethics and privacy impacts of UASs which demonstrates that the use of these devices needs to be regulated. One of the most difficult parts of this task is that the regulatory parameters for the use of UASs is that UAVs range between small size model aircrafts for recreational purposes and military aerial vehicles such as planes and helicopters which are remote-operated. Consequently, UAS law frame are likely to present variations depending on the model, size, weight and speed, leading to regulations significantly more complex and difficult to understand and enforce. The second issue that presents difficulties when it comes to imposing new regulations is the wide range of UAVs applications. The legal frameworks should include policies ranging from surveillance to delivery of goods. Thus, there will inevitably be many legal issues: accidents involving personal injury and property damage, intellectual property issues implicated by the technology used to control UAVs, individual privacy rights, as well as criminal laws coming into play such as stalking, harassment, and wiretapping.

In the States the Federal Aviation Administration (FAA) is in charge of overseeing airspace in the US and the guidance for non-commercial users. What it holds at the moment is that the commercial use of UAVs is illegal although many entrepreneurs envision the next killing?? commercial application of the drones, like amazon's air prime. The rules that apply for the UAV operators can be found in (Faa.gov, 2015). According to FAA's road map of the integration of drones by the self-imposed deadline of 2015, the FAA looks at the use of drones for commercial purposes in order to develop a plan for boosting the use of drones in the US.

In the UK the Civil Aviation Authority (CAA) governs the use of drones. A summary of the legal requirements related to the UAVs can be found in (Caa.co.uk, 2015). Anyone who is using a drone under 20kg for commercial purposes has to be licensed to ensure that they are sufficiently trained to fly the plane and have the appropriate insurance in place.

#### A.1.4 Industrial impact

Over the past few years, the prospects for a UAV civil market have distinctly improved. The UAV industry is an emerging domain in a worldwide scale. It is dominated by the US and Israeli suppliers followed by the European companies. Less aerospace-developed countries such as China, Turkey and Pakistan are focusing on UAV development. It is predicted that Asia is set to become the second most important UAS market behind the US. China and Japan are likely to be the primary industrial players (Royal Aeronautical Society, 2013). Other countries showing signs of related industrial activity are Poland and South Korea.

The diversity of the companies, which are engaged, with the industry of the UAVs is also an interesting point to investigate. The emergence of the UAS and predictions of future business growth has led established aerospace companies to take an interest either by developing technology by themselves or by acquiring smaller specialist companies. For example I can refer to

Boeing, BAE, Thales and many more. At the same time partly due to the relatively primitive nature of the standard UAV platform, it was made possible for new companies to enter the market and stake their percentage. For instance, there are many cases of spin off companies that combine innovative research concepts, produced in the institutes, with practical engineering suitable for manufacture.

#### A.1.5 Economic impact

A recent study (Jenkins and Vasigh, 2013) by the Association for Unmanned Vehicle Systems International (AUVSI) predicts that in a matter of years UAV industry in the U.S. could produce up to 100,000 new jobs and add \$82 billion in economic activity between 2015 and 2025. Of course this prediction is based on the fact that federal law mandates FAA to open up the National Airspace System (NAS) by 2015. The UAV industry is looking forward to this development since current restrictions prohibit individuals from flying drones for commercial purposes. It has been estimated that every year that this integration is delayed, the US loses more than \$10 billion in potential economic impact (a loss of \$27.6 million per day that UAS are not integrated into the NAS).

In Europe the landscape is almost the same. The European Commission likens the economic impact of UAVs to the development of the Internet in the nineties. However, in order to avoid problems emerged from the ethical and legal issues they address the need of regulation.

Unlike the US and EU, Canada is one of the leaders in commercial applications for UAVs and this happens due to progressive legislation. UAVs are already being used in Canada for the monitoring of piping and power lines, as well as various other uses including crop monitoring.

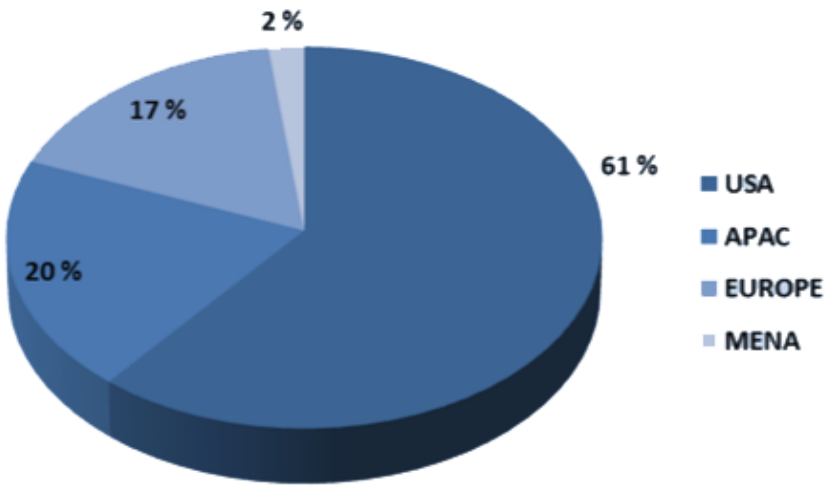


*Fig.A.3 Regional breakdown of the global commercial and civil UAV market in 2013,  
source (INEA consulting, 2015)*

## A.2 Interface Analysis Centre (IAC)

Interface Analysis Centre is a university research group, hosted in the School of Physics at Bristol University. IAC combines material scientists and engineers that concentrate on answering why the materials have certain properties and behaviors and how these can be exploited to compose something better or cheaper. Using special equipment, IAC aims to deduce how the properties (like strength, transparency, flexibility, conductivity) are related to the structure (like crystal size, alignment of fibres). After all, the challenge is to use this knowledge to design and manufacture materials, which have better properties for the required purpose (Bristol.ac.uk, 2015).

One of the specific tasks in which IAC focuses is the visual and thermal monitoring of radiation after a release of nuclear material. It has already developed a semi-autonomous drone, called Advance Airborne Radiation Monitoring (AARM) system, which was jointly funded by the Engineering and Physics Sciences Research Council (EPSRC) and Sellafield Ltd. The latter is the national organization tasked with the managing and safely storing the

UK's nuclear waste. The initiation of this idea happened in response to requirements for radiation monitoring needed at Fukushima Daiichi Nuclear Power Plant and in the surrounding affected prefecture. After the first successful mission (Imitec, 2014) of flying at Sellafield nuclear site in spring 2014, a small team led by Dr. Tom Scott employed two AARM systems to provide an initial assessment of contamination in one of the most highly contaminated prefecture areas within the Abukuma river basin, in the Kawamata area of Japan (Scott, 2014). Sellafield and the Bristol-Kyoto Strategic Partnership Fund jointly sponsored this expedition.

### A.3 The project

The purpose of this project is to advance the existing capability for radiation surveillance at civil nuclear sites of the first generation AARM system. The primary goal is to utilize commercial off-the-shelf (COTS) technologies combined with algorithms used in the robotics fields to design a more sophisticated AARM version. More precisely, it is desirable to develop an assisted flight method in which the UAS operator is aided actively during the flight to avoid collisions with obstacles. In addition to that, a mobile application for visualising the individual gamma energies and intensities (cps) on a map is implemented. Using this app, the users will be able to observe in real time the contamination levels being recorded by the UAS and focus accordingly to the areas of interest.

The overall task can be divided to the following individual objectives:

- Literature review of up-to-date related papers found in IEEE explore website. The subject of the research is the development of autonomous UASs and collision avoidance techniques as well as UAV stabilization, proximity sensors, radiation mapping and UAV simulations.

- Experimentation with a range of proximity sensors, from ultrasound to laser scanners, and comparing them in terms of functionality, power consumption and size. Ensuingly, the sensors are adapted to the UAS and are used to take measurements in various conditions. During that procedure, existing problems and the limiting factors are identified. Moreover, possible solutions are proposed including additional 3D-printed structures that improve the performance.
- Employment of a realistic 3D simulation to experiment with various collision avoidance maneuvers that can be used in an assisted flight method. Henceforth, the same techniques are applied to a real UAV. Comparison of the performance in both situations is conducted.
- Design and development of a mobile application that depicts the level of radiation contamination on a map in real time, taking wireless measurements from a gamma spectrometer. This task improves the human-robot communication to a friendlier interface and takes advantage of the ubiquity of the smart devices.

As a general approach in this project, it has been decided to engage with a range of different tasks like sensors, simulation, real UAV and human-robot interface rather than focus and specialise in a specific task. This decision is preferable in order to gain experience and understanding from a wider range of domains. The work of this project was conducted in the IAC lab using the provided equipment and parts that were acquired only for the specific project. For all the objectives, the approach was to study the available options and follow the one that was the best suited for my case.

## Part B

### Literature review

In this section, an extended literature review is presented which is conducted in the individual sections of the dissertation. Most of the sources are conference papers and journal articles on the basis that they are published recently and thus are more up-to-date compared to books. They reflect the latest developments in each discipline. The vast majority of the sources are less than four years old (dating from 2011 to present). Thorough research is undertaken for every major part of the dissertation in order to get a rounded view of the undergoing research and development that is being carried out.

#### B.1 Radiation mapping

The radiation anomalies mapping procedure is one of great importance since it can ensure the public safety in cases where disaster happened or in monitoring of nuclear power stations. There are many examples that can show the importance of radiation mapping. In March 2011 The Fukushima Daiichi nuclear power plant was severely stricken by a tsunami causing Units 1 – 4 to contaminate the environment with significant atmospheric release of radioactive material (MEXT, 2015). This case clearly illustrates the requirement for technology that allows rapid and accurate mapping of ground and plume radiation contamination. Moreover, in nuclear power plants there is a constant need for validation of safe operation. This can be achieved by continuous routine surveys to identify contamination releases. Finally, Radon mapping is also important because it can affect the public health as it accumulates inside buildings and basements, greatly increasing the risk of lung cancer.

There are three methods of radiation mapping. Static ground based surveys, which performed by arrays of above ground in situ measuring stations or handheld devices. In situ ground level measurements improve spatial averaging at the cost of vertical profiling. The handheld measurement devices produce an accurate and sensitive representation of how radioisotope concentrations vary spatially or depending on depth. On the other hand, this method is time consuming and captures a limited snapshot of radionuclide distribution (Sanderson et al., 1995). Car-borne radiation surveys conducted using vehicles equipped with detectors, which are calibrated and deployed quickly, and can map 400–1000 km every 24 hours (Mellander, 1995). Using this process, more measurements can be collected compared to the first method but data collection is limited to the road network (hence rural data is often sparse) and to low driving speed (< 30 mph) to maintain an adequate resolution. The third approach, which is the one the project refers to, relates to airborne radiation surveys. This can cover great areas of interest expeditiously. Coverage per unit is  $10^6$ - $10^7$  times greater than that of ground based and  $10^2$ - $10^3$  times that of car-borne surveys because of the greater ground clearance, coverage and the lack of obstacles (Schwarz et al., 1995). It can also be considered the safest since the remote nature of the sensing removes pilots from a percentage of the ground based radiation exposure, although this is not true of radiation plume mapping. In this method, the most influential factor is altitude. Air attenuates radiation and consequently as altitude increases, the intensity detected decreases rapidly (fig.B.1).

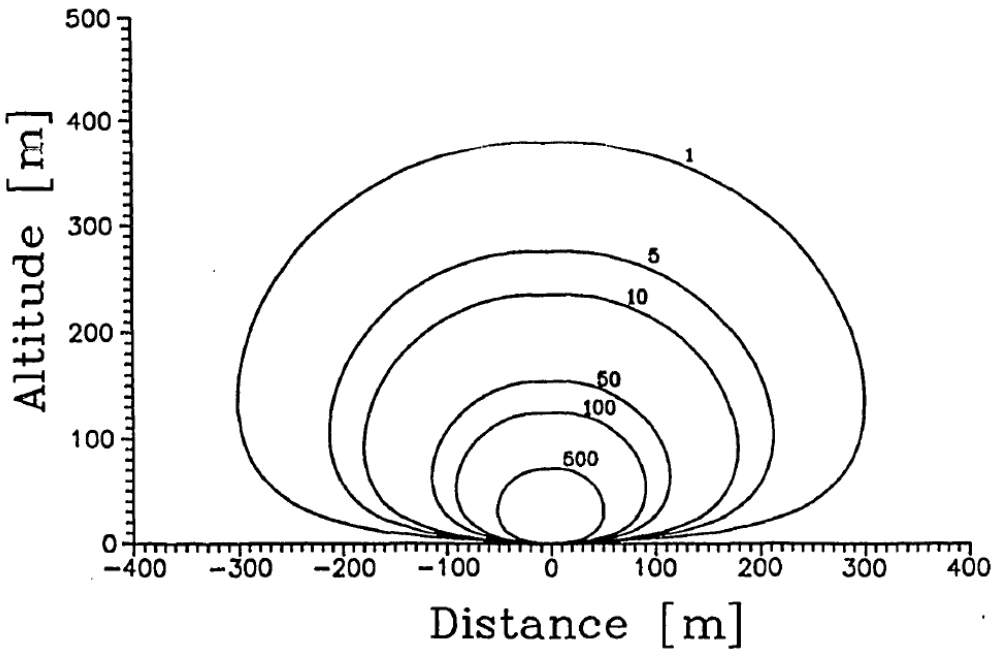


*Fig.B.1 Modeled count rate (counts per second) isolines, using a large volume NaI scintillation detector, of a 1.9 GBq (50 mCi)  $^{137}\text{Cs}$  source buried at 1 cm depth. (image from Schwarz et al., 1995)*

A subcategory of the third approach, which offers the benefits from all three methods, is radiation mapping using UAVs. The utilization of this method seems ideal for the following reasons:

- It can produce high resolution mappings similar to the hand held based surveys since UAVs can hover in low altitudes and follow dense trajectories in given areas.
- UAVs approach the territories of above and avoid local obstacles resulting in a low sampling density. In addition, they have the ability to fly steadily with low velocity in close proximity to nuclear premises and collect accurate measurements.
- UAVs require lower initial expenditure than airborne radiation surveys.
- UAVs ability is not influenced from radioactive debris that could contaminate the UAV like car tyres, which are in constant contact with the road and stick materials from the surface of the road.

One successful approach that managed to implement a UAV based airborne radiation survey comes from Imitec (Imitec Limited, 2014), a University of Bristol spin-out company. They have developed a remote isotropic analysis system, which consist of a lightweight gamma spectrometer and positioning devices, integrated in a UAV (fig.B.2). Using this combination, it is possible to measure meter resolution maps of radiation including over high dose areas and inaccessible locations. It can also provide aerial imaging and observation in conjunction with the radiation measurements. Finally, there is the ability to perform pre-programmed flight paths, which is advantageous for scenarios where routine monitoring is required.



*Fig.B.2 The Imitec's Advanced Airborne Radiation Monitoring (AARM) UAV (image from [www.imitec.co.uk](http://www.imitec.co.uk))*

## B.2 UAV flight

In every mobile robot application, semi-autonomous or autonomous, the task of mapping, localisation, navigation and collision avoidance is important decision in design. The implementation of each part can be done using properly adapted versions of popular methods and probabilistic algorithms available in the robotics literature. This literature review includes the knowledge of related papers concerning UAVs. In order to be more precise I

focused my research on quad or multi copters in order to exploit the strengths and combat the weaknesses in this specific configuration.

The Mendes and Ventura 2012 paper (Mendes and Ventura, 2012) proposes an interesting approach to tackle the problem of assisting tele-operation to safely pilot a UAV; a concept that is closely related to the current project. More precisely, according to the environment in which the UAV flies, driven by the operator, the researchers designed a process that overrides this operator input either by modulation, inhibition, or replacement with a different input. The desired goal is to use sensor data to determine an appropriate assisted tele-operation in order to guarantee, to the best of sensor capabilities, a safe flight.

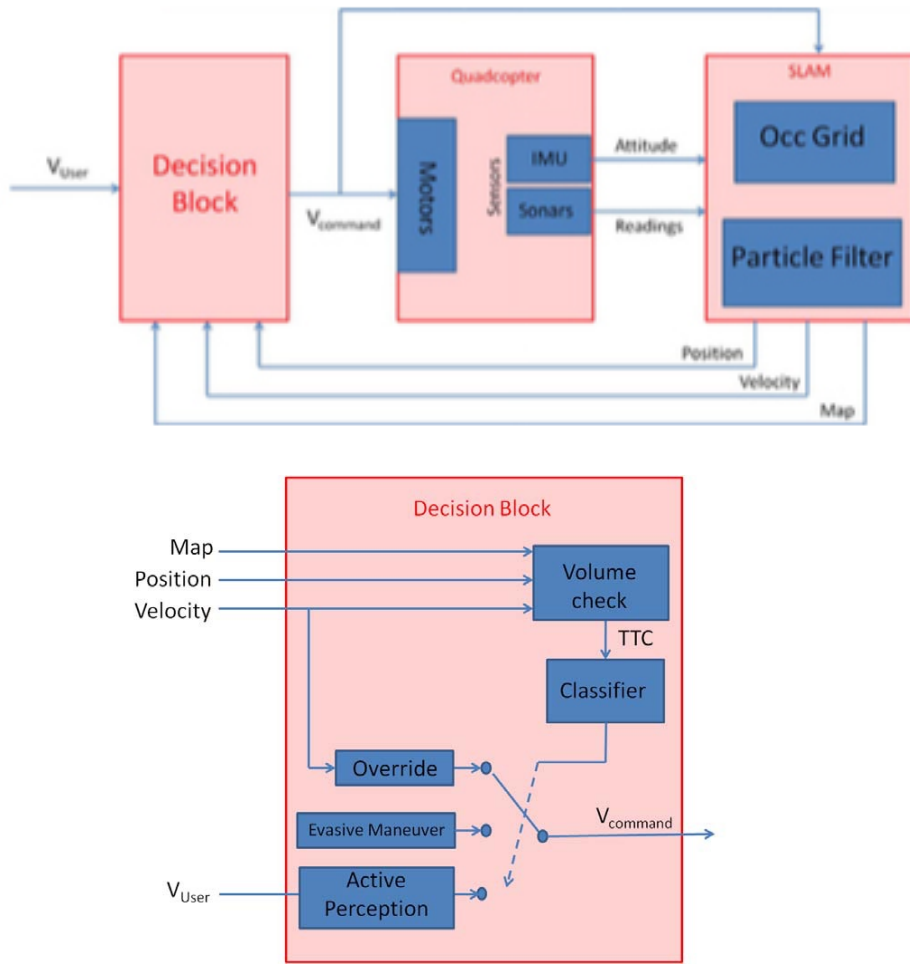


Fig.B.3 Full architecture of the proposed approach and flow chart of the decision block  
(image from Mendes and Ventura, 2012)

The investigators assume that the UAV operates in unknown, unstructured, GPS-denied, and indoor environments, therefore the main potential threat is collision with obstacles. Thus, distance sensors are used to detect and map these obstacles. The approach is based on the FastSLAM algorithm, together with 3D occupancy grid mapping. Using these techniques they are able to estimate the vehicle's position in the map. At this point a classifier makes a decision based on danger assessment. This classifier overrides the user's inputs if they compromise the quad copter's physical integrity in the near future. Overriding may extend from simple velocity reduction to, in extreme cases, an evasive manoeuvre (fig.B.3).

The approach assumes that the attitude is known using the on-board IMU so the problem is to define the position of the UAV. Using FastSLAM they can estimate both the position and the map of a robot simultaneously. The classifier takes the position estimation and the map as inputs. It categorises each cell of a 3D occupancy grid in one of 3 states Free, Unknown and Occupied. Given the operator's inputs, the classifier computes the desired direction for the vehicle and the distance to the first non-Free cell. If the closest cell is occupied, the inputs are altered accordingly so that the UAV will remain safe and then they are applied to the navigation. If the closest cell is Unknown and if the distance to it is higher than a certain threshold, the algorithm checks whether there is any sonar aligned with the desired direction. Otherwise, the algorithm will autonomously rotate the vehicle and then applies the same speed that the user demanded.

This remarkably interesting approach is based on short-term, rough mapping of the nearby environment. The researchers argued that the real world experiments were successful and thus verified the design. However, it is also mentioned that the four sonars, which were used as proximity sensors, recorded the readings with the quad-rotor's motors set off, for safety issues. Despite the safety benefits in such a procedure the result of the tests could be inaccurate, considering that sonars with their rotors switched on take error prone readings.

In the Chen 2013 paper (Chen et al., 2013) the effort of the research team to develop a UAV system capable of autonomously navigating in a one-level building and producing a 2D map of the space is presented. Moreover, there were specific requirements from the academic partners that needed to be satisfied. More precisely, the system had to be based on an inexpensive, upgradeable, and reconfigurable solution with commercial off-the-shelf (COTS) products.

The hardware of the project consists of an AeroQuad quad copter, a 54-Pin Arduino Mega SDK microcontroller, a Samsung Galaxy SIII Android smartphone, and MaxBotix ultrasonic range sensors.

For the navigation task of the project they decided to use Voronoi Fast Marching motion planner. They argued that this approach offers a thorough description of the exploration process, the ability to integrate with SLAM, and the potential to safely and effectively navigate with a limited field of view. In the SLAM part of the project they evaluated different existing approaches like GraphSLAM, EKFSlam, GridSLAM and FastSLAM. They resolved on choosing the latter, since FastSLAM is computationally efficient and likely to overcome inaccurate data making it the preferred algorithm for this project

Having made these decisions about the algorithms the research team designed the simulation part of the project. In the paper, they presented the results related to the mapping algorithm and the navigation one. They cited that they hadn't managed to construct the localization prototype due to the lack of time and the complexity, thus they couldn't present results of the FastSLAM approach. As expected, they did not present results from any real experiments.

Due to the lack of actual experimentation and the incomplete state of the simulation results this paper could be deemed a premature project Nevertheless, it is interesting to read since it assesses available methods for

navigation and SLAM and also describes their experiences from the sensors' behaviour (in the calibration stage).

On the contrary to the previous study, a complete and interesting approach is presented in Hrabar's 2011 paper (Hrabar, 2011). In cases where UAVs performs real applications there is a need to move in cluttered environments, making collisions a real possibility. This paper comes to propose an interesting 3D reactive obstacle avoidance technique suitable for UAVs flight in point-to-point trajectories.

In the introduction the author presents us with common disadvantages in the existing approaches. He refers to techniques that check only current sensor's field of view without keeping memory and also refers to techniques that propose escape points without taking into account the goal point. Ensuingly, he counterpoises an approach where a cylindrical volume in front of the UAV checks for potential collisions and when one is detected an intermediate waypoint (Escape Point) is found in free-space that provides a route past the obstacles that have been mapped (fig.B.4). The Escape Point search proceeds on a series of concentric ellipses, the shape and orientation of which can be adjusted to favour horizontal or vertical avoidance manoeuvres (fig.B.5). Since a waypoint is produced, the technique is suitable for integration with global path planners that plan between waypoints.

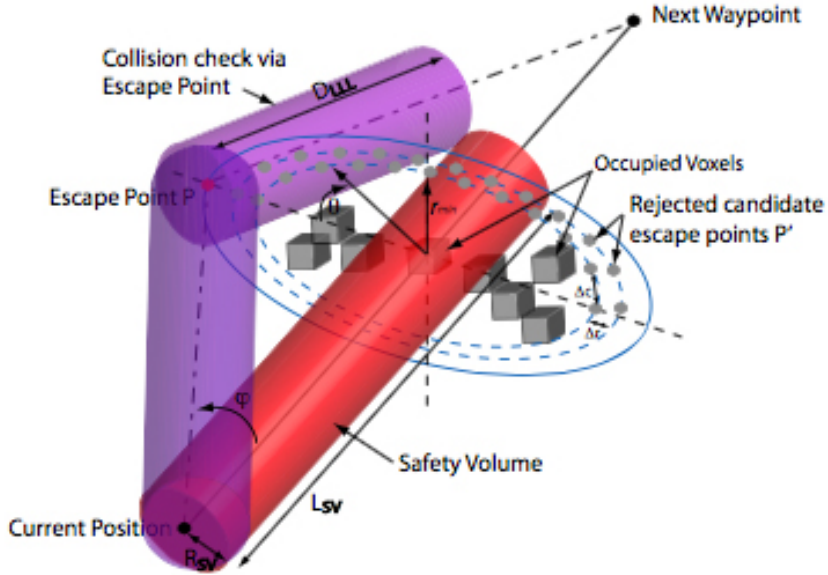


*Fig.B.4 The expanding elliptical search for a valid Escape Point (image from Hrabar, 2011)*

A voxel-based representation of the 3D environment has been employed to be the basis in which the algorithm is going to be operating. The algorithm maintains an occupancy grid in which both global path planning and reactive avoidance cooperate. In this map-based approach the reactive avoidance mechanism is easily tuneable to favour horizontal or vertical avoidance manoeuvres and generates reactions based on all the previously sensed obstacles, producing an intermediate waypoint which can be used as input for a waypoint-based global path planner.

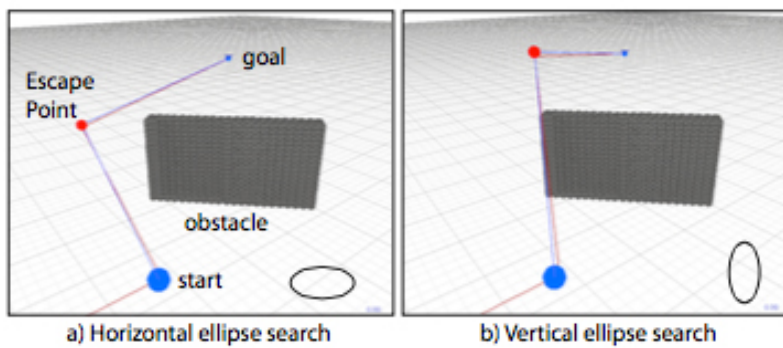


*Fig.B.5 With the major axis of the ellipses aligned horizontally, horizontal manoeuvres will be favoured (a), while vertically aligned ellipses will produce vertical manoeuvres (b) (image from Hrabar, 2011)*

Special care has been taken to enable the execute of the algorithm in the on-board hardware. The author cites that one of the most demanding tasks of the algorithm is the checking within the occupancy map for occupied voxels, required when testing for potential collisions ahead of the UAV and when evaluating candidate Escape Points. He used a balanced kd-tree (Bkd-tree) structure to represent the occupied voxel centres. Moreover, he compared the Bkd-tree based query times to a traditional brute-force linear search. For smaller voxel populations the techniques show similar performance, however as the voxel count grows the search time increases linearly for the linear search while remaining almost constant for the Bkd-tree search.

After an extensive and detailed explanation of the algorithm, the author presents the experimental results. The UAV was tasked to fly between pairs of waypoints either side of an obstacle, requiring it to detect and avoid the obstacle in order to reach the second waypoint. The results were very promising and the failures that occurred were due to obstacles not being detected and not due to the reactive avoidance algorithm.

The paper is well structured and presents its approach in great detail. Not only the theory of the approach is well defined but also the author presents a wide range of real experiments results. This is highly valued from a researchers standpoint since other papers I have read only include simulations and poor real world experiments, promising improvements in the near future. A possible limitation of this approach is the computational complexity. The UAV was equipped with (1.83GHz Core 2 Duo, 2GB RAM) system rather than popular Arduino based micro controllers (APM or even PX4) that usually be found. However, the progress in the field of SoCs (System on Chip) makes these kinds of tasks easier to be executed. It should be taken into consideration that the experiments were held successfully in 2011 with systems, which were available 4 years ago.

One more paper that presents a flight control system for autonomous UAVs is described in Wang 2014 (Wang et al., 2014). The design is a low-power,

small-size autopilot and the research team performed various tests in order to verify its stability and reliability. The hardware used consists mainly of a microprocessor ATmega 2560, GPS, barometer and an MPU unit (gyroscope and accelerometer). In addition, it has a laser distance sensor to achieve a more accurate altitude for automatic take-off and landing. The autopilot system controls a small UAV, having wingspan of 3.8m and powered by a gasoline engine, rather than a multi-copter but the principles of control remain the same.

The design of controller of the autopilot is based on a cascade control method. The outer loop is a trajectory controller; the inner loop is an attitude controller. Among them, the role of the trajectory controller is to calculate the desired attitude and throttle, based on the desired trajectory and current UAV position and height. The attitude controller controls the size of aileron, elevator and rudder, in order to control the attitude of UAV consistent with the attitude calculated by the trajectory controller.

The trajectory controller contains two parts: a lateral controller and a longitudinal controller. Firstly, the lateral controller's role is to reduce, eliminate cross track error, making the UAV flight along the desired trajectory as far as possible. For this part, they used the L1 control method especially suited in the situation where the desired trajectory is a complex curved path. Secondly, the longitudinal controller tries to eliminate the altitude error. In the meantime, the airspeed of UAV remains within a safety range, avoiding under-speed. For this task, the researchers used the Total energy control system (TECS). The principle of this theory is that coordinating the throttle and the desired pitch angle of the UAV controls altitude and airspeed.

Further to the model, the paper includes the experimenting results. In general, the small-scale UAV flight presented an accuracy of trajectory control of about 1.5m and altitude error no more than 0.5m. The paper was coherent but it failed to adequately explain the control methods. However, it

presented in great extent the hardware that was used but this did not add something to the novelty of the approach they were trying to offer.

### B.3 UAV Stabilisation

One of the requirements for the UAS that I intended to design is the ability to fly low, slow and with augmented precision so as to measure accurate radiation values close to the source. Consequently, there is a need for enhanced stability during the flight. A typical fixed wing aircraft is inherently stable while in flight because the forward motion and airflow over and under the wings create stability. On the contrary, the task of keeping stable a helicopter during hovering requires constant minute corrections to throttle, pitch, roll, and yaw. Turbulences that would not trouble a fixed wing UAV can send a helicopter into a settling with power state or some other unrecoverable situation. The advantage of using multi-copters compared to the helicopters is that the former are simpler platforms since they can control all degrees of freedom by simply redistributing the thrust among the rotors. However, small UAVS flying in a low altitude need to respond very quickly to turbulences so as to avoid crashes.



*Fig.B.6 Hovering flight above the landing pad (image from Herissé et al., 2012)*

In (Herissé et al., 2012) the writers present an image-based visual control algorithm inspired from biological models like bees. Their purpose was to achieve UAV stabilization relative to the moving platform that maintains a constant offset from a moving reference and secondly automatic vertical landing onto a moving platform (fig.B.6). The image information that is considered is the average optical flow that is obtained from a textured target plane, using additional information delivered by an embedded IMU for de-rotation of the flow. The implementation is based on two nonlinear controllers, a proportional-integral (PI)-type controller designed for hovering flight, while the other is responsible for exploiting the vertical optical for the vertical landing.

In terms of hardware configuration, the system consists of an inertial measurement unit (IMU) and optical-flow measurements yet it additionally includes a digital signal processing (DSP) board, which runs at 150 MIPS and performs the control algorithm of the orientation dynamics and filtering computations. A spherical camera pointing directly down transmits video to

a ground station via a wireless link. The data are processed by the ground station and incorporated into the control algorithm where the desired orientation and thrust are generated and sent back to the UAV. A challenging part for the implementation lies in the relatively large time latency between the inertial data and visual features.

The paper is oriented towards the capability of stabilizing the motion of the UAV with respect to a dynamic moving environment. A disadvantage of this approach is that the data cannot be processed on board in the UAV because of the algorithm's complexity. It can be also considered the requirement of contrast textures in order to gain better performance from the optical flow algorithm. On the contrary, it is easily inferred that the use of an optic flow sensor could enhance the stability in challenging situations and environments by giving more flexibility compared to the noise prone acoustic sensors of the range limitations of the infrared ones.

A more focused paper describing the benefits of optical sensors regarding the stability is presented by Fowers, 2007 (Fowers et al., 2007). It approaches the system by developing quad-rotor UAV using a low resolution (640x480) CMOS image sensor and a custom, low-power FPGA platform to perform computationally intensive vision processing tasks on-board, without the need for wireless tethers and computational support on ground stations. Deeper on the algorithms side, it uses Harris feature detection and template matching, giving the UAS the ability to be stable and almost drift-free hover.

The very small payload that the UAS can handle and the limitations in power consumption turns the use of the low power and small size FPGA (fig.B.7) a radical solution for the on-board calculations of the demanding image processing algorithms. The on-board vision system performs the drift-corrections that are not detected by the IMU, by tracking feature movement through consecutive images captured by the camera facing the ground.

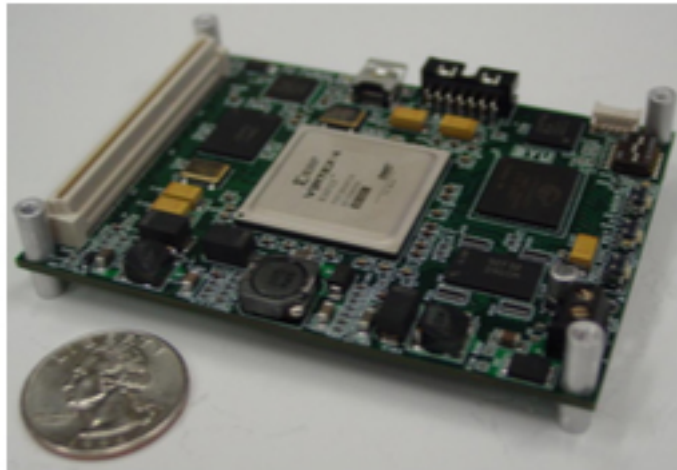


*Fig.B.7 FPGA-based helios board (a Xilinx Virtex-4 FPGA) for embedded vision processing (image from Fowers et al., 2007)*

Another approach using more advanced configuration is proposed in (Romero, Salazar and Lozano, 2009). This paper proposed an eight-rotor configuration whose translational and rotational displacements are decoupled. Four rotors perform the stabilization of the orientation copter, and the other four are used to drive the lateral displacements. The authors argue that the proposed configuration is useful for image processing since it keeps constant camera orientation. This is particularly important since systems that rely on optic flow for estimating range information need to remove components of optic flow that are induced by rotations of the aircraft, and use only those components that are generated by the translational component of motion. This happens because only the translational components of optic flow provide information on the range to objects in the environment. However, the experiments exhibited that the estimation of translational speed in outdoor environments using optic flow has several limitations, such as the light intensity and the contrast. In indoor environments this strategy seemed to have worked better. Nevertheless, the design of this configuration (fig.B.8) is custom and cannot be applied in commercial Off-The-Shelf (COTS) products without major modifications.

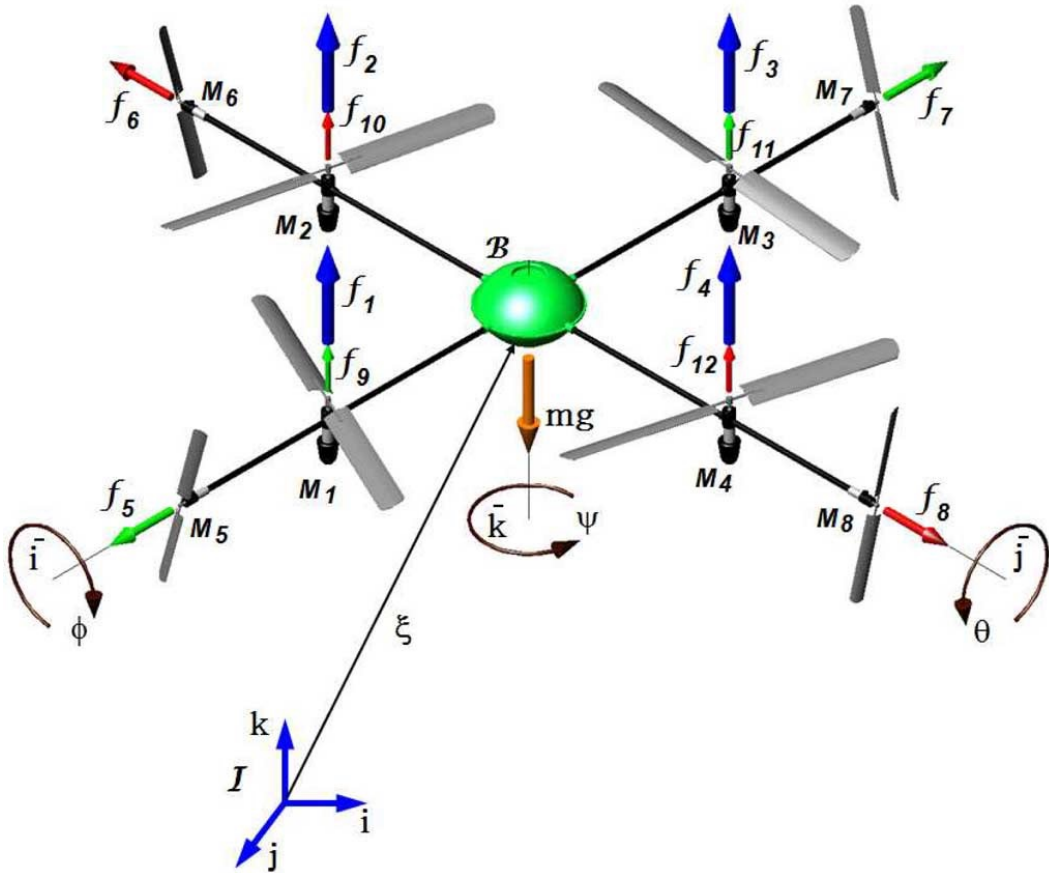


Fig.B.8 Eight-rotor rotorcraft scheme (image from Romero, Salazar and Lozano, 2009)

#### B.4 UAV sensors

Having reviewed interesting approaches related to UAV collision avoidance and stabilisation I realize that the availability of reliable and flexible sensors will facilitate the task. My project is based on the use of COTS technologies and the research of existing distinguishable hardware is required. In the field of mobile robot navigation there is always the need for an accurate, low power, compact and ideally low cost distance measurement sensor. Pulsedlight (Technology Brief, 2015) has managed to implement a very interesting design (fig.B.9). It measures distances from zero to 40m with +/- 0.025 m accuracy at a reading rate of 100Hz. According to the developers the existing optical sensors solutions was either high accuracy phase-based measurement based on the transmission and reception of a continuously

modulated, typically red, pointing and measurement beam or long range low accuracy pulsed measurement using the delay between the transmission and reception of higher power, short duration, infrared pulses. The innovation in this approach is that they implement a device based of the latter, time-of-flight distance measurement method, but using low power and low cost signal digitization hardware unlike the existing solutions, usually military applications. In order to achieve that goal they had to develop a new signal processing approach to optical distance measurement, known as signal correlation technique, which still allowed implementation using a very simple hardware configuration while eliminating the time consuming and processing intensive signal reconstruction of existing approaches. The implementation of this design is released as a single programmable logic chip or System-on-Chip (SoC).

In the stabilisation section, the optical flow measurement seems to play a dominant role in this task. PX4 project, which is an independent, open-source, open-hardware community, has developed a remarkable optical flow measurement device (Honegger et al., 2013). They present low consumption, lightweight and low cost SoC (fig.B.9) that can compute optical flow and compensate for rotation. It is suitable for indoor and outdoor applications having very high light sensitivity. The software implementation and hardware design is open sourced. The system consists of an ARM Cortex M4 microcontroller that performs optical flow processing at 250 frames per second at a subsampled resolution of 64x64 pixels using a CMOS machine vision sensor. An ultrasonic range sensor is also installed to measure the distance towards the scene and to scale optical flow values to metric velocity values. Up until the presentation of this implementation it was a more popular approach to use computer mouse hardware sensors to carry out similar tasks but they suffer from lighting limitations since they require strong lighting to provide accurate measurements. Other systems using more advanced CMOS sensors send the data via wireless links to ground stations for processing or employ dedicated hardware designs implemented in field programmable gate arrays (FPGA) to perform all computations on-board in

real-time. The evaluation experiments were conducted in indoor and outdoor environments, with different illuminations. The system is validated with several experiments comparing the presented flow sensor to a standard mouse sensor and GPS and measurements with ground truth using a VICON motion tracking system. The results demonstrated that the sensor operates accurately at high frame rates.

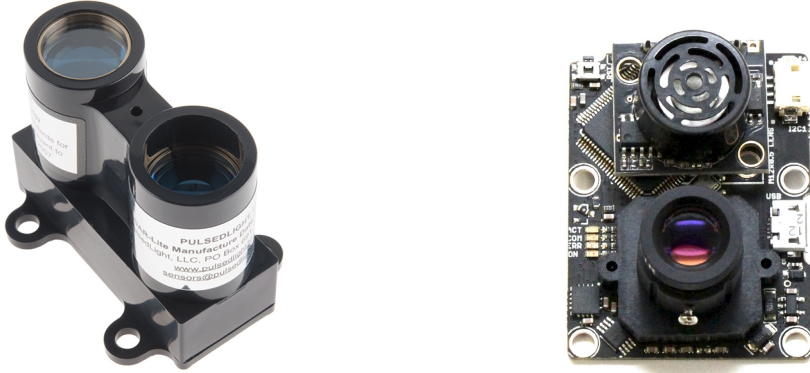


*Fig.B.9 PulsedLight's Lidar-Lite laser distance measurement device and PX4Flow optical flow smart camera (images from <http://pulsedlight3d.com> and <https://pixhawk.org/modules/px4flow>)*

## B.5 UAV Simulations

In recent years, computer simulation of robotic concepts has become popular since many tools have been introduced to facilitate the designer's work. The advantages of doing a simulation (Richards, 2015) is that it is cheaper and less risky to experiment using computer models rather than real hardware. Regarding the UAVs, there is a plethora of available simulators each of them targeting a specific task. The problem with these is that they complicate the evaluation of the designed tasks and have steep learning curves. On the other hand, there is always the option to develop a custom simulator only for the given task that the designer requires. The downsides of this approach are the amount of time is spent building things from scratch as well as the absence of

some advanced features that the simulators have, such as visualization, readymade environments (indoor and outdoor) and advanced dynamics.

For the specific project I need a simulator that can be used in different environments, to assess the efficiency of the collision avoidance algorithms by employing different proximity sensor technologies as well as to prove the stability of the configuration. For these tasks, I need to be able to plan a path, to build different environments and finite states machines, which add the required intelligence to the UAVs. Most importantly, I need to change the UAV model and add additional sensors in specific parts of the UAV. This set of requirements makes the use of available simulators difficult for my task. I reviewed some of them in order to assess their suitability.

The Robot Operating System (ROS) is a framework for writing robot software. More precisely (Ros.org, 2015), it is a collection of tools, libraries, and conventions that aim to simplify the task of creating complex and robust robot behaviour across a wide variety of robotic platforms. Gazebo is a robot simulation tool that is used in combination with ROS to test algorithms, robot designs and perform regression testing using realistic scenarios.

The usage of these tools is very popular in the robotics community and it is a standard in many robotics fields. For the quad-rotor UAV systems case there is a published package related to modelling, control and simulation called hector\_quadrotor (Meyer et al., 2012). This approach allows simultaneous simulation of diverse aspects such as flight dynamics, on-board sensors like IMUs, external imaging sensors and complex environments. In order to exploit them, the user needs to have experience in C++, preferably, or python. In addition they need to be familiar with working in Linux environment and server – client programming. Like many open-source projects, support is provided mainly from the support forums. There are several tutorials, but in my opinion these cover a small and low-level area of required knowledge. In addition to that, there is a wiki but one needs to be an experienced user to take advantage of it. One drawback that I also discovered is the existence of many

distributions (distros) and the complexity that this adds to the available third-party libraries and packages. On the bottom line ROS and gazebo is a very powerful (fig.B.10), professional and popular tool yet it needs lot of time to become a user-friendly tool and start producing useful results. It produces a difficult learning curve if the user comes from different background.

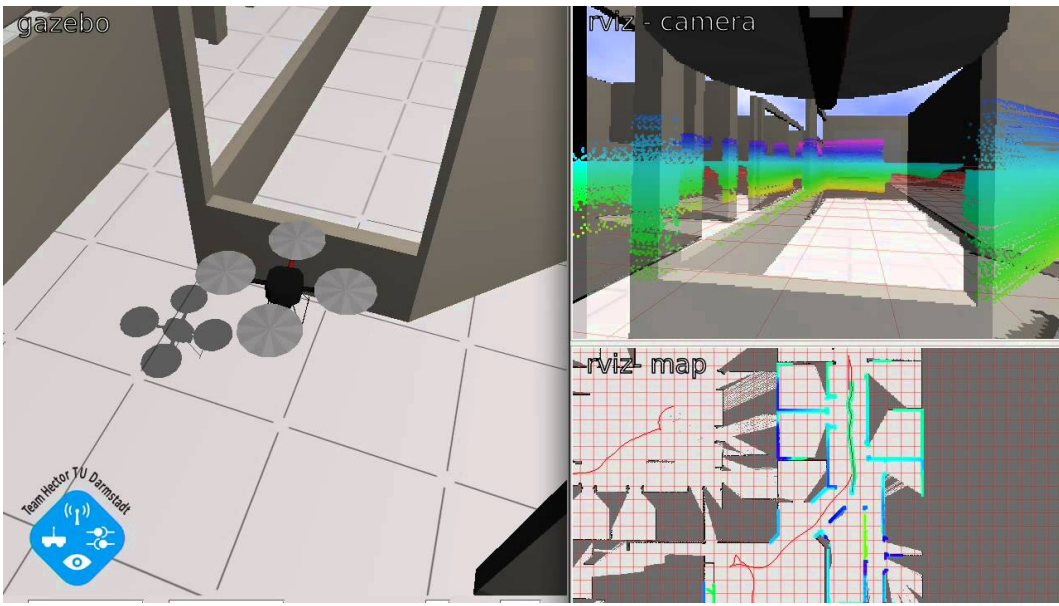


*Fig.B.10 Screenshot of an indoor quad-rotor UAV simulation using ROS with rviz and gazebo (image from Meyer et al., 2012)*

Very recently (available in Matlab R2015a), complementary to the previous approach, is the release of a new robotics system toolbox trying to resolve some of the weaknesses and bridge some gaps I referred to previously. The system toolbox (Uk.mathworks.com, 2015) provides an interface between MATLAB and Simulink and the ROS that enables the testing and verifications of applications on ROS-enabled robots and Gazebo. It also supports C++ code generation, enabling the generation of a ROS node from a Simulink model and deploy it to a ROS network. It is worth mentioning that if the users need to alter and build custom models they need again to cope with ROS architecture and code. Consequently, I admit that this approach is friendlier than the stiff approach of plain ROS but it needs to have knowledge of this in order to be flexible and creative.

Another package that I tried was a 3D Integrated Simulation Platform for Indoor Quad-rotor Applications provided by (A.R. Al-Omari, A. Jaradat and Jarrah, 2013). It is built entirely in Matlab without the use of Simulink. It offers impressive 3D views and a nice graphical user interface (fig.B.11). On the other hand, it lacks serious documentation and the code is not well commented. There are no instructions on how to edit it, to add sensors or construct new maps. Unfortunately, in the current state it cannot serve its initial purpose, as stated, which was the ability to implement and inspect algorithms in different scenarios.

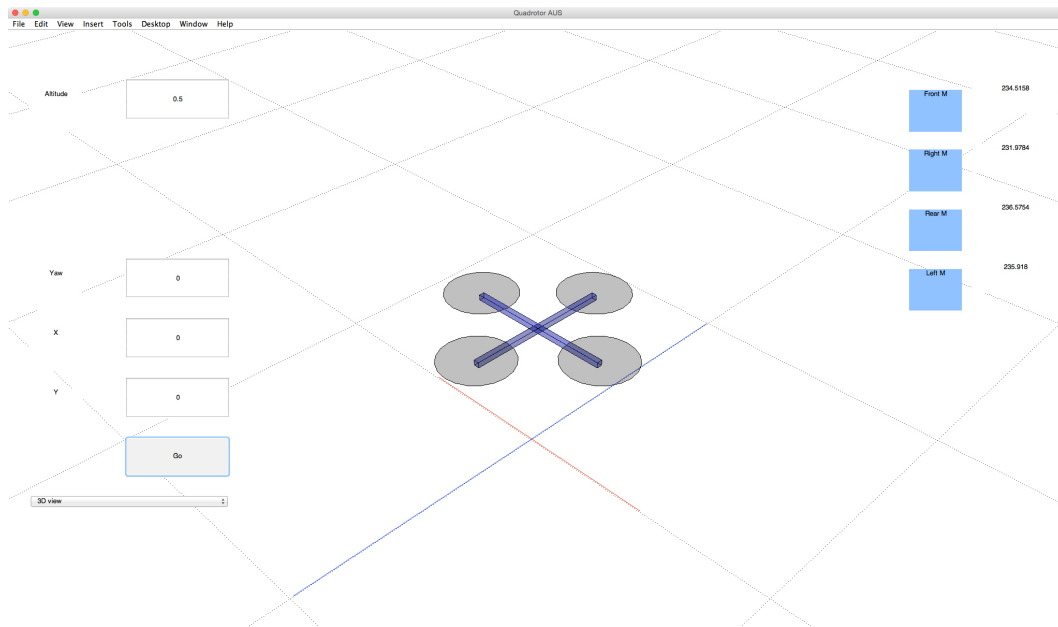


*Fig.B.11 Screenshot of the Integrated Simulation Platform for Indoor Quad-rotor Applications (image from A.R. Al-Omari, A. Jaradat and Jarrah, 2013)*

A better approach in UAVs simulations is presented in Hartman, 2014 (Hartman et al., 2014). They presented a quite detailed quad-copter dynamic modelling and Simulation package accompanied with extended documentation and instructions. The researchers have built the simulation making extensive use of Matlab and Simulink. Using this tool the designer can define the exact geometry of the dominant parts of the UAV like motors, electronic speed controllers, central hub and arms (fig.B.12) and simulate scenarios with different initial conditions and paths. The documentation does not include instructions on extending the model with various sensors nor does it include the ability to build custom maps with obstacles and to test

different behaviours. It is an admirable attempt but, in my opinion, it is intended to different testing scenarios where the designers experiment with the geometry and the configuration of a UAV rather than have a given UAV and test behaviours in different stimuli.

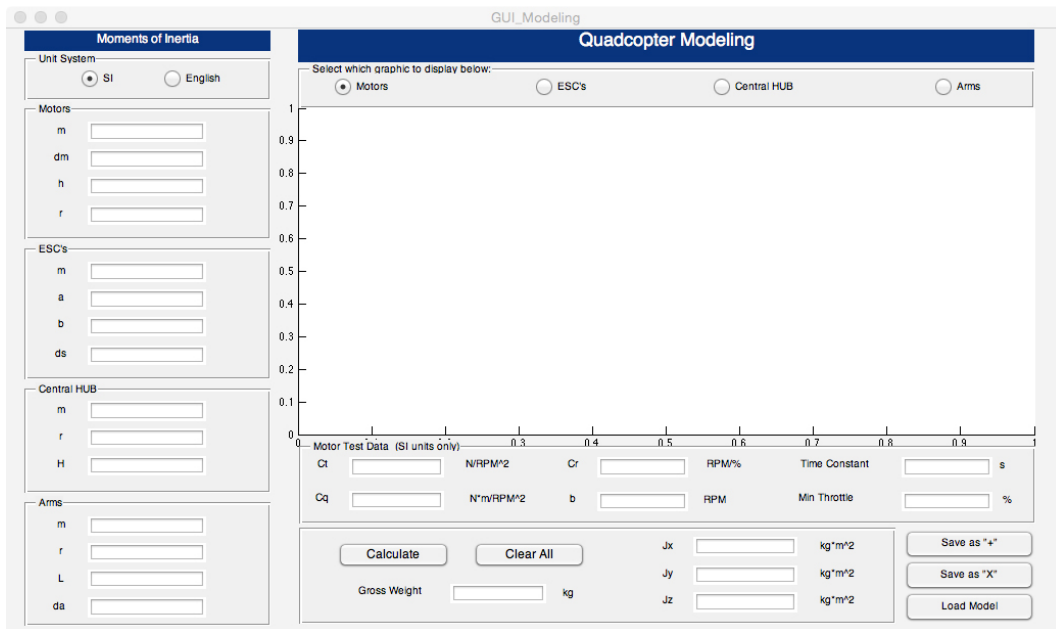


*Fig.B.12 Modelling graphical user interface of quad-copter simulation using (image from Hartman et al., 2014)*

## Part C

# Sensors

### C.1 Ultrasonic sensor

Ultrasonic sensors are transducer devices that can convert ultrasound wavefronts to electrical signals. To illustrate, a sound is emitted by the sensor, then it bounces on the surrounding environment and comes echoing back. This sound takes time to travel distances. The further the distance it needs to travel, the longer time it takes. After that, the sonar's microcontroller, which keeps track of the time that passes, can calculate the distance of the reflective objects detected and it produces an appropriate voltage to the host circuit.

#### C.1.1 Devantech SRF02 Ultrasonic Range Finder

SRF02 is a single transducer ultrasonic rangefinder in a small footprint PCB that supports both I2C and Serial interfaces (fig.C.1). According to the specifications, the minimum measurement range is approximately 15cm and the maximum 6m with 3-4cm resolution. Resolution is simply the smallest measurement increment that the device is capable of reporting. It's the same as the smallest increment of measurement on a tape measure or ruler. SRF02 can report the distance in cm, inches or uS.

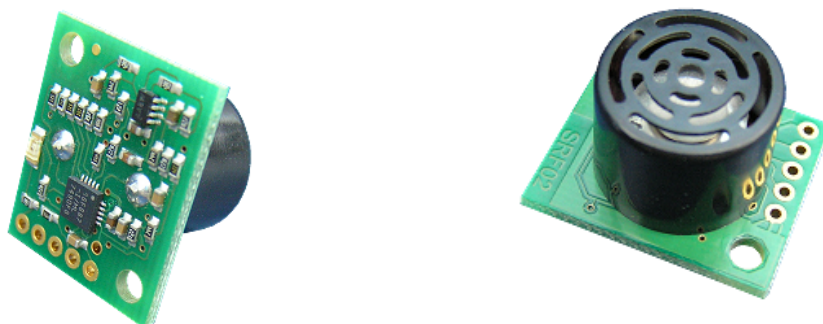


Fig.C.1 Devantech SRF02 Ultrasonic range finder

The advantages of this device can be summarized in the following points:

- Low-cost
- Light-weight
- Low-power consumption: 5V, 4mA Typ.
- The use of serial bus, which can be connected up to 16 devices to any uP or UART serial port, since individual addresses can be allocated.
- There is no need for calibration since it supports full automatic tuning.

In order to test the SRF02, experiments in various shape spaces were conducted to verify the behaviour related to the shape of the lobe. In the first stage of experimentation there is no noise caused by airflow (wind).

*Table C.1*

*(All measurements taken with a surface perpendicular to the sonar)*

Distance (cm)	Measured Distance (cm)	Difference (cm)
10	27	17 (dead zone)
30	29	3
80	78	2
130	128	2
170	169	1
210	207	3
310	306	4
400	396	4
500	495	5
600	595	5
> 600	0	NaN

By examining the table (tbl.C.1) the following conclusions are apparent:

- Reflective objects closer than the minimum are in the sensor's dead zone.
- For distances lower than 2m, it has an accuracy of 2cm. For distances longer than 2m, it has an error approximately 3 to 5cm.
- For distances greater than the maximum, it returns 0.

There is huge variation of the measurements according to the angle in which the reflective objects is hit by the sonar. The sensor can not accurately measure the distance of an object that has its reflective surface at a shallow angle, as a result the sound will not be reflected back towards the sensor. The other case is when the object is too small to reflect enough sound back to the sensor. The sensor's behaviour becomes clear by examining the beam pattern in (fig.C.2)

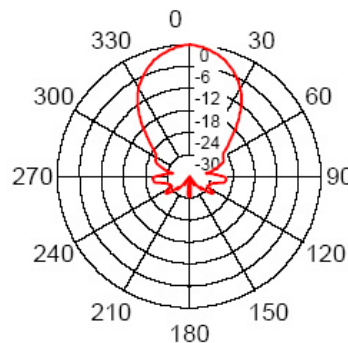


*Fig.C.2 The SRF02's beam pattern, showing the sensitivity of the transducer in dB  
(image from robot-electronics.co.uk)*

To experiment with the different behaviour, I performed a range of measurements in different angles. The set-up is illustrated in figure (fig.C.3).

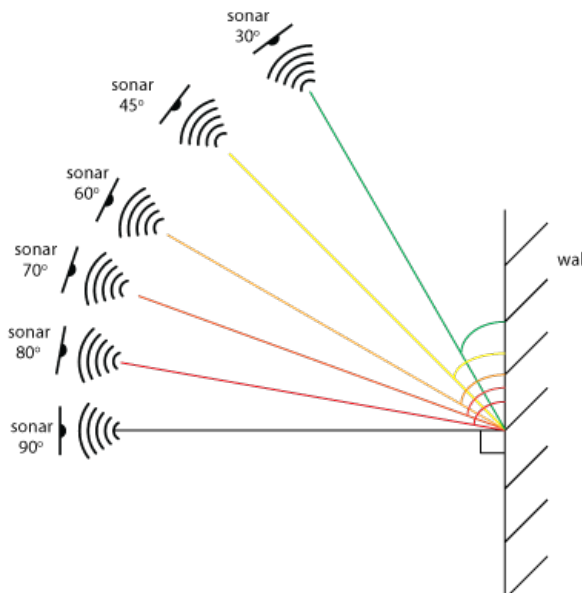


*Fig.C.3 Measured distances in different angles to the wall*

As it is illustrated by the beam pattern, in angles larger than 30 degrees the sensors sensitivity has already been reduced 8 times. The situation deteriorates for angles larger than 60 degrees where the performance of the sonar sensor is unacceptable. The table below (tbl.C.2), based on the experiments, verifies what I have described.

*Table C.2*  
*(Measurements taken in different angles towards the wall)*

Distance (cm)	Angle (degrees)	Measured distance (cm)	Difference (cm)
100	90	98	2
100	80	97	3
100	70	94	6
100	60	90	10
100	45	145	45
100	30	149	49

An additional unwanted behaviour that the SRF02 displayed in the experiments was the wrong measurements due to the beam width. As an example, if the sensor is used in a 1m-width corridor, even though the distance in front will be clear and the wall perpendicular to the sensor, the measured distance will most probably be approximately 124cm. This is clearly illustrated in figure (fig.C.4).

I conducted two experiments that verified this behaviour. The set-ups are depicted in (fig.C.5). In both cases the measured distance were incorrect. The sonar detects the echo by listening for the returning wavefronts. In our case, points that were in periphery and not in the target responded with strong wavefronts and the sonar reported incorrect measurements. Another possible reason could be the phasing effect where the echo does not come from a point source. For example, in the case where a wall is in front of the sensor, not only the central reflection is encountered but also the reflections

from the surrounding area are slightly behind of the central. The sum of all reflections, which the sensor receives, can be either strengthened or weakened by phasing effects. Therefore, if the echo is fainted then it might be the following wavefront that is detected (Robot-electronics.co.uk, 2015).

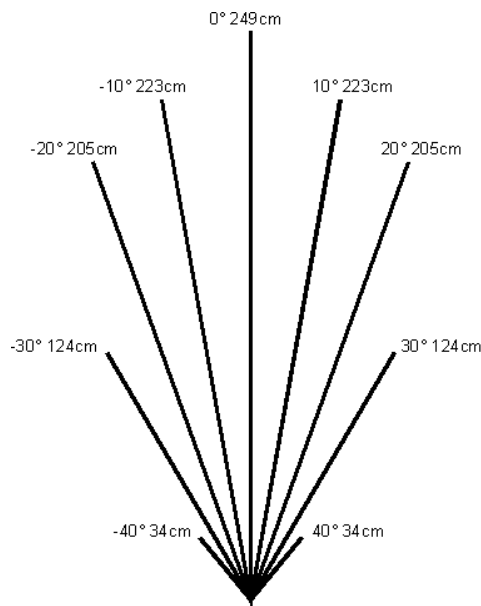


*Fig.C.4 Measured beam pattern for the SRF02 (image from robot-electronics.co.uk)*

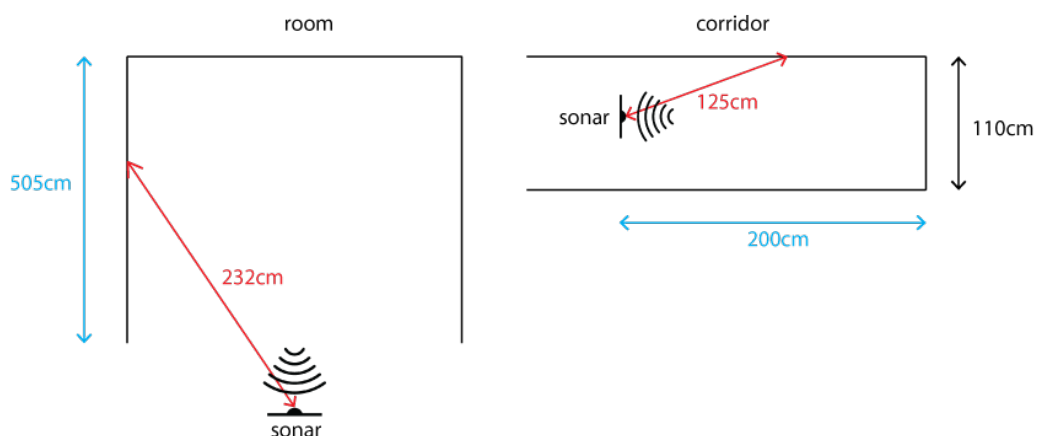


*Fig.C.5 Side lobe points lead to incorrect distance measurements even though the space in front is clear and the reflective surface perpendicular aligned.*

The second experiment using an ultrasonic sensor was to explore its behaviour related to the wind. It is an important factor since it will be used outdoors, mounted on a UAV and the acoustic frequencies might be affected by it. Inside a lab, a simple way to simulate wind was to use a pedestal fan.

Under certain conditions, it produces airflow, not too focused but in a certain directions. I tested the setup with the fan, in highest speed, in different positions related to the ultrasonic sensor. I was cautious enough not to place the fan in a point where it could be identified as an object and thus could alter the results because of the presence of an object and not due to the airflow (fig.C.6).

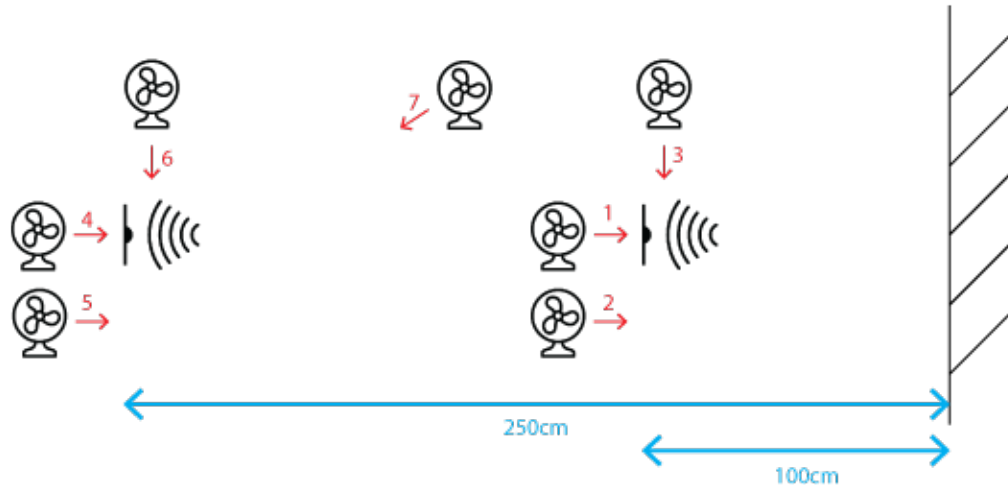


*Fig.C.6 Experiments of ultrasonic sensor with the presence of airflow (the fan was operating at the highest speed)*

The outcomes of the described experiment proved the stability of the sensor in most of the cases (tbl.C.3). More precisely, when the airflow was not directed towards the ultrasonic sensor, the influence was minor (positions 1-6). The only interesting behaviour was observed in position 7. In this position, when the fan was switched-off, the measurement was always 250cm. Whenever the fan was turned on, some of the measurements (approx. 1 every 5) reflected the distance between point 7 and the sensor, including an error. Generally speaking, it seems that the ultrasonic sensor is affected only when the airflow is directed towards the sensor and it is near or inside its sensitivity field. Unfortunately, I couldn't move the fan in many other positions since it was sensed as an object. Moving the sensor to greater distances was not attempted since the sensor itself is prone to side lobes and the measurements would not be stable.

*Table C.3**(Measurements with a source of airflow in different positions and directions)*

<b>Distance (cm)</b>	<b>Position</b>	<b>Measured distance (cm)</b>	<b>Difference (cm)</b>
100	1	98	2
100	2	100	0
100	3	103	3
250	4	248	2
250	5	250	0
250	6	247	3
250	7	249*	1*

## C.2 Infrared sensor

Infrared sensors base their functionality on the emission of light. This sensors use Light-Emitting Diodes (LEDs) as a source of light. The sensor detects a specific light wavelength in the infrared spectrum. Any light with wavelengths longer than 700 nm is called infrared and is not normally visible. The LED produces light at the same wavelength as what the sensor is able to receive. Moreover, it can calculate the distance by measuring the intensity of the received light. For instance, when an object is close to the sensor, the LED light bounces off the object and returns into the light sensor.

### C.2.1 Sharp GP2Y0A02YK0F

The Sharp's infrared red sensor (fig.C.7) consists of an integrated implementation of a PSD (Position Sensitive Detector), IRED (Infrared Emitting Diode) and signal processing circuit. It exploits the triangulation method to detect the distance. Because of that, it is not affected by the environmental temperature and the operating duration.



*Fig.C.7 Infrared proximity sensor Sharp GP2Y0A02YK0F (image from sparkfun.com)*

The key features of the sensor are the following:

- Distance range: 20 to 150 cm
- Analog output type
- Consumption: 5V, 33mA Typ

Various experiments were performed with the IR sensor to test its behaviour in different distances and situations. The conversion between the voltage and the distance is not a straightforward issue. According to the specifications (GP2Y0A02YK0F, 2006), the measurements' characteristics of the output follow a certain graph given in figure (fig.C.8)

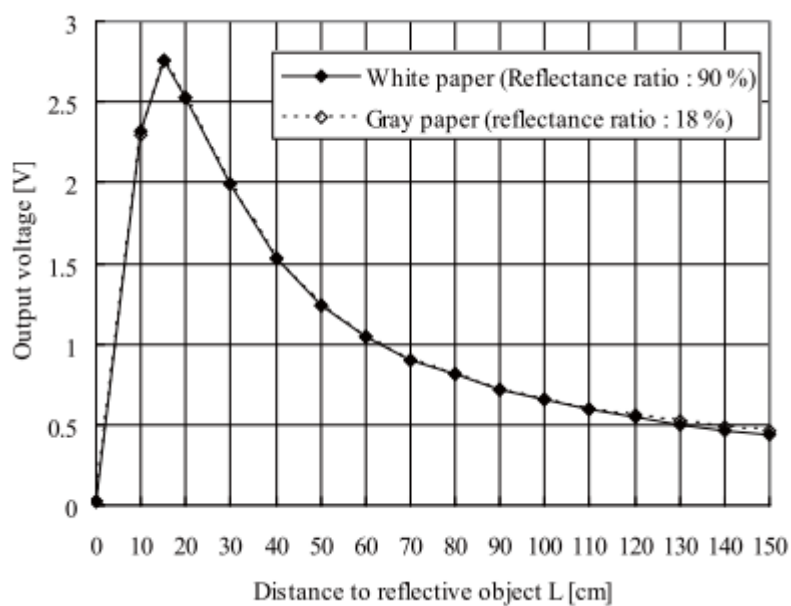


*Fig.C.8 The relation of the output voltage with the distance for the Sharp IR sensor*

(image from (GP2Y0A02YK0F, 2006))

The relation of the output voltage over the distance is not linear. One approach could be to use this graph and attempt to find the best fitting line equation. To facilitate the coding, the output voltage is converted to values from 0-1023, which is the analog reads that the Arduino measures (5v/1024 units). Matlab was used to draw the graph and evaluate the corresponding best-fit equation (fig.C.9). Using a two-term power series model, the estimated equation is the following:

$$V = 3965d^{-0.6257} - 86.46$$

Where V is the output voltage and d is the corresponding distance. An approximate solution of the above equation regarding the distance is the following:

$$d \approx \frac{2.7655 \cdot 10^8}{50(50v + 4323)^{0.593625} \cdot v + 4323(50v + 4323)^{0.593625}}$$

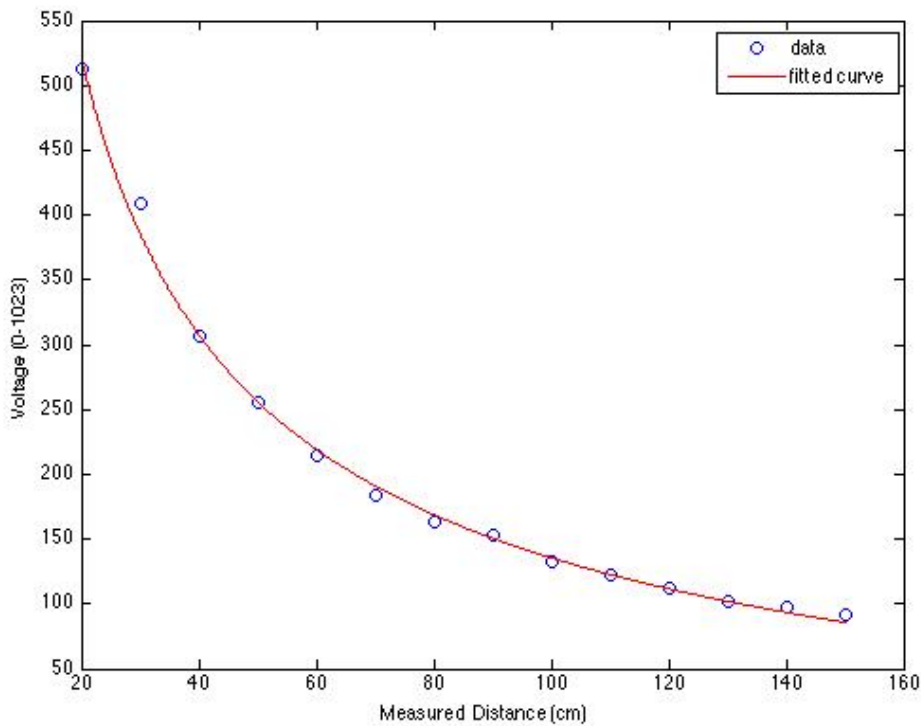


Fig.C.9 Best fit equation for the non-linear relation of voltage and measured distance

Using this equation, a range of measurements was performed as shown on table (tbl.C.4). The set up was the IR sensor pointing towards a yellow wall. The performance was not acceptable. The error in distances above 100cm is huge. This behaviour could be justified because of the following reasons:

- The best-fit approximation in the range from 80 to 150cm is not well adjusted. This happened because the Sharp's graph is not so detailed and minor changes in the voltage correspond to major changes in the distance. Consequently the resolution is poor. Moreover, an approximate solution was used in order to calculate the distance from the voltage since the exact was too complex.
- The specifications mention that it is recommended to stabilize the power supply line, by inserting a by-pass capacitor of  $10\mu F$  or more between  $V_{cc}$  and GND. Unfortunately, it was not implemented.

*Table C.4*

*(All measurements taken with a surface perpendicular to the sonar)*

Distance (cm)	Distance measured (cm)	Difference (cm)
13	18	(Dead zone)
30	30	0
50	53	3
80	89	9
110	128	18
140	164	24

Similar behaviour with the sonar was observed in the cases where the objects were not perpendicular aligned with the IR sensor. In addition, an influencing factor was the reflectivity of the object. For example, white paper has a reflectance ratio of 90% while grey paper 18%. This is particularly important for distances above 110cm where the sensor's resolution is poor.

In conclusion, the performance of the sensor could be improved if a voltage to distance graph made from scratch and not based on the one shown in the specifications. This would facilitate accurate correspondences between the pairs instead of having to guess from the graph, especially in the low-resolution part. In addition, since it is analog, the output is depended of the stability of the input voltage and the flatter is the input the less noise will be present in the output. Nevertheless, the range of the IR sensor is very restricted and since it is not suited to the UAV applications, it is not worth spending more time on it.

### C.3 Optical flow sensor

Optical flow sensors are mainly utilized to provide precise measurements of ground speed and therefore the position of mobile robots. They are particularly useful in GPS denied environments allowing long-term dead reckoning navigation.

#### C.3.1 Px4flow smart camera

One of the first attempts to use this type of sensors in the UAVs was based on mouse sensors. The mouse sensor returned the average movement of the visible surface's features. In order to convert these values into real distances, which correspond to the movement, the altitude should be known. By combining the measurement of a barometer or an ultrasonic sensor, this distance can be calculated. Other factors that affect the optic flow are the vehicle's roll and pitch changes. If these rotations have known values, reported from the IMU for example, it can be introduced to the calculations and provide the correct distances covered.

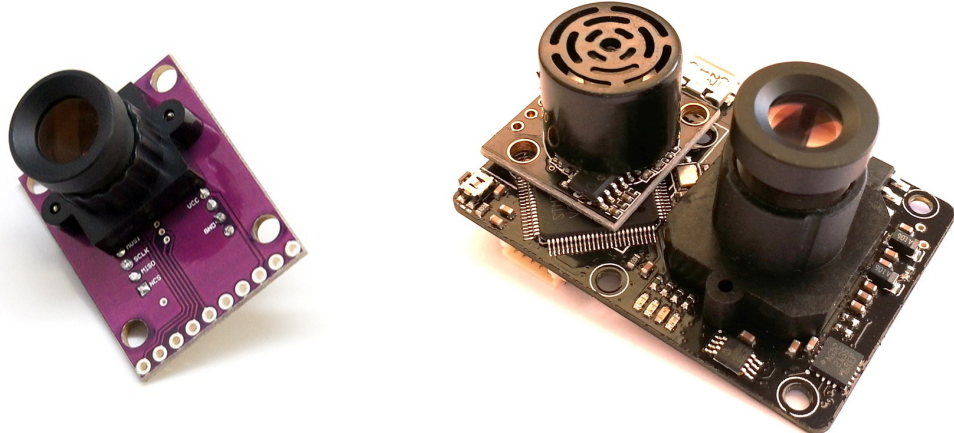


*Fig.C.10 Mouse-based optical sensor and p4flow smart camera (images from [copter.ardupilot.com](http://copter.ardupilot.com))*

The main disadvantages of using mouse-based optical flow sensors are the following:

- They operate satisfactorily only in well-lit environments. In typical indoor and outdoor low-light conditions, their practical use is limited.
- They need additional devices to be present such as sonar and IMU to have all the required data for the calculations.
- They require a fast MCU (microcontrollers) for the calculations. The flight controller is already used and loaded with the coordination operation of all the other connected devices.

A highly improved optical flow sensor that can support more advanced operation scenarios is the px4flow (fig.C.10). The main features that improve its functionality can be summarized as follows:

- It has a CMOS image sensor with a  $752 \times 480$  resolution having a very high light sensitivity.
- It is equipped with an ARM Cortex M4 CPU customized with a special imager bus peripheral for real-time image processing reaching a maximum rate of 250Hz in optical flow calculations.
- It has a high precision on-board gyroscope to compensate angular velocity.

- It is equipped with an on-board ultrasonic range sensor to measure the distance towards the surface and to scale optical flow values to metric velocity values.

Up to this point I have explained that the optical flow sensors can measure the ground speed or translational velocity. This is based on the following equation:

$$v_{trans} = v_{optic} \frac{Z}{f}$$

where Z is the current distance to the scene, f the focal length and  $v$  the optical flow. It is assumed that the rotational velocity is either zero or known, measured by the gyroscope. An interesting aspect of this equation is that it can be used to calculate, with high accuracy, the altitude instead of the translation speed if the latter is known. The ground speed can be known either using the GPS or the airspeed measurements.

Before moving to the experiments regarding the px4flow smart camera it is important to cite some restricting factors of the optical flow sensors in general. The optical flow equation (OFE) is defined as:

$$I_x v_x + I_y v_y + I_t = 0$$

where  $I_x$ ,  $I_y$  and  $I_t$  are the spatial and temporal derivatives, respectively, of the image sequence  $I$  at a given point, and  $(v_x, v_y)$  is the 2D velocity at that point. The underlying model on which OFE is based on is that the luminance remains constant between frames along the motion trajectory, so that the total derivative of the image function is zero, hence the OFE. The OFE is one equation with two unknowns,  $v_x$  and  $v_y$ . Hence further constraints are needed to obtain a solution. The Lucas and Kanade method (LS) makes the assumption that the motion field within a small window is constant and this constraint is used with the OFE to construct a least squares problem and

hence estimates of the vector  $(v_x, v_y)$ . All points in the region are assumed to have the same velocity, hence giving multiple equations in 2 unknowns, enabling a LS solution to be obtained. All in all, the method should work well within textured regions with anisotropic intensity variation, which means changing in all directions, and in which the motion is locally constant and can be approximated as such.

There are various tests that can be carried out using this sensor. They can be divided to two categories, tests related to the ground speed estimates and tests related to the altitude. Unfortunately, for the first category the testing configuration is rather complicated compared to the other sensors. The best way to assess the ground speed is to compare them with data computed using a VICON motion tracking system. Alternatively, the ground speed can also be compared with the corresponding values obtained using an on board GPS unit. Considering that the calculated ground speed will not be exploited from the radiation mapping UAV and that the testing is time consuming, it was decided not to proceed with this procedure. However, the device will be part of the configuration for the UAV's altitude hold mode and as such is going to be tested for the purposes of my project.

The px4flow device is equipped with a high quality ultrasonic range finder, the Matbotix HRLV Maxsonar EZ4. The specifications cite that it supports 1 millimetre resolution having a maximum range of 5000mm and a dead zone at 300mm. The special property of EZ4, which makes the difference from the competitors, is the narrow beam width providing the least sensitive to side objects. Consequently, the HRLV-MaxSonar-EZ4 is a very good choice when only larger objects need to be detected since it may ignore some small and medium targets. Another advantage of using the EZ4 is that it provides the most noise tolerant acoustic sensitivity compared to the other ultrasonic sensors of the same category. The Matbotix EZ4 range finder supports three different interfaces, analog Voltage, RS232 Serial and Pulse Width. However, since the sensor is part of the px4flow, the commination has to be accomplished through this. As it is described in the special section "Sensors

Circuits", I utilize two individual ways to access the data, Adruino microcontroller and ROS packages.

Similarly with the Devantech SRF02 sensor I conducted various experiments to verify the accuracy of the sensor (tbl.C.5). The setup of the experiment was the sensor facing a wall in the perpendicular direction. The measured distances were very precise. Above a dead zone of the 30cm, the performance was excellent. A very interesting aspect in the behaviour of the sensor was the narrow beam width. I repeated the same corridor test like with the SRF02. It is very impressive that the EZ4 sensor was measuring the correct distance till the value of 350cm (fig.C.11).

*Table C.5*

*(All measurements taken with a surface perpendicular to the sonar)*

Distance (cm)	Distance measured (cm)	Difference (cm)
25	30	(Dead zone)
40	40	0
60	60	0
100	101	1
150	151	1
200	201	1
300	301	1



*Fig.C.11 Matbotix EZ4 tested in a corridor experimenting with the beam width.*

## C.4 Laser sensor

Laser sensors belong to the high-end devices of the proximity sensors. They are more expensive than the others but they offer higher ranges with enhanced accuracy. Unlike infrared LED sensors, the semiconductor laser emits light from a very tiny area in only one direction and at one wavelength or a few closely spaced together.

### C.4.1 LIDAR-Lite

PulsedLight's laser is an innovative device. It offers competitive features in low price, compared to other laser sensors, and with the ease of I2C or pulse width modulation (PWM) connectivity. According to the specifications, it supports up-to 40-meter range capability with 2.5cm accuracy, 1cm resolution and fast acquisition rate equals to 50Hz. In addition, it has a small size, low power consumption and it is lightweight (fig.C.12).

In the manufacturer's site it is stated that the success of the LIDAR-Lite is based on the specific implementation. They use a customised version of the Time-of-Flight distance measurements approach, originating in military applications. These systems transmit relatively high power infrared pulses using a laser diode. The distance estimation is accomplished by measuring the time delay between the transmitted pulse and the detected return pulse. In general, it is a long-range operation with low accuracy. In order to improve the accuracy of these systems they had to use signal processing. The challenge was to avoid complex and expensive hardware to achieve this as other existing systems implement it. PulsedLight manage to develop a signal processing technique using a simple approach without the complexity and cost of direct analog-to-digital conversions (Technology Brief, 2015).



*Fig.C.12 LIDAR-Lite Laser Rangefinder (image from sparkfun.com)*

The experiments of the sensor was conducted in various distances and angles. In the first table (tbl.C.6), where the reflective objects were aligned perpendicular, the performance followed the specifications, showing accuracy close to 1-2cm. In greater distances like the 10m, I should admit that even my verification method, using a tape measure, was error-prone so the accuracy is negotiable but in favour of the device. Especially for the 10m measurement, it should be mentioned that it was conducted in a corridor (1.1 meters wide). Consequently, in contrast with the sonar where the wide acoustic lobe is problematic, laser sensors have a concentrated beam and perform uninfluenced of the location's shape.

*Table C.6  
(Reflective objects are perpendicular aligned)*

Distance (cm)	Distance measured (cm)	Difference (cm)
30	34	4 (close to dead zone)
60	60	0
100	100	0
250	250	0
400	402	2
500	501	1
1050	1040	10
> 4000	0	NaN

Another useful aspect that emerged from the tests was the behaviour regarding the material of the object and the hit angle. The following table (tbl.C.7) shows that glass degraded the performance only when the beam was hit in angle. On the other hand, when the material was concrete the hit angle was not an influencing factor.

*Table C.7  
(Measurements in different angles and materials)*

Distance (cm)	Angle (degrees)	Material	Distance measured (cm)	Difference (cm)
100	90	Concrete	100	0
100	45	Concrete	101	1
100	90	Glass	101	1
100	45	Glass	135	35

To conclude with, LIDAR-lite showed an impressive performance compared with the previous tested sensors. It offers a long range, good accuracy and its behaviour is not restricted to the surrounding environment.

## C.5 Applications

An interesting and creative task is to use the sensors to build more complicated and useful devices, which can be used in localization and navigation applications in robotics. The most versatile and promising sensor to use from the previous presentations is the LIDAR-Lite. The px4flow was delivered as an autonomous operating package ready to use and does not allow any space for modifications.

The LIDAR-Lite is a reliable laser sensor having high reading rate and accuracy. It can be used as a simplified version of a lidar that essentially provides laser scans. To leverage the full features of the LIDAR-lite, I needed

to combine it with a microcontroller and a servomotor. The most popular choice was to utilize an Arduino Uno with a small yet classic servo in inexpensive robotic applications Hitec HS-422 Deluxe (fig.C.13).

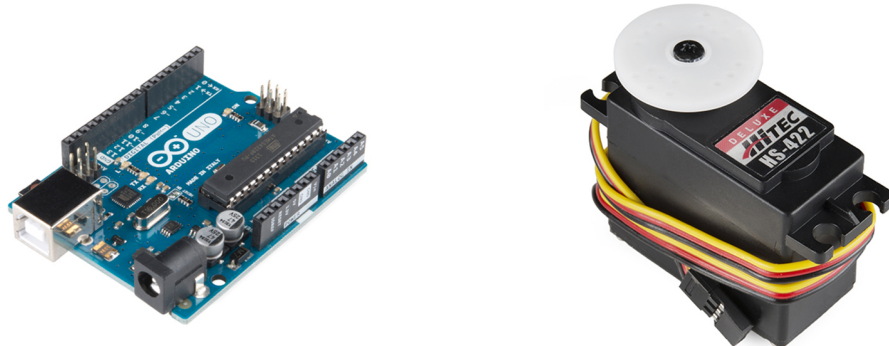


*Fig.C.13 Arduino Uno and Hitec's HS-422 Deluxe (image from sparkfun.com)*

### C.5.1 Mapping application

One of the most common applications of a laser scanner is the mapping. To map the surroundings, I need a servo to rotate the laser in continuous angles and measure the related distances. In order to accomplish this task the laser was mounted on the servo using a specific bracket (fig.C.14). This mechanical construction was pretty stable although the integration of 3D printed case could offer a more compact design for easy use in robotics applications.

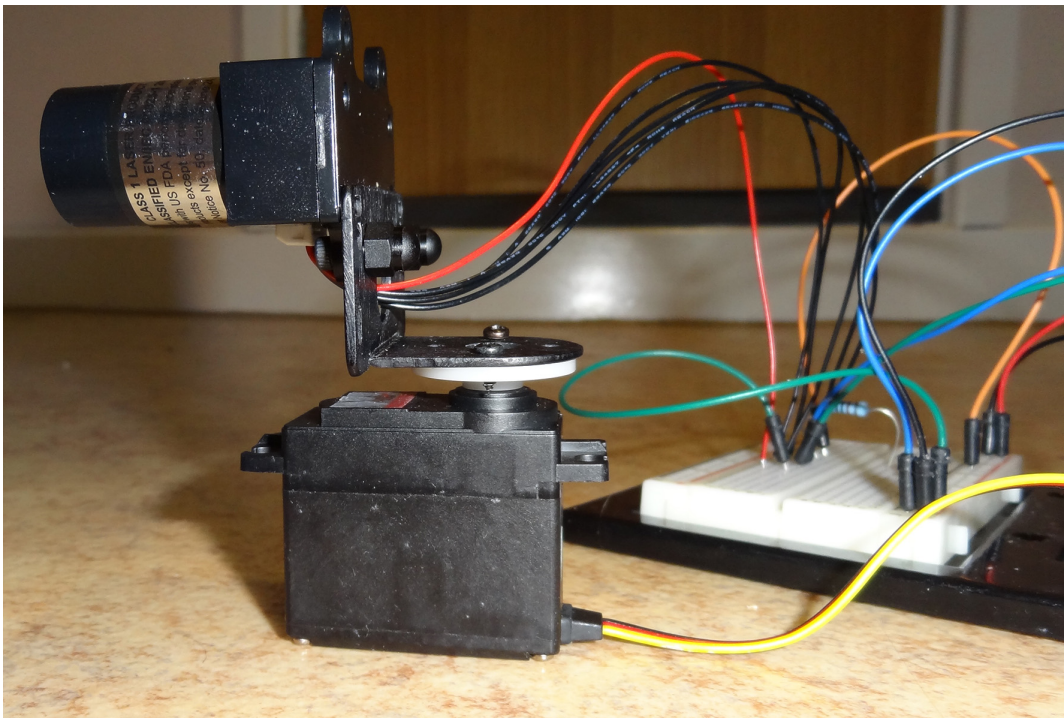


*Fig.C.14 Mapping device consists of a servo, a mounting bracket and a laser sensor*

The structure of this task consists of two working parts (fig.C.15). For the first part an Arduino sketch has been developed which is responsible for the following functions:

- To read the angle of the servo
- To measure the related distance. More precisely, it gets two measurements and provides the mean value of them so as to avoid a fair amount of noise.
- To send both data to serial port with a rate of 9600bps

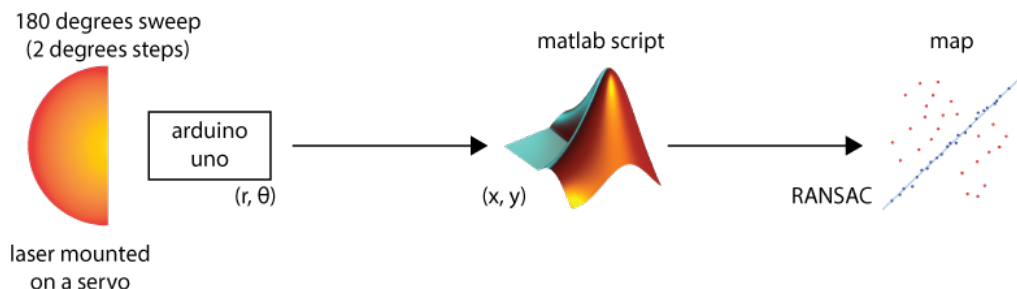


*Fig.C.15 The logic flow of the proposed mapping algorithm*

This part is attached to the hardware and utilizes the microcontroller to gather the useful information and transmit it to the other end for processing. The servo rotates the laser forward and backward by 180 degrees. Every 2 degrees it stops and performs the tasks I have previously described. Consequently in a loop, the total number of readings is equal to 180, the first 90 taken during the anticlockwise transition from 0 to 180 degrees and the remaining 90 during the clockwise rotation.

On the other side, a Matlab script has been developed as a client. This script takes input from the serial port using the USB, which is connected to the Arduino Uno. Particularly, the script accomplishes the following tasks:

- Reads the angle and the related distance
- Filters values outside the LIDAR-Lite range
- Converts from polar coordinates to Cartesian, x and y
- Feeds the points to a RANSAC method to detect potential lines in the data.

This script exploits the measurements to yield useful patterns in the space that could be the base of a map. It makes use of the random sample consensus (RANSAC) algorithm (Fischler and Bolles, 1981), which is an iterative method to estimate parameters of a mathematical model from a set of observed data, which contains outliers. The assumption is that the data consists of inliers and outliers. By referring inliers I mean data whose distribution can be explained by some set of model parameters. However, inliers are expected to be noisy. On the contrary, outliers are data that do not fit the model.

For the estimated lines the following balance should be kept:

- Enough lines to describe details of the environment. Consequently, the total points should be divided into subgroups and feed the algorithm individually.
- Elimination of repeated lines of the individual subgroups of points that give the same equation. In order to avoid that, the implemented approach

discards the lines, which have less than 5 degrees difference in the direction.

A sample of the mapping output is illustrated in (fig.C.16). In this case the mapping device has been placed in the middle of the room. Since the device covers 180 degrees, the output should look like a  $\pi$  (pi). The outcome of the mapping approach is similar to the expected one for this simple case.

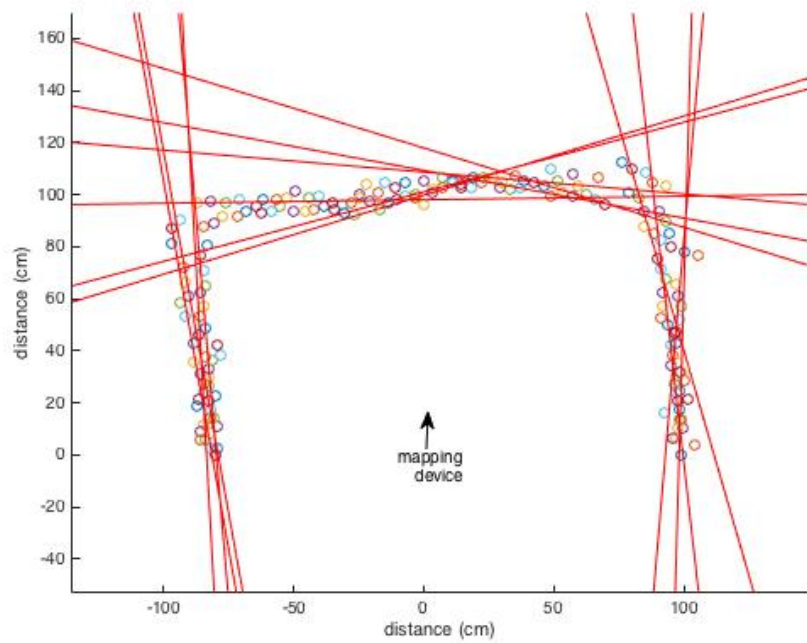
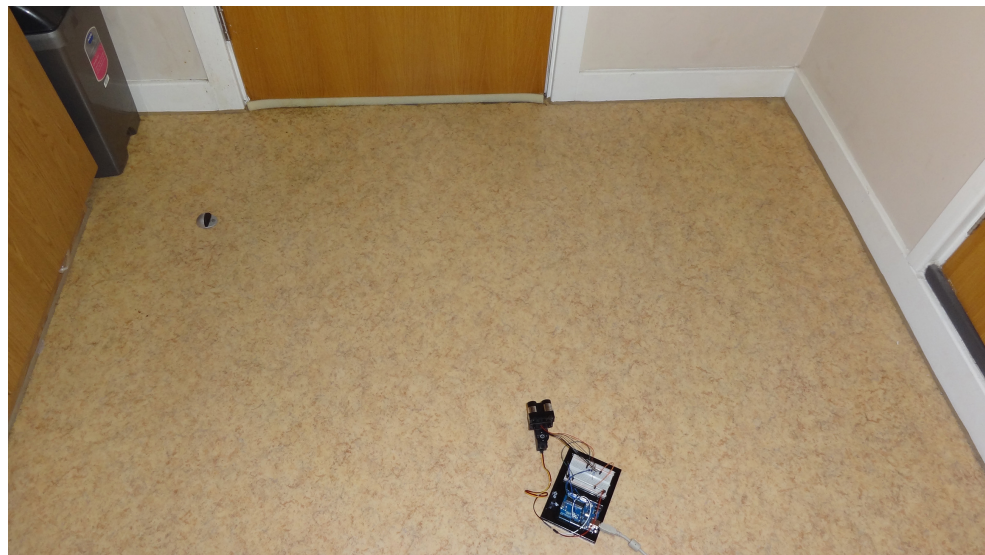


*Fig.C.16 The setup of the experiment and the outcome of the mapping algorithm*

The required code, both for Arduino IDE and Matlab, as well as the circuitry is available in the “Sensors Circuits” section.

### C.5.2 Proximity application

For this section, and after having implemented a simple mapping algorithm, I wanted to develop a ROS enabled application ready to be employed in any compatible system. My initial plan was to deploy a LIDAR-like application where the laser sensor would continuously rotate and transmitted, via a topic, an appropriate sensor message of type *sensor\_msg/laserScan*. Although I put a lot of effort into it, this was not feasible, mainly due to the instability of the system. More precisely I encountered the following problems:

- The Arduino memory was 80% occupied by loading only the required libraries (*ros.h* and *i2c.h*), leaving limited space for the working sketch.
- The power source was overused since both laser and servo were fed from the 5V output of the Arduino Uno.
- The servomotor under complex and tedious continuous translation was drifting sometimes and in addition it couldn't provide an absolutely stable cycle to compose the *laserScan* ROS message.

The combination of the laser sensor and the servo driven from an Arduino Uno controller was not adequate to support such a complex and precise task and provide the expected reliability. As an alternative, since I wanted to develop a working ros-enabled sensor, I utilized the existing hardware configuration to deploy a proximity sensor. This sensor provides three distances, the front and the sides ( $0^\circ$ ,  $-90^\circ$  and  $90^\circ$ ). To improve the accuracy, in every position the laser sensor measures the distance twice and returns the average. In my attempt to implement more complex scenarios, like sweep ranges of 20 degrees for every main direction, I faced drifts and synchronisation problems. Consequently, I kept the design simple and reliable for the given hardware.

One of the great features that ROS provides is the ability to utilize in robotics systems simple and cheap sensors using the Arduino microcontroller. It exploits the fact that the Arduino is connected to the computer using a serial connection and data is transmitted using this port. Providing a specific interface package called *rosserial*, it allows transmission and reception of ROS messages by coding Arduino IDE sketches with just including the ROS library. The entire flow of the information from the laser sensor to the published topic is summarized in the following figure (fig.C.17)

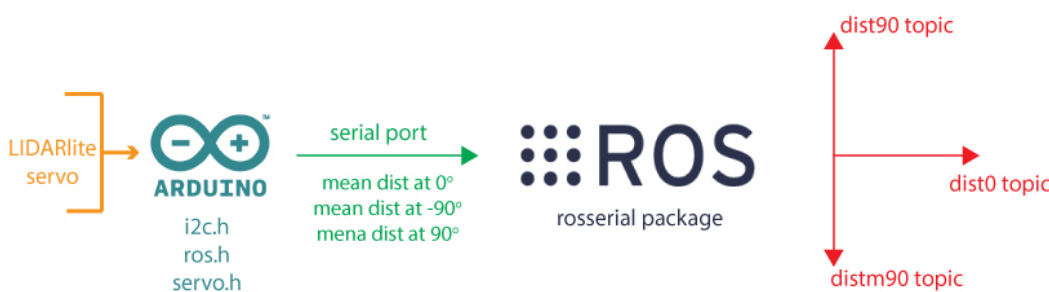


Fig.C.17 The flow of the information for the proximity application algorithm

Since I had already found the pathway that I had to follow, the implementation was straightforward. On the Arduino side the sketch included specific ROS commands. More precisely, aside from including the servo and the I2C libraries, this time the ROS library was added in complementarily. By doing this, I could declare in the Arduino IDE objects like ROS nodes and publishers. Consequently, I declared three publishers, one for every measured direction. For every publisher, an appropriate message was transmitted with a rate between 0.5 and 1Hz, as explicitly measured with convenient time function. This unstable period was one reason why I couldn't compose a laserScan message, since for this type of messages, it is a requirement.

It is also worth citing the different approach that I followed for the movement of the sensor. Unlike the mapping application, this time I did not use the convenient servo methods *write* and *read*. For this specific task I wanted total control and accuracy of the movement. With the given controller this

could be feasible with a simple scenario. To move the sensor accurately, in the three directions, as fast as it was possible without drifts and lost of synchronisation I had to use the *writeMicroseconds* method. The signal consists of positive going pulses ranging from 544 to 2400uS long. The servo positions its output shaft in proportion to the width of the pulse. At the beginning, I discovered the exact values for the 0°, 90° and 180° or in the -90°, 0° and 90° according to the measurement device frame (heading). After the calibration, I investigated the synchronization issues related to the time that it allowed the servo to move before issuing the next move command. I optimized to the shorter interval without having instabilities. As soon as the servo had moved to the desired position and the laser ha estimated the average distance, the microcontroller emitted the distance by publishing a message to the specific topic.

As I have described so far, the ROS topics are composed by the Arduino and are transmitted. However, the last stage -in order to have a working system- is to employ the *rosserial* protocol. There is a need for a specific protocol for wrapping standard ROS serialized messages and multiplexing multiple topics and services over a character device such as a serial port or a network socket. In my case, I needed to execute the serial node python script, having as input the USB that the Arduino was connected to. After that, the proximity topics were visible in the entire ROS ecosystem.

To validate the implementation, I tried out the device at the end of a corridor (fig.C.18). As can be seen in the table (tbl.C.8) the measured distances lie inside sensible margins. It is clear that the deviation from the case where I tested the laser sensor in a static setup was greater but still usable in proximity check approach. One additional issue that I noticed was the degradation of the accuracy when I increased the servo speed. This had occurred not because of the laser sensor, since it had a high operating rate (~50Hz), but mainly because of the instability and drift of the servo.

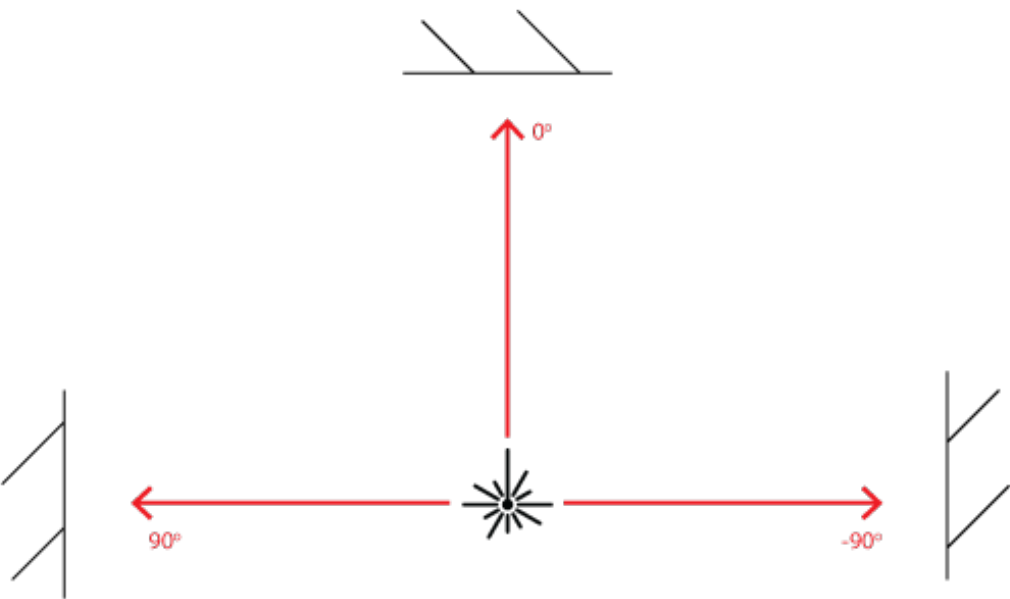


*Fig.C.18 The set up of the experiment for testing the proximity application*

*Table C.8*  
(Measurements in the three individual directions)

	Distance Measured (cm)	Distance (cm)
<b>dist0</b>	52, 57, 55, 54, ...	55
<b>dist90</b>	77, 79, 78, 81, ...	79
<b>distm90</b>	84, 86, 87, 88, ...	86

By following this implementation I created a ROS enabled device that could act as a laser proximity sensor. It is a feasible system since the housing of the device can be easily designed and composed in a 3D printer. In terms of the microcontroller, there is no need for an Arduino Uno since an Arduino Nano v.3.0 (45mm length and 18mm width) can effectively do the work. This is because both of them are based on the ATmega328 chip, which provides 2 KB of SRAM and 1 KB of EEPROM. The circuit with the Nano board was implemented so as to test the behaviour and the stability in reality (fig.C.19). In essence there was no difference in the behaviour compared to the Arduino Uno. The main difference was in the available power to drive the servo and the LIDAR-Lite and a compatibility issue. More details about the implementation can be found in the “Sensors Circuits” part. To conclude, it is

possible to have a compact and simple design that can report three accurate distances in a reasonable rate.

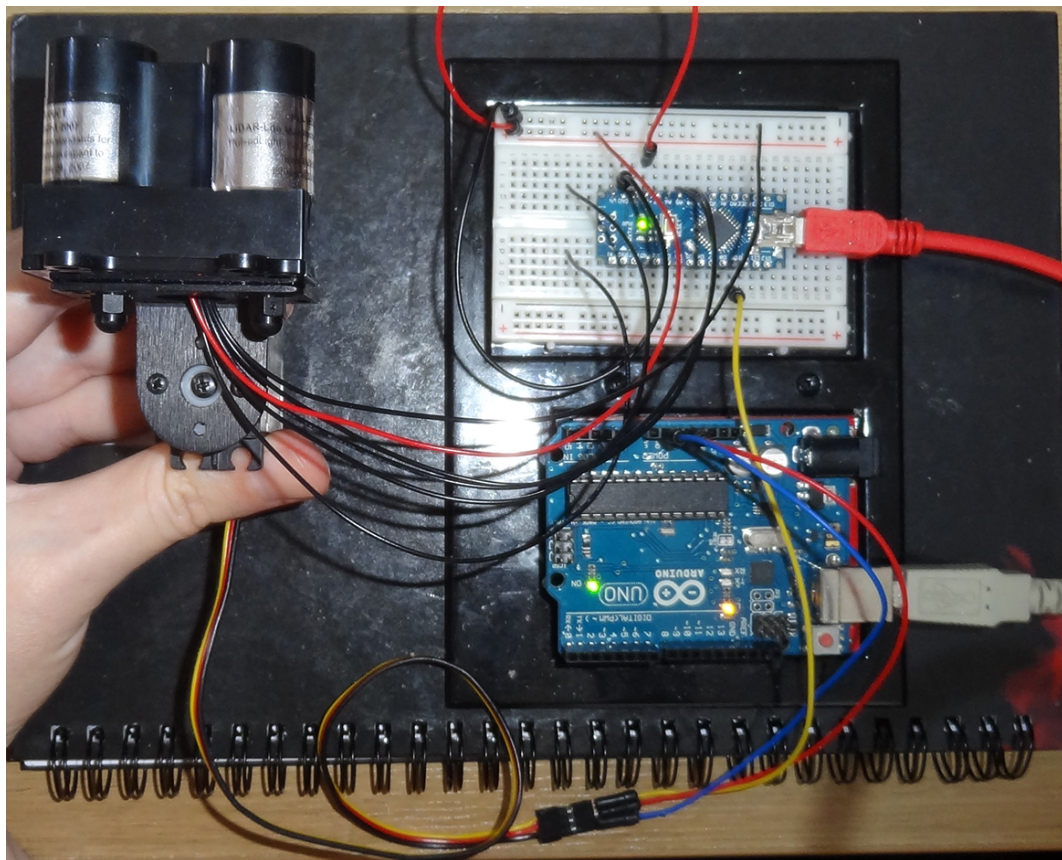


*Fig.C.19 The proximity application implemented using an Arduino Nano board. In this picture Arduino Uno feeds only the  $V_{dc}$  and GND pins of the servo*

## Part D

# Simulation

### D.1 Introduction

Simulation in Unmanned Aerial Vehicles is a very broad topic. It mainly depends on the application which is under testing. There are different simulators if the operators need to learn how to fly a UAV compared to the ones that are useful for the engineers to help them design an effective chassis. In my project's case, I need a simulation in order to investigate the behaviour of developed applications in certain circumstances. The key features that I needed were the following:

- A realistic UAV simulation in terms of the physics and dynamics that applied.
- Ability to utilize different types of sensors and customise their specifications.
- Ability to build custom landscapes and test the behaviour of the algorithms for various different cases.
- Be as close as possible to the structure of a real UAV in terms of the flight controller, to the input commands for navigation and to the individual devices from which it is built, like the global positioning system (GPS) or the inertial measurement unit (IMU).
- The ability to apply the developed algorithm to a real UAV with minor modifications.

After an extended research of many available approaches, all the aforementioned requirements lead us to a specific solution, which is the combination of ROS and Gazebo. Some of the solutions that were explored but were rejected were the following:

- Building a custom simulation from scratch using Matlab. During the second semester there was a related unit that gave us the opportunity

to build a simple UAV simulation. However, it was assumed that the UAV moves in 2D and it did not simulate the flight dynamics of the UAV. Generally speaking, the simulation was intended to test UAV swarm robotics algorithms. Consequently, the effort to build a simulation in this way from scratch was a time consuming procedure with uncertainty about the effective fulfilment of the requirements.

- Available simulation found on Internet based on Matlab and Simulink. There are several simulations of this type and a possible approach could be to adapt one of those and customise it. Most of them have been built as master or part of PhD theses. The disadvantages of using them are that they are primarily focused on simulating the dynamics and they do not include sensors. Moreover, they do not offer a build in feature of designing realistic landscapes. In general, depending on the quality, most of them have poor comments on the code and most importantly they do not offer support. Consequently, this solution was ineffective since it may have meant debugging others' code rather than building creative tasks.
- There was the possibility to use Webots (Cyberbotics.com, 2015). This is a development environment used to model, program and simulate mobile robots. It offers the choice of using a wide range of simulated sensors and actuators. The robot behavior can be tested in physically realistic worlds. It is a popular tool for research, well documented and continuously maintained for over 18 years. The reason why it was not adopted in my research was that it is not free of charge. It offers a 30-day trial version but after this period a valid license should be acquired.

In short, various approaches were considered for simulating a UAV executing different behavioral algorithms. The most promising and professional way seemed to be using the combination of ROS and Gazebo. Following this method in order to carry out my experiments finally proved a successful decision considering the outcomes of my research.

In the “Simulation Topics” appendix there is a section related with a general description of ROS, Gazebo as well as a terminology section, which is extensively used in the remaining of this chapter.

## D.2 UAV package

When using ROS and Gazebo in robotics simulation what the roboticist want to avoid is the reinvention of the wheel. Therefore having these tools installed and working, the users could utilise packages that implement UAVs equipped with all the required features. Depending on the application, there are UAV implementations available which have many common characteristics but also differences that help us when decision making. For my project, I explored the following three packages:

- Tum simulator

This package ([goo.gl/ZBjaAY](http://goo.gl/ZBjaAY)) contains the implementation of a Gazebo simulation for the Ardrone 2.0 (fig.D.1). It is a nice simple quad-rotor simulator developed at the Technical University of Munich. The simulator supports both Ardrone 1.0 and 2.0 versions but it is optimised for the latter. It has a built-in support for joystick manipulation, which means that the users can use it to fly the real drone as well as the simulator. The Tum-simulator is equipped with 2 cameras, one front and one bottom and a height sonar sensor.

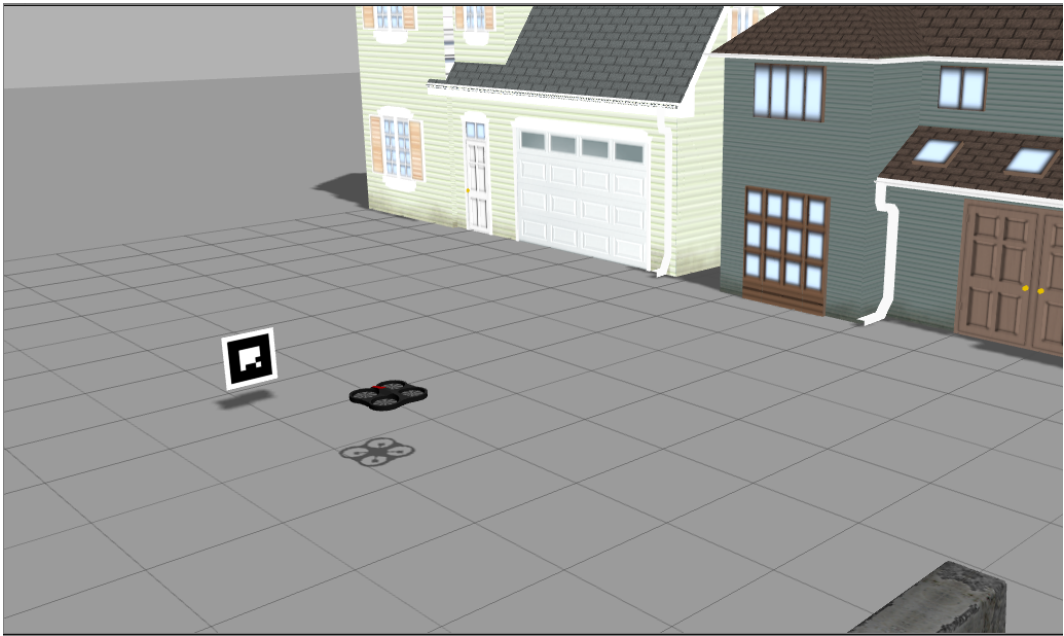


*Fig.D.1 Tum simulator in action (image from answers.ros.org)*

There are two reasons why this simulator was not adapted in this project. Firstly, it is executable in ROS Fuerte released in 2012, four versions older compared to the current. After this version, ROS changed completely the low-level built system macros and infrastructure (catkin). Consequently, I wanted to avoid working with an outdated framework, which would downgrade all the other tools to ensure compatibility. Secondly, the provided sensors are not suitable for my project. This simulator is more focused on computer vision applications where the users capture video from the cameras and process data, using for example OpenCV, to make navigation decisions. There is always the choice of adding or developing custom sensors but it is safer to find a simulator that already integrates them.

- **PX4 SITL**

This simulator developed by PX4 Autopilot Project for the software in the loop simulation (Pixhawk.org, 2015). The ROS SITL setup allows the users to run certain PX4 Firmware modules, which use the multiplatform wrappers within ROS. These applications publish data in the related ROS topics. The PX4 simulator is compatible with ROS Indigo, which is a very recent ROS version. Likewise the previous, it allows joystick manipulation. It is

noteworthy that includes two UAV simulators, one based on Ardrone and the other on Iris (fig.D.2).

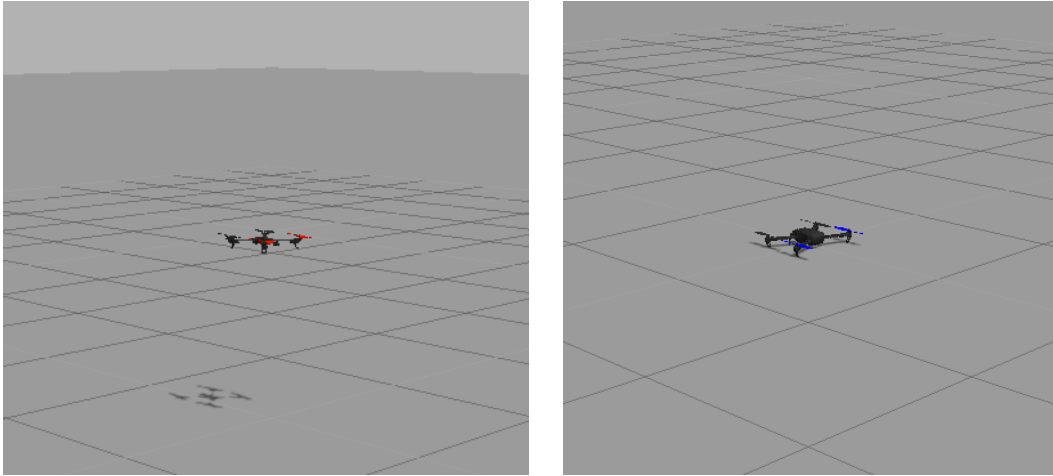


*Fig.D.2 PX4 SITL simulation using Ardrone and Iris UAVs in action*

The additional characteristic that this simulator includes, compared to the others, is the MAVROS (Micro Air Vehicle ROS) package. This package provides a communication driver for various autopilots with MAVLink communication protocol. In addition, it provides UDP MAVLink bridge for the ground control station. Using this protocol ROS can send specific commands to the UAV, which is essentially what this simulator is specialised for. To illustrate this, using ROS in a companion computer, navigation commands can be sent directly to the flight controller produced by a robotics algorithm via MAVROS. This is called off-board control. This simulation is intended for those cases where the users want to test the MAVROS commands before applying them to the real UAV.

Since it is actually a port of the PX4 flight stack in ROS, it is a high fidelity simulation coming with plenty of capabilities like real UAV. For example, in order to begin it is required to arm. Some of the available features provided are:

- Inertial measurement unit (IMU) which provides linear acceleration, angular velocity, atmospheric pressure and altitude
- Compass which provides heading

- GPS which provides longitude, latitude and altitude
- PX4flow optical flow sensor which is integrated to provide ground distance
- Manual set of the motor speed for each individual motor

There are reasons why I did not select this simulator for my task. Firstly, it has some problems when I used it in combination with the RViz, the ROS visualization tool. This is the all-seeing ROS visualisation utility. This tool becomes very important when there is a need for customisation of the sensors since it visualises the laser scans and the ultrasonic lobes. Secondly, it did not include laser or ultrasonic sensors and my preference was to have them integrated to avoid misconfigurations because of my short experience. Thirdly, that fact that it is equipped with MAVROS and includes highly detailed UAV configuration, it introduces an unwanted complexity for performing behavioural analysis of navigation algorithms. As I already explained, from my perspective the PX4 SITL is focused on different tasks compared to my requirements.

- Hector quad-rotor

The Hector quad-rotor simulator is a framework that implements the simulation of quad-rotor UAVs employing ROS and the Gazebo simulator (fig.D.3). It is developed by the Research Training Group in Darmstadt Technical University (Meyer et al., 2012). The dynamics model of the quad-rotor has been parameterized using wind tunnel tests and validated by a comparison of simulated and real flight data. It is available for all the latest ROS versions from 2012 and on (Fuerte, Groovy, Hydro and Indigo).

Hector quad-rotor comes with a wide range of available sensors. It is equipped with an Inertial Measurement Unit (IMU) measures the angular velocities and accelerations of the vehicle's body in the inertial frame. It provides ultrasonic sensor to measure the distance from the ground in a specific range. In addition, it has a Magnetic Field sensor to measure the heading of the UAV. A GPS receiver is also installed to provide pseudo range

measurements. Aside from the standard devices, it also offers additional and more sophisticated ones. More precisely, it provides the Hokuyo UTM-30LX as laser scanner, a depth camera like Kinect and a normal camera. Furthermore, like all the other simulators, it is possible to manipulate it using joystick (like x-box controller) as well as keyboard.

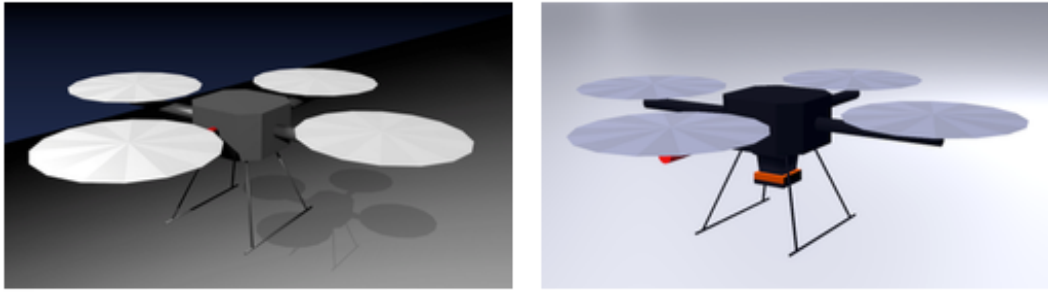


*Fig.D.3 The Hector quad rotor model with a Hokuyo UTM-30LX laser scanner mounted in the second picture (image from (Meyer et al., 2012))*

The Hector quad-rotor is delivered as a ROS stack, which means that is a collection of packages and not only a single one. So, aside from the packages that are responsible for the modelling, the control and the Gazebo simulation of the UAV, it also includes a visual SLAM (Simultaneous Localisation and Mapping) package to demonstrate the great potentials to build robotics applications.

Hector quad-rotor combines all the types of the sensors, which I wanted to employ in my simulation in a well-structured package, as complex as it is required for a comprehensive realistic simulation. Everything is located in the place where I expected to find it. This enabled me to customise the configuration and move it closer to my real setup. It is also well documented with many related questions in the ROS support forums. My working system is configured in ROS Hydro version with all the related tools working flawlessly like RViz. The same implies in the ROS Indigo as well. All in all, from my experience with working with it, it is a reliable and stable tool that helps to focus on the details of the developing robotics applications leaving away all the other distracting points.

### D.3 UAV configuration in simulator

The rich features of Hector quad-rotor package were utilized for simulation in the current project. In order to build a UAV close to my working scenario, I needed to refine the sensors positions and operation. The selection and the settings of the sensors were based on the available equipment I had for the real UAV.

From the available sensors provided in the hector UAV I utilized the following:

- IMU

The IMU was exploited to report the heading of the UAV (yaw angle). An alternative method to obtain this value was the Magnetic Field Sensor (the compass).

- Sonar

The ultrasonic sensor transmits short ultrasound impulses. Sonar reports the distance corresponding to the first echo returned from the ground or any other object within its FOV (Field Of View). The comprehensive way that the simulator was built allows modifying all the related parameters of the ultrasonic sensor. More precisely, in the file ([goo.gl/RCZ1u8](http://goo.gl/RCZ1u8)) the users can change the following characteristics:

- Update rate (in Hz)
- Minimum and maximum range (in m)
- The name of the published topic
- The position, the orientation and the parent frame link in which is attached

If the users want to experiment with more advanced characteristics, using the parameters inside the file ([goo.gl/dalwSo](http://goo.gl/dalwSo)), they can alter parameters such as resolution, Gaussian noise, moments of inertia and many more. In this project the sonar was used twice. Firstly, an ultrasonic sensor

installed under the central hub, facing the ground, to report the distance from the ground –that is the altitude. Secondly, an ultrasonic sensor installed in the frame arm oriented to the back in order to measure the distance between the UAV and any object in the back. To add more devices in the UAV configuration, the users should edit this file ([goo.gl/XJU7TU](http://goo.gl/XJU7TU)) accordingly.

- Laser scanner

The Hokuyo UTM-30LX Scanning Laser Rangefinder is a great device having features like 270° area scanning range with 0.25° angular resolution at a speed of 25msec/scan. However, it is very expensive with a price approximately 5.000\$. In my project the principle of using relatively cheap COTS technology did not justify the use of this device. Therefore, I did not use this device as it is. The simulator structure allowed me to alter the characteristics and degrade it in a simple laser sensor. Using this ([goo.gl/ZzL6HI](http://goo.gl/ZzL6HI)) file I could change:

- The minimum and maximum angle from 270° to 180°.
- The ray count from 1800 (in the 270° range) to 180 (one scan per degree for my 180° range)
- And the update rate.

Likewise, the users that want to experiment with advanced features of the laser can alter the related parameters in this file ([goo.gl/FhyLzY](http://goo.gl/FhyLzY)).

Aside from the devices that I tested and utilised, I additionally experimented with the following:

- GPS

The GPS reports longitude, latitude and altitude measures. There are two useful ways to exploit these data. The first is using an approximation, to estimate the distance between two points. This accomplished by converting the (lat, lon) coordinates to meters. The second is to use the altitude. However, in my case it was not accurate, as it is expected. Furthermore, I couldn't rely on that value in order to hover constantly in low height.

- Barometric sensor

This sensor measures the air pressure as the primary means for determining altitude, also called Pressure Altitude. Like with the sonar sensor, the reported height is utilised to lock the altitude during the flight. However, if the air pressure is changing in the flight area due to extreme weather, the UAV will follow the air pressure change rather than actual altitude. In reality when the altitude is less than 8 meters, the sonar is the main device of obtaining the altitude and not the barometer. In the simulation, the measurement of the barometer in 1m above the ground was even a negative number. Consequently, this sensor was not used in the simulation.

- Front camera

In the default configuration of the Hector simulator a front camera is enabled. I did not experiment in depth with this device because I did not have any intention to use computer vision as part of my application.

The complete setup of the simulated UAV is shown in the following figure (fig.D.4). In this screenshot, a hector quad-rotor UAV equipped with a laser scanner and two sonars is visualised in rviz.

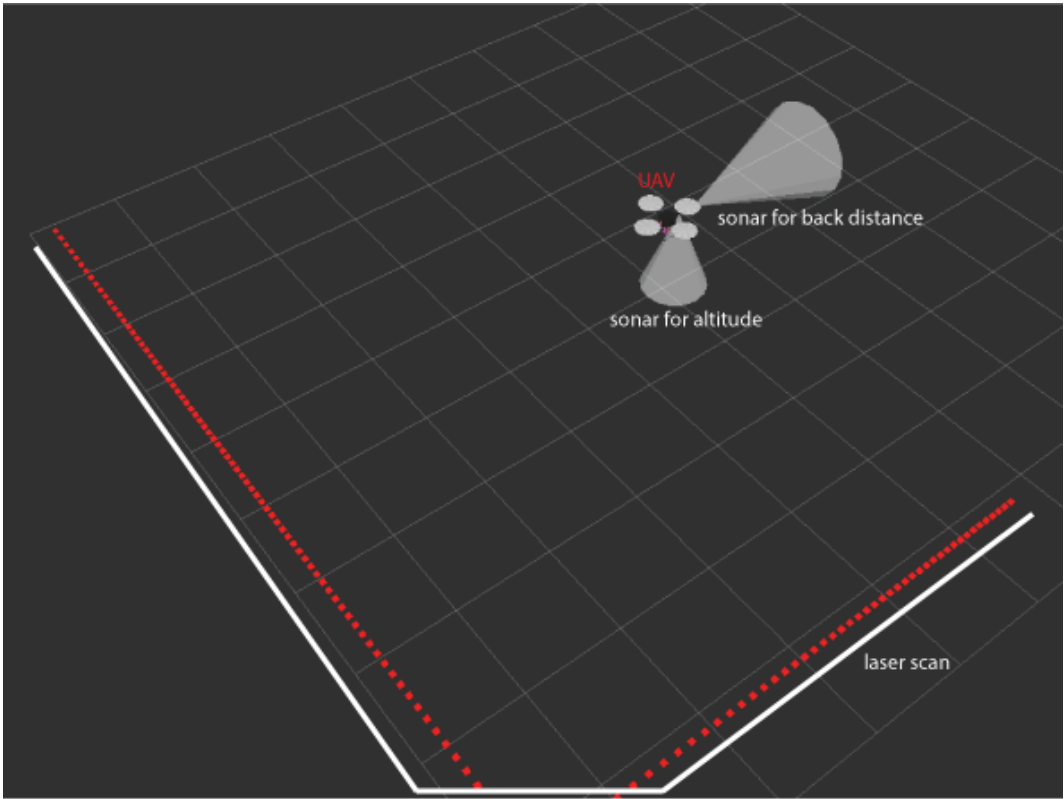


*Fig.D.4 Visualisation of a simulated UAV using the ROS rviz tool. This screenshot illustrates the two sonar lobes and the laser scanning of a corner (two perpendicular walls)*

#### D.4 The radiation mapping and simulation requirements

It is important to explain clearly the task of UAV taking radiation measurements so as to gain better understanding of the simulation. In a real UAV for radiation measurements, a gamma spectrometer is also installed in addition to the proximity sensors. Based on the radiation mapping techniques, to obtain high quality measurements, the UAV should fly close to the inspected surface and in a constant distance. This means that the UAV should fly in low height above the surface and this distance should be locked. In the real UAVs there is flight mode for this case called Altitude Hold Mode.

A desired feature during the radiation mapping is the obstacle avoidance capability. To illustrate this, as the operators control manually the UAV, if

this gets near an obstacle, in the direction of its movement, an assisted behaviour will be performed. Thus, if the UAV finds an obstacle in front of it, it will assess the surrounding environment and accordingly it will accomplish an avoidance maneuver. At the end of this intervention the position of the UAV should be pointing to the open space and in the predefined locked altitude. After this point the control returns to the operators who are free to continue without worries till the next one. Simultaneously, if for any reason the UAV sense an object around it that is closer than one meter, it will proceed to emergency landing.

The described obstacle avoidance algorithm was implemented in the simulation environment to test its behaviour and get an assessment of its effectiveness. The technical details of the implementation are explained in the following sections. All the source files created for the obstacle avoidance teleoperation algorithm has been grouped in a ROS package called `my_hector` ([goo.gl/DpgSre](http://goo.gl/DpgSre)). The required changes in the existing files of the Hector quad-rotor ROS stack are explicitly cited in the related chapters with direct links.

## D.5 Topics nodes

The key feature of the radiation mapping is the capability to maintain a constant distance from the floor, even if this is the ground or the terrace of a building. The sensor that was employed for this task was the sonar, which is mounted under the central hub looking downwards. This device in the simulation publishes continuously, with a rate of 10Hz, the measured distance. It has a range from 3cm to 3m.

In order to implement the required behaviour, I designed the hover node ([goo.gl/vTajQO](http://goo.gl/vTajQO)). Essentially, this node gets input from the sonar to access the actual altitude of the UAV. In addition, it takes input from a custom topic `hover_height` with messages of type `geometry_msgs` (fig.D.5). This is the

interface of the node with the ROS ecosystem. Every node that wants to adjust the altitude hold of the UAV can set up a publisher for this topic and send the appropriate message to the hover node. Inside this message the z component commands the node to lock the altitude in this specific value.

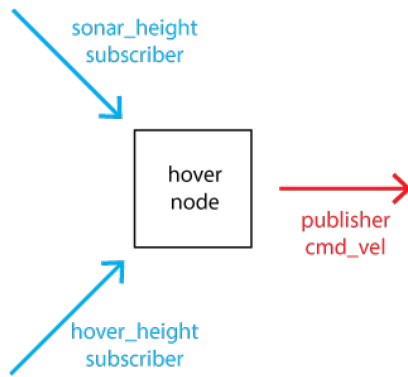
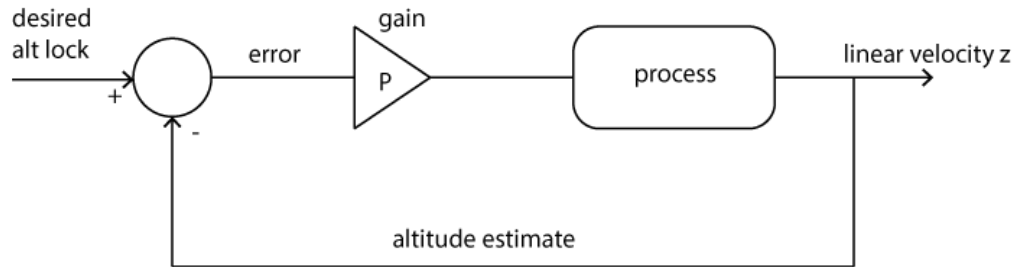


Fig.D.5 The messages' flow for the hover node

Since the node has all the data needed for its operation, it proceeds to the requested behaviour. Technically, both subscribed topics are connected with callback functions. The *heightCallBack*, related to *hover\_height* receives the desired altitude hold and checks if it is inside the range of the ultrasonic sensor. In the second callback function *heightCallBack*, which corresponds to the *sonar\_height* topic, the real work of this node takes place. Inside this function there is a simple P-controller (fig.D.6). This controller calculates the difference of the desired and the current height and outputs a value adjusted according to a gain. This outcome is basically the linear velocity in the z direction. Consequently, using this value a *geometry\_msgs/Twist* message is prepared and sent to the *cmd\_vel* topic. As long as the altitude of the UAV is stable and equal to the desired, the node does not need to act. It is worth noting that this node is active throughout the simulation since the altitude hold is a requirement in the flight mode. To achieve this automatically, the relevant command has been included inside the simulation launch file, for example in ([goo.gl/jBtQsi](http://goo.gl/jBtQsi)).



*Fig.D.6 The schematic of the P-controller inside the hover node*

Besides the hover node, a node responsible to change the heading (the yaw angle) is also developed called turn node. The operation principal is the identical to the hover node. The difference is that it gets the reading from the IMU sensor and publishes an angular velocity in the z axis instead of a linear velocity. A figure that summarizes the subscribed and published inputs is depicted in (fig.D.7). This node, based on topics, was replaced at the final obstacle avoidance application from a node, based an actionlib, for reasons that will be explained further on.

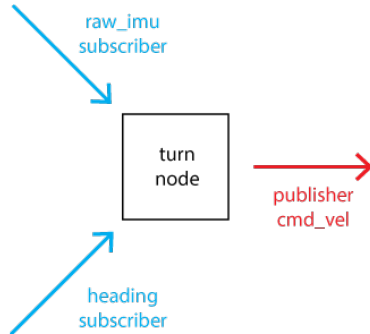


*Fig.D.7 The messages' flow for the turn node*

## D.6 Actions nodes

In the introduction of ROS, it was described that there are many ways for the nodes to communicate with each other. Aside from the topics and the services, actionlibs is a powerful tool to design communication channels

between nodes. In particular cases, when the following conditions exist, there is the only way.

- When the task is required to take time and feedback of the progress is needed, as well as a sign of completion or failure at the end. In this way, the application knows exactly the state of the ordered task and when the correct time to continue has come. This cannot be implemented using topics or services.
- When the application needs a way to cancel the ordered command.

For these reasons I decided to build action servers nodes in order to change UAV's heading and altitude lock. There is a predefined way that an actionlib server is built. In this section I will explain how the change-heading server was designed. First, in order for the client and server to communicate, there is the need to define three different types of messages on which they communicate. More precisely, the Goal, Feedback, and Result messages with which clients and servers communicate should be defined.

- Goal: To accomplish tasks using actions, the notion of a goal is introduced that can be sent to an action server by an action client. In my case the desired heading (in radians) is sent.
- Feedback: This message provides server implementers a way to tell an action client about the incremental progress of a goal. In my case, the difference between the desired heading and the current heading is published.
- Result: A result is sent from the action server to the action client upon completion of the goal. The difference with the feedback is that it is sent only once. This is also useful when the purpose of the action is to provide some sort of information at the end. In my case the result message means the successful completion of the ordered task and it is the accomplished heading.

Technically, to create new type of messages there is a need to define them in a specific action file. Then this file should be properly declared in the

*CMakeList.txt* file of the package. The next important step is to execute the *catkin\_make* process. Upon the completion of this, the required C++ header files containing the messages definitions have been created in a specific folder in the *devel* section of the ROS project. Now, the developers can use these messages merely by including the required headers.

The moment the infrastructure is complete, the design of the server can be implemented. For this particular server there is a need to know the actual heading. An easy and reliable way to obtain the heading is to employ the IMU sensor. Consequently the heading-change server has to subscribe to the *raw\_imu* topic. In this topic *raw\_imu* transmits quaternions. Using a couple of convenient methods it is possible to convert a quaternion to roll-pitch-yaw and access the UAV heading.

Following the creation of the server, three required function callbacks should be declared (fig.D.9). The first one is responsible for setting the goal in the action server. In my case, the *goalCB* callback function sets the desired heading. The second one is the preempt callback function. This action is event driven. It only executes when the callbacks occur, therefore a preempt callback is created to ensure that the action responds to a cancel request. In my case this callback function called *preemptCB*. The third callback function is the IMU callback function. Inside this function the change of heading takes place. At the beginning the current heading is obtained, as I described before. Then, the difference between the actual and the goal is calculated. At this point the feedback message is published. After that, this difference combined with a constant gain, form the input of a P-controller (fig.D.8). The outcome of this procedure is the angular velocity in the z axis. As it is expected at this point *geometry\_msgs/Twist* message is created and published to the *cmd\_vel* topic. At the end of this method, a termination condition is evaluated. More precisely, when the absolute difference between the desired and the actual heading is less than 3 degrees, the procedure terminates successfully. At this point the result message is published, only once. The reason why I introduce a 3-degree angular tolerance is that it is very easy to overshoot the rotation

and even a slight angular error can ruin the operation of the entire application. Empirically it was found that a tolerance of about 2.5 degrees gives acceptable results. The complete source file of the change-heading server can be found in this location ([goo.gl/qbZDVR](http://goo.gl/qbZDVR)).

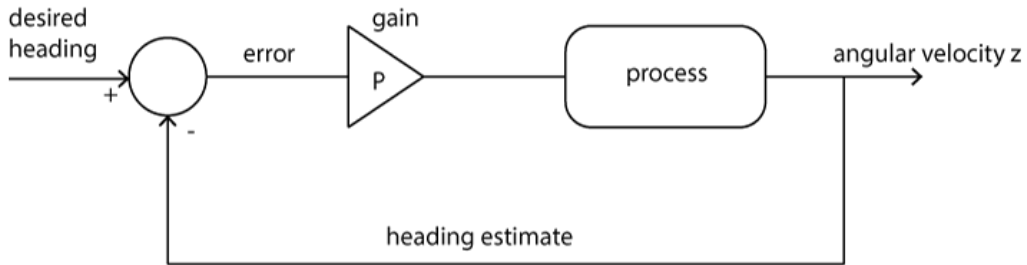


*Fig.D.8 The schematic of the P-controller inside the change-heading server*

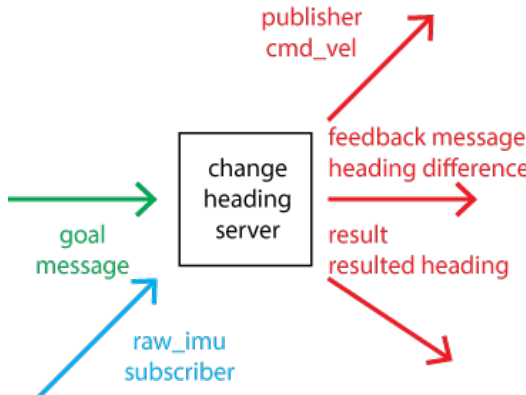


*Fig.D.9 The messages flow for the change-heading action server*

Before the action server was utilized as part of the application, the debugging and testing stage could be performed using a simple action client. In this client the goal heading is sent to the server. After that, the timeout duration is defined. During this period the client receives and reports the feedback messages. If the procedure ends within the time limit, it is considered successful otherwise the action has failed and an appropriate message is printed out. Since the actions are more complex than the other approaches, for every individual action server I have developed a suitable action client.

An additional important action server of the application is the hover-height server. This server is responsible to change the altitude to the new desired

value, which has been set as goal. The underlying logic and the structure of source file are similar the change-heading server that I have already described. The few differences that exist are the following as depicted in the figure (fig.D.10).

- The device that has undertaken the task to inform the current height is the sonar.
- The action server does not implement any controller. Instead of this, it takes advantage of the hover node and sends the required message to this mechanism in order to move the UAV vertically.

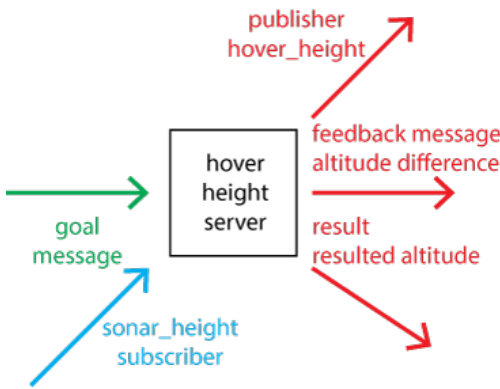


*Fig.D.10 The messages' flow for the hover-height action server*

The importance of both action servers in the obstacle avoidance algorithm will become apparent when the application will be explained. Nevertheless, before settling on the final version I had experimented with other implementations as well, which I included in my source code as available tools in the toolkit. The first one is a server ([goo.gl/k60jVX](http://goo.gl/k60jVX)) which -instead of the desired altitude- accepts a vertical distance as its goal. For instance, if the goal is 1 the hover-distance action server will move the UAV 1m upwards. The second one is a server ([goo.gl/KhdlHm](http://goo.gl/KhdlHm)) that performs the same action as the hover-distance but the measured height depends on the GPS altitude instead of the sonar's distance from the ground.

## D.7 Obstacle Avoidance

Having developed a complete toolkit of useful tools, it is time to present the design of the obstacle avoidance algorithm. The heart of algorithm is the finite state machine (FSM). This allows adding intelligence to the UAV since it is able to switch between different behaviors according to its sensors readings.

It is important to describe the scenario of the simulation. In this simulation, as in the real UAV as well, the operator controls the flight manually using a joystick or the keyboard (fig.D.11). If the UAV encounters an obstacle in front of it or senses something closer than 1m around it, then the control passes to the obstacle avoidance algorithm. From this point, the UAV based on the FSM will perform a single or a series of maneuvers. When it assess that there is no obstacle to avoid, it will pass the control back to the operator. After the avoidance procedure, the algorithm will try to deliver the UAV in the initial heading that this had before the algorithm took the control. In complicated cases, when the UAV performs a sequence of maneuvers this could not be possible. This description corresponds to an assistive teleoperation solution where the application helps the operator by performing the avoidance maneuvers.

The aforementioned approach can be translated technically using the following techniques. The control input devices, described extensively in “Simulation Topics” appendix, send traditionally the *geometry\_msgs/Twist* commands in the *cmd\_vel* topic. To enable the obstacle avoidance application to alter the predefined flow of the commands, I structured it as a message getaway or a filter. To illustrate this, the input control devices have been remapped to publish the navigation commands to the *obs\_cmd\_vel* topic instead of the initial *cmd\_vel*. The *obs\_cmd\_vel* is the one that the application listens to. If there is no need for intervention, the node is transparent. Whatever navigation message comes from the inputs, it is published automatically in the *cmd\_vel* topic. If there is need to perform avoidance

maneuver, the node overrides the control and sends the algorithm's messages as input to *cmd\_vel* topic.

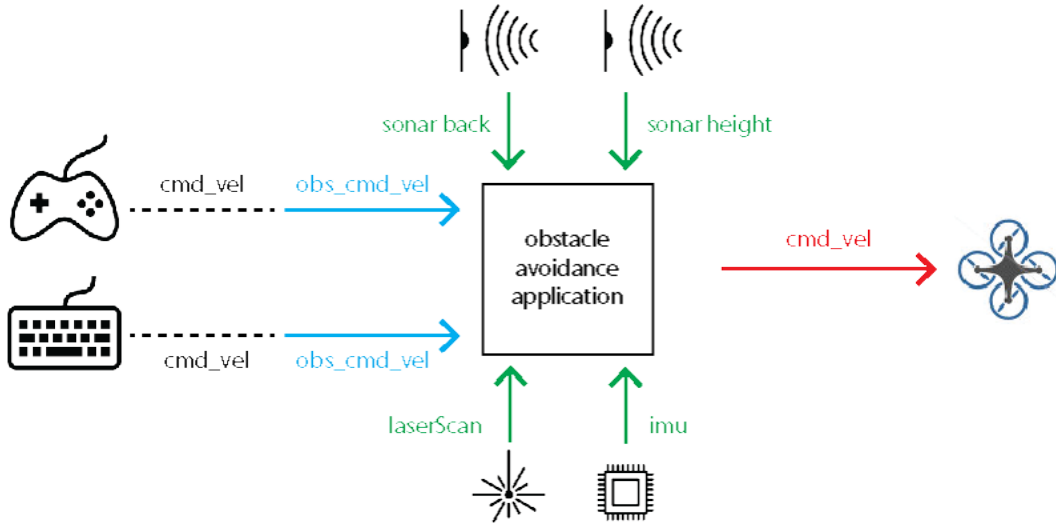


*Fig.D.11 The messages flow for the obstacle avoidance application*

At this point I should clarify the way that the UAV measures the distances that were used in the algorithm. The height and the back distance are measured using two ultrasonic sensors pointing towards the ground and back accordingly. For the distances in front and on both sides the laser scanner is used (fig.D.12). More precisely, having configured the laser to take measurements every 1-degree in 180° range, it is possible to choose these directions from the related positions of the distances in the reported scanning. Consequently, the front distance is given by getting the minimum distance in the range from 70° to 110° heading. The left is the minimum distance in the range from 0 to 20° and the right from 160° to 180°. This approach is closer to the real UAV since I do not have laser scanner sweeping of 180°. Instead of this, I have an individual sensor on each side or a single laser taking measurements for every perpendicular direction.

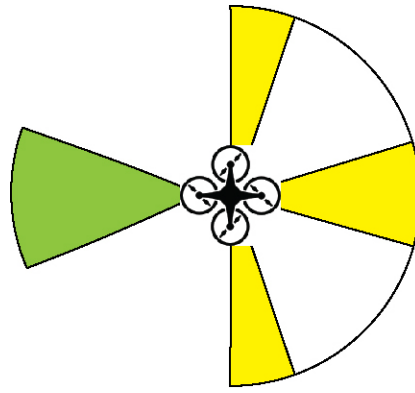


*Fig.D.12 UAV proximity sensors. The sonar lobe in the back (green) and the segmented laser scanning in front and on the both sides (yellow)*

Having talked about the finite state machine (FSM), a detailed explanation includes the description of the individual states and conditions that should hold to move between them (fig.D.13). The loop that executes the FSM is repeated at a constant rate of 20Hz.

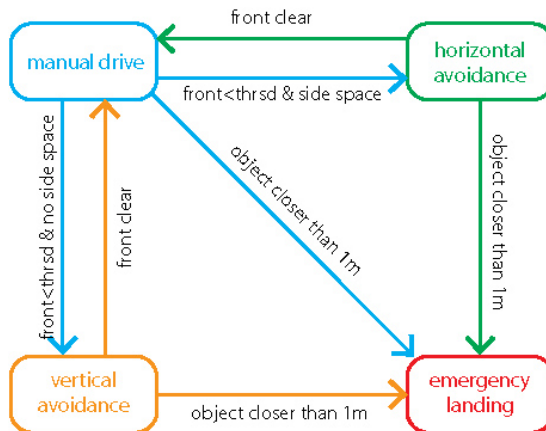


*Fig.D.13 The UAV's finite state machine*

#### State 0 – manual drive

In this state, input devices such as a keyboard or joystick control the UAV. Every time this state is executed, a safety check is performed. If the distance in front is less than a defined threshold a transition should occur. The destination of the transition depends on the distances on the left and the right of the UAV. There are the following possible cases:

- The distance on both sides is less than a threshold. This means that the UAV is at the end of a corridor, like a dead end. If this is the case then it changes to state 2.
- The distance on the left is greater than the one the right or vice versa. In situation like this, the UAV seems that flies near a corner. In this case the UAV will change to state 1 by rotating 90° to the side where the open space is sensed.
- The distance on the left is equal to the distance on the left. This happened when there is no obstacle on both sides and the laser reports its highest range, or when there are obstacles further to the maximum range. In this case the UAV will randomly turn on one side or the other side and change to state 1.

Finally, if the UAV senses an object in distance closer to 1m at any direction (front, back, sides) then it performs emergency landing in state 3.

#### State 1 – Horizontal avoidance

In this state the UAV has already sensed that there is space to move in the one or the other side. Before entering this state a 90° change of heading has been performed during the transition from state 0 to the side that has the greatest open space. The UAV starts to move forward and continuously measures the distance on the side where the obstacle exists. If at one point it is noted that the distance gets higher than a threshold, this means that there is no obstacle any more. This signs the end of the obstacle but not the end of the maneuver. After that the UAV will move a bit more and it will correct the heading back to the initial one which it had before the override. During the aforementioned procedure two simultaneous safety checks are executed at the same time.

- Since the UAV moves till it finds the end of the obstacle, it always measures the distance in front of it. If it finds that there is another obstacle ahead of it, it repeats the avoidance maneuver again and continues, maintaining the state to 1.
- If at any point for any reason it senses an object closer to 1m on the proximity directions (back, front, sides), it changes to state 3.

At the end of the procedure, if the avoidance maneuver completed successfully, the UAV moves back to state 0.

### State 2 – Vertical avoidance

In this state the UAV has already discovered that it is at the end of a corridor. There is no point to explore the sides for horizontal escape. At this point, it will attempt a vertical overcome of the obstacle. Depending on the height of the obstacle in front of the UAV there are two available options:

- The first case implies if the obstacle's height is lower than the sonar's range. In this situation, the UAV will start to elevate and simultaneously measure the front distance. At a point before it reaches the upper limit, the UAV will sense that there is space ahead. Consequently, at this point it will stop the vertical translation and it will move forward to overcome the obstacle. After a certain predefined distance, the UAV will move back to the altitude hold position and the control will return to the operator in state 0.
- The second case happens when the UAV reaches the limit of the sonar range. At this point I do not want to move further up and obtain the height altitude measurement using the barometer or the GPS. These devices are not so accurate and the altitude hold mode becomes unstable. So if this is the case, the UAV will stop the vertical translation and it will change heading by  $180^\circ$ . After that, it will move back to the predefined altitude hold position. Eventually, the UAV control will return to the manual operation in state 0. Similarly to the previous states, it is possible to change towards the emergency landing state 3 if any object is sensed closer than 1m.

### State 3 – Emergency landing

During the movement of the UAV in manual mode or even when it performs avoidance maneuvers a safety check is concurrently run. In this check the UAV gathers the measurements in every perpendicular direction ( $0^\circ$ ,  $90^\circ$ ,  $180^\circ$ ,  $270^\circ$ ) and if it encounters an object closer to 1m it will proceed to emergency landing. Since the altitude is locked to a low height this solution is

workable to enhance the safety of the UAV and the surrounding environment. The landing was preferred because it is difficult to trust a subtle maneuver with a hazard so close. However, if there is time for exhaustive testing, a more complicated behavior could be developed. In this emergency situation the control doesn't return back to the operator and it requires the physical intervention in the location of landing.

The source file in which the obstacle avoidance application has been implemented is located in ([goo.gl/eG2mXn](http://goo.gl/eG2mXn)). It is a ROS node that acts as a central hub since it is subscriber to all the sensor and input control devices, publisher to the velocity control topic and client to action servers related to the heading and altitude.

## D.8 Testing

During the development of the code the proper debugging took place in order to produce a functional application that will allow me to experiment with the behavior of the model. At this point, I exploited the dynamic features that Gazebo 3D simulator offers to the users. There is online an available library of objects which can easily be utilized to construct a landscape. These objects are declared in an XML-like file by defining the exact positions and orientations. In my case, the wall object was an ideal choice since I could place it in various combinations and explore how the UAV reacts. The specific file in which the landscape is defined can be found in this location ([goo.gl/vfi9NH](http://goo.gl/vfi9NH)).

In the following figures the scenarios of some of the experiments, which have been conducted, are illustrated (fig.D.14), (fig.D.15), (fig.D.16) and (fig.D.17). The experiments were successful and the behavior of the UAV was stable and as it is expected to be. There are available online videos of the experiments

in this address ([goo.gl/JyTzGp](http://goo.gl/JyTzGp)). The code of the project can be found online at the following git repository ([goo.gl/BU1ydu](http://goo.gl/BU1ydu)).

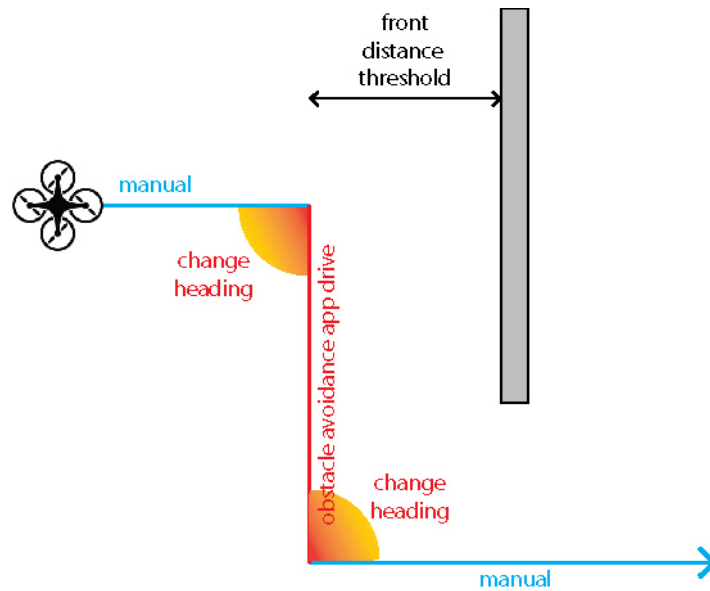


*Fig.D.14 The avoidance maneuver when there is no obstacle in both sides of the wall*

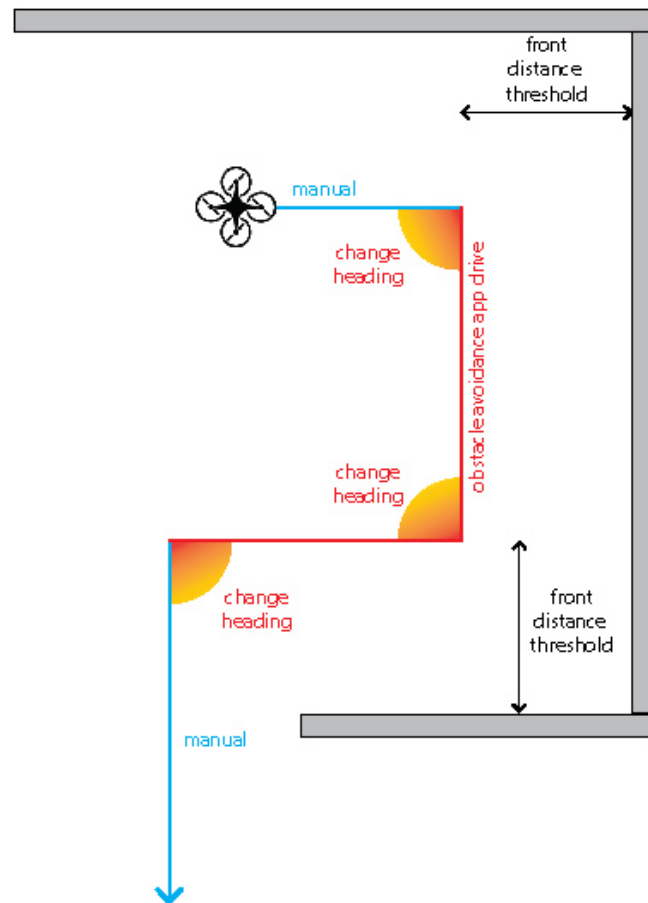


*Fig.D.15 The avoidance maneuver when there are multiple obstacles in the path of the*

*UAV. Two avoidance maneuvers in sequence.*

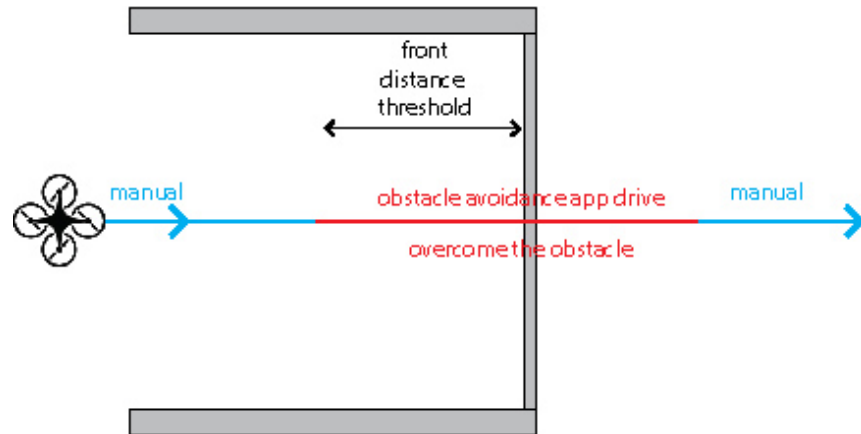


*Fig.D.16 The UAV moves towards a dead end. The obstacle in front is lower than the maximum range of the altitude sensor. The UAV overcomes it and returns to alt hold.*

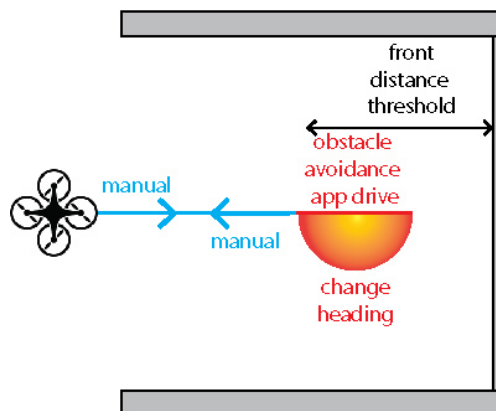


*Fig.D.17 The UAV moves towards a dead end. The obstacle in front is higher than the maximum range of the altitude sensor. The UAV changes heading by 180° and returns to alt hold.*

## Part E

# Human Robot Interface

In this part, the design and development principals of the two iOS mobile applications, which have been implemented in the context of this project, are presented. Both applications aim to enhance the user's experience in the field of human robot interface. The first is related to the visualisation of the radiation mapping and the second to the teleoperation of a UAS.

### E.1 UAV teleoperation application

One of the popular and traditional methods of teleoperating a quad copter is using a Remote Control (RC). It is a well-established and tested method, which has its origin before the era of the UAV. Nowadays, advanced UAVs are equipped with many sensors and specific purpose equipment such as cameras or radiation spectrometers. An alternative method of getting high bandwidth data from a UAV, which is also convenient, is using telemetry. This method uses a client application, installed in a laptop, in order to make all the data transmitted from the UAV available.

The approach, which has been developed for this project, is based on the utilisation of smart devices (fig.E.1). These devices are equipped with powerful CPUs, extreme visualisation capabilities and a wide range of connectivity options. Needless to say that it is very popular and almost everyone in the developed countries has one of them.

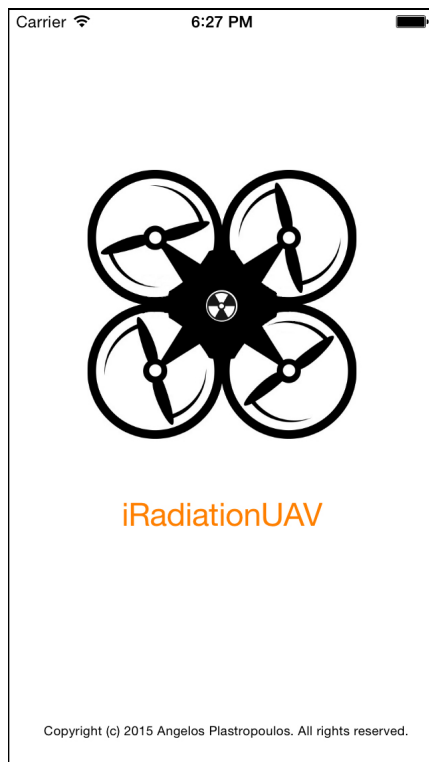


*Fig.E.1 The splash screen of the teleoperation application*

### E.1.1 Topology

The communication between the iPhone and the UAV is accomplished via wireless connection (Wi-Fi). I have chosen this method because TCP/IP is the native communication protocol supported in ROS ecosystem and a wireless connection will be available in the next generation AARM system since it is going to have a companion computer.

Since I chose the communication method the next step was to decide the format in which the data should be encoded in and exchanged between peers. The selection of JSON (Javascript Object Notation) is a commonly accepted method. JSON is a lightweight data interchange format, easy for people to write and read yet, at the same time, it is easy for machines to parse and generate. In addition, there is a wide variety of available libraries that can be utilised to provide apparent and reliable implementations.

## A. UAV Peer

In the side of the UAV there is one important requirement that has to be satisfied: UAV should be ROS-enabled. This is not restrictive because ROS is a very popular and trustworthy action plan in robotics' communities. Moreover, as it has been implemented in this project for safety and convenience reasons, it is possible to use a simulator for the development. The advantage here is that in ROS systems the same code can be used with a real robot without any change.

In a ROS system there is a messaging mechanism called topics (fig.E.2). The data from the installed on-board devices which are publicised in relevant topics and control commands related to the linear and angular velocities are also accepted from the appropriate receivers using associated topics accordingly. These topics should be available to the iPhone in order to have access to the data and control commands. At this point a specific ROS package comes to play. *Rosbridge* (Crick et al., 2011) which provides a JSON API to ROS functionality for non-ROS programs. This sounds ideal for the requirements of my project. *Rosbridge* provides a wide range of supporting interfaces. For my case, it was important that it included a WebSocket server for web browsers' interaction. The WebSocket Protocol is a network protocol designed for the web that enables browsers to have bi-directional communication with a server. Using this package, communication mechanisms can be provided to the non-ROS systems following a ROS-style approach. It supports topic publishing and subscribing, service request and response as serialized JSON objects.

One of the advanced equipment that a UAV could carry is a camera. It is extremely helpful and interesting to have real-time streaming of the video to the app. While *Rosbridge* allows streaming videos, seeing as it is just another message type from ROS, I preferred to use a different component. *MJPEG* (Motion JPEG) server (Pitzer, 2011), which is a ROS package, optimised for efficiently transferring stream images in binary format. Consequently, an

additional communication channel was used to increase performance and enable clients to request specific video quality and frame size according to their needs.

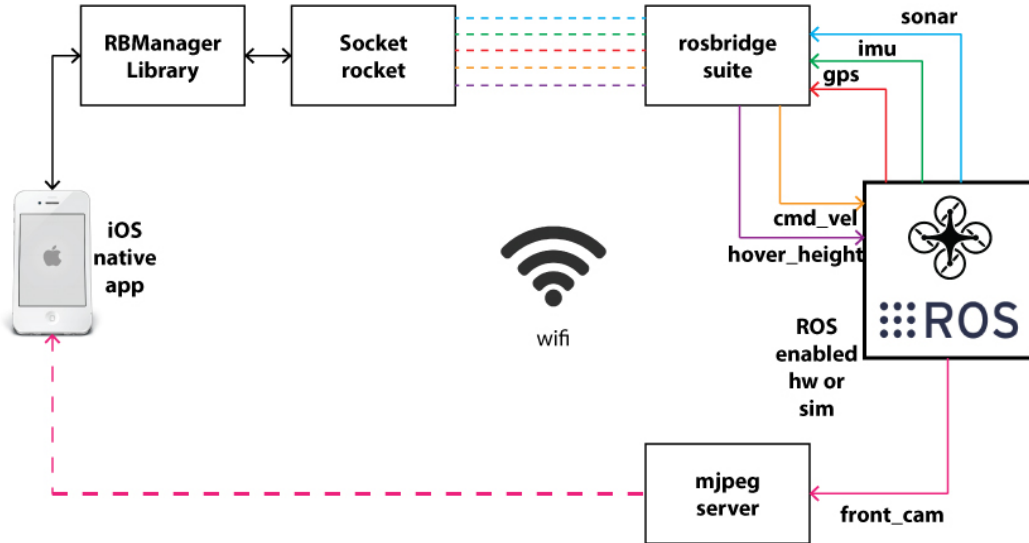


Fig.E.2 Topology of the teleoperation application

## B. iOS device peer

On the other side there is a native iOS application developed using Objective C. As with the ROS side, the application should leverage the appropriate libraries to gain access in the data generated in the ROS ecosystem as well as to send compatible data. For this case, a *WebSocket* library should be used. *SocketRocket* is an objective C *WebSocket* client library (Lewis, 2015) useful in native mobile applications. By using *WebSockets*, existing tools built for the web can be easily reused for the mobile applications. It is similar to how most mobile apps reuse *HTTP* for their APIs. One level deeper in the architecture, there is the powerful *RBManager* library (Goodhoofd, 2014) for communicating between iOS and ROS. This library is a wrapper for the *SocketRocket* *WebSocket* library in iOS. This approach follows the standard publisher, subscriber and service call architecture to send packets compatible with the *Rosbridge* protocol. It is well structured and easily expandable. It allows adding new message types and building on top of that. It has a simple syntax as long as the developer knows ROS.

Regarding the processing of the streaming video the case is simpler. The stream of the MJPEG server is essentially a video sequence in which each frame is separately compressed as a JPEG image. In the iOS library there is a *UIWebView* component (Developer.apple.com, 2015) available that enables the embedding of web content in iOS native applications.

Specific implementation details regarding the application are described in the related appendices chapter.

### E.1.2 Functionality

The teleoperation application is a prototype of a fully working application yet has not optimised in areas such as functionality and appearance to be commercially available. The application consists of three main screens. The first screen appears when the application is loaded as the central hub (fig.E.3). From this point, the operator has a complete overview of the sensors' feedback. It shows data collected from the GPS unit, the IMU unit and the sonar, which measures the distance from the ground. In addition, in this screen the operator can enable the control tab. This tab provides the ability to control the linear velocity in the plane, x and y direction, as well as change the heading by manipulating the angular velocity in the z direction. This tab includes also the altitude lock mode. More precisely, the user can adjust the constant distance from the ground in which the UAV flies. Whenever the operators need to freeze the UAV (zero the velocities components of the control), they just have to toggle the enable/disable button. In this procedure the altitude remains constant. Finally, it contains a button to disconnect from the UAV and to terminate the application.

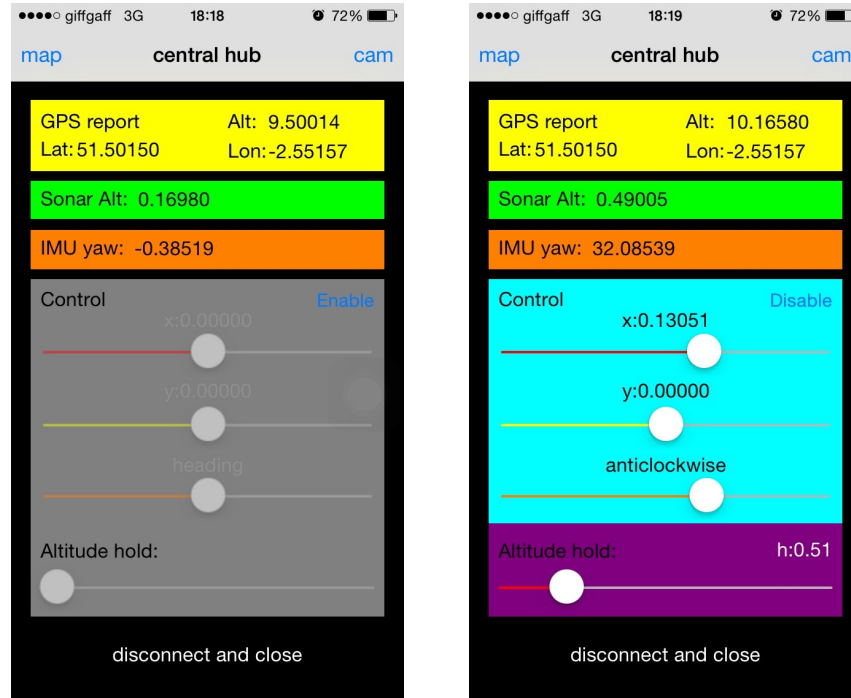


Fig.E.3 The central hub screen with control tab enabled and disabled

The second screen shows the exact location of the UAV in a map (fig.E.4). It takes the longitude and the latitude from the on-board GPS unit. The third screen shows the streaming video of the on-board front camera (fig.E.4). The user having locked the altitude could also drive the UAV from this screen.

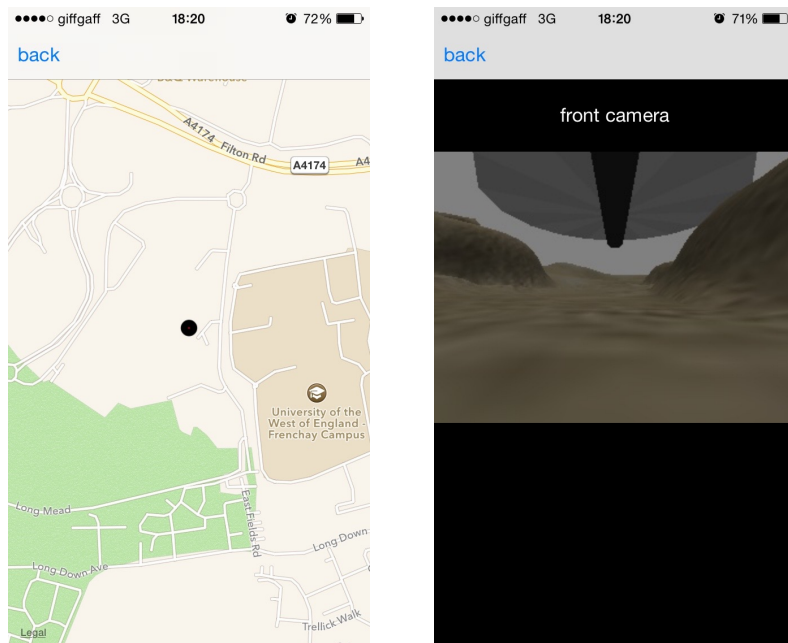
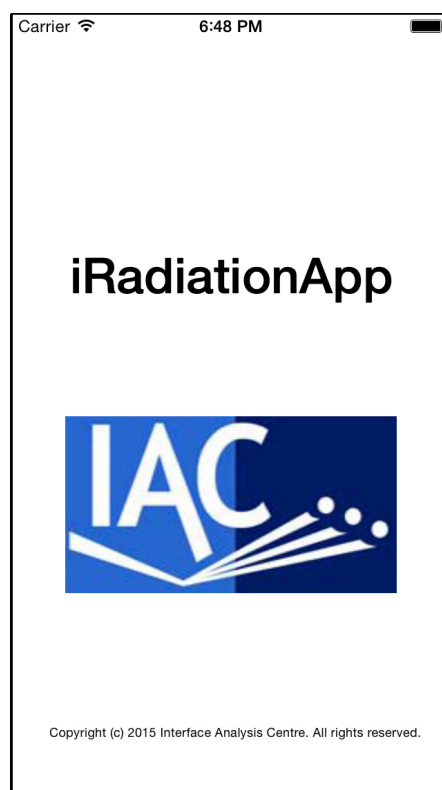


Fig.E.4 The map and the camera screen

More technical details about the implementation of the application can be found on the “Mobile applications Configurations” section in the appendices.

## E.2 Radiation mapping application

This mobile application constitutes an important part of this project since it is directly related to the radiation mapping visualisation. Up until now the radiation mapping is a procedure which is conducted offline. To illustrate, the operator could carry a hand held measurement device that stores the data in a SD memory card. Upon the completion of the procedure, the researcher should access this memory card by inserting it in a memory reader using a laptop. The desired requirement at this point is that the researcher will be able to get the status of the radiation measurement unit and the measurements displayed on a map during the procedure in real-time (fig.E.5).



*Fig.E.5 The splash screen of the radiation mapping application*

### E.2.1 Topology

The communication between the iPhone and the measurement unit is accomplished via Bluetooth low energy (LE). BLE is a wireless personal area network technology. It provides considerably reduced power consumption and reduced cost while maintaining a similar communication range with the classic Bluetooth. In addition, using BLE I avoided the process of requesting a specific license from Apple, called MFi ("Made for iPhone/iPad/iPod"), which is required when the classic Bluetooth is employed.

The operation of the measurement is based on an Arduino IDE sketch developed at Interface Analysis Centre (IAC). This sketch was used as a base to build the server-part of my application. The architecture of the sketch, as it was built, was to enable the GPS connection to get the longitude and latitude and then to obtain cps measurements via the USB protocol from the spectrometer. When all the required data were available, the sketch was forming a data entry to the text file stored in the SD card. My task was to maintain the working part while simultaneously integrating the required parts for the iOS application.

The first addition for the measurement unit was to install the BLE shield. After that, the sketch had to change in order to access desired bits of information, form compound packets and send them to the link. The formation of specific data packets was a demand since the payload of the transmitted package has a maximum size of 20 bytes for the gives BLE shield (fig.E.6)

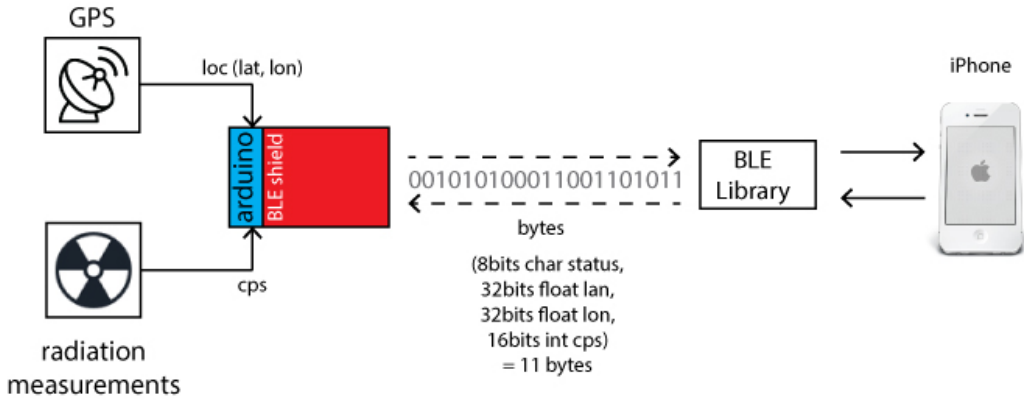


Fig.E.6 The overview of the radiation mapping scenario

According to the application's specifications the status of the GPS should be reported. To save space in the messages payload, I encoded the status information in one byte. Consequently, since the GPS lock is an on-off condition, it needs one bit. The remaining 7 bits of the byte are used to report the number of connected satellites. After that, the latitude and the longitude should be represented using 32bits floating-point numbers. To manage this, I break each value to four parts of byte size and I assemble them again in the iPhone side. Moreover, the radiation counts per second is encoded as a two bytes integer. Finally, having formed the payload of the BLE message (fig.E.7), this message is transmitted to the other side at the end of every cycle.

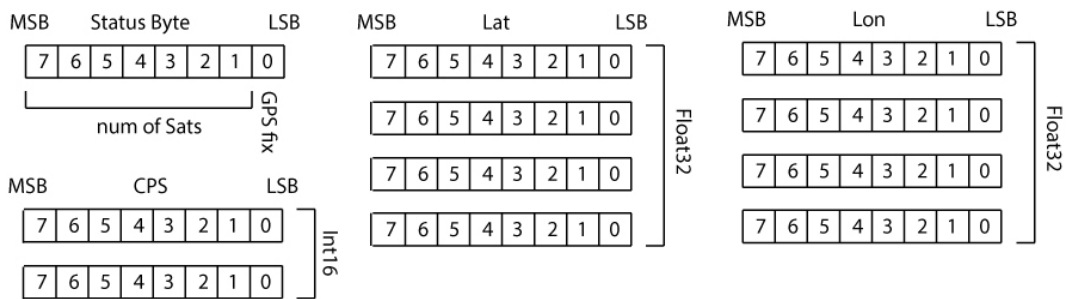


Fig.E.7 The payload of the BLE message

On the other side there is an iPhone device with the Bluetooth connection enabled. In order to decode the transmitted messages, a specific library is needed. The manufacturer of the BLE shield has released an appropriate library for this task, called BLE. Using the provided features, the iPhone can

search for compatible BLE devices to connect and disconnect with them. When the iPhone has connected to the measurement unit, there is the possibility to measure the RSSI level (Received Signal Strength Indication) and access the contents of the payload. Using the reverse procedure, the iPhone script assembles the primitive data types from the raw bytes and visualises the information using various means.

### E.2.2 Functionality

The radiation mapping application has been developed using the directions of the experienced IAC researchers. It is a very specific application and in order to be useful and a real tool in the hands of the user, it has to be specifically defined and designed according to their needs.

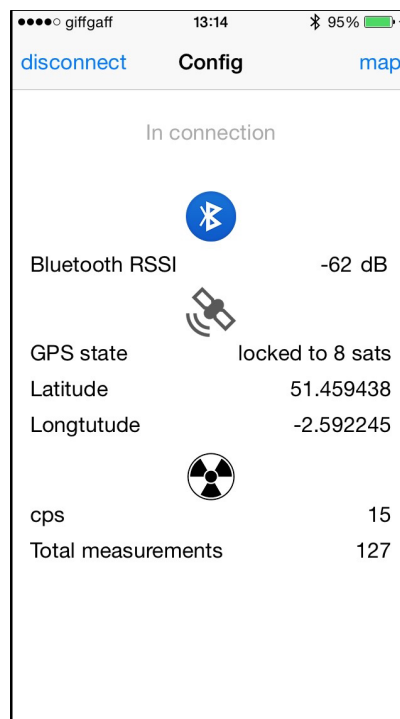


Fig.E.8 The configuration screen of the radiation mapping application

The configuration screen displays all the useful information to the user (fig.E.8). In the first part of the screen there is a message board that displays informative messages regarding the Bluetooth connection. In this display,

the user can be informed about the availability of other BLE devices, the name of the device that they are eventually connected to and other relevant information. After a successful connection the RSSI value is continuously updated to reflect the signal strength of the Bluetooth connection between the measurement unit and the iPhone. At this point, with an active Bluetooth connection, the user can read the status of the measurement device in the iPhone screen. Consequently, when the GPS unit locks, both the relevant message and the number of the connected satellites will be displayed to the screen as a sign of the signal strength. Finally, there is a section related to data which come from the radiation spectrometer. In this part, the actual CPS value is reported together with total number of measurements that has been performed.

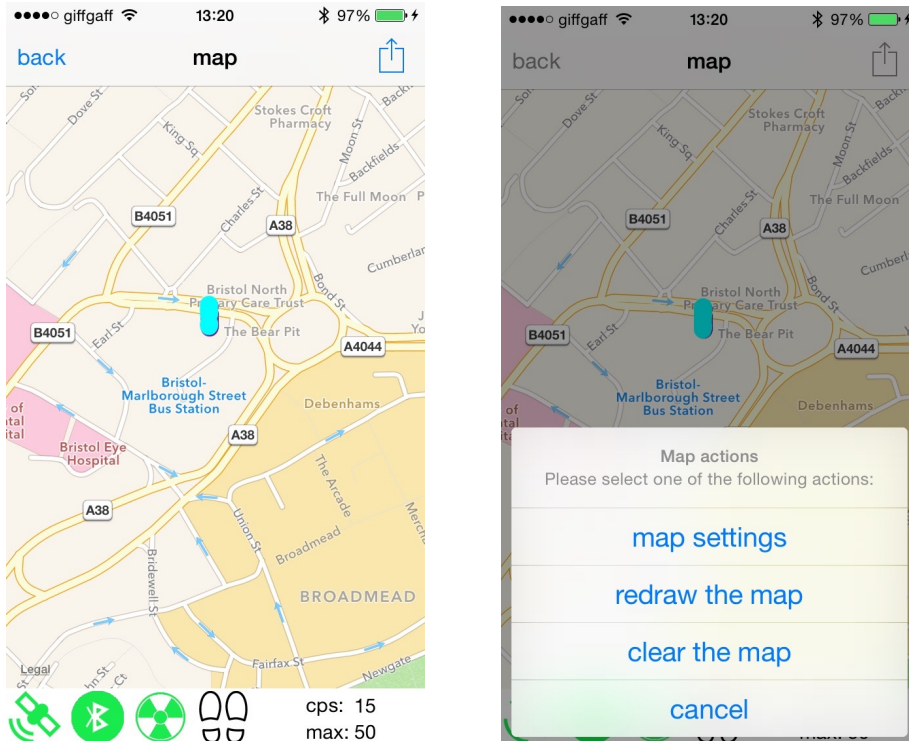


Fig.E.9 The map screen (left) and the map screen with the actions button enabled (right)

The next screen displays the visual representation of the measurements in a map (fig.E.9). Every time a new measurement is received, the application stores this value in an internal data structure and at the same time it displays a colour-encoded point at the exact longitude and latitude in the map. Colour

depends on the CPS value. At the lower part of the application there is an information tab. Since the users spend most of the time on this screen, they need a way to know the overall status of the procedure. The summary part, which is available, contains the following:

- Three status icons corresponding to GPS, Bluetooth and radiation device connectivity. The first two are green when the connection is active, otherwise they are grey. The third one is animated like a heart pulse to indicate that the CPS storing and visualisation proceeds flawlessly.
- There is an additional icon in the tab that represents the method of the radiation mapping. Furthermore, there are two character strings displaying information about the current CPS value and the visual colour-encoded CPS range.

There is a button in the navigation part of the screen, which contains a set of map related tasks. Using this button the user can clear and redraw the map. An additionally important task is the display of the map settings screen.

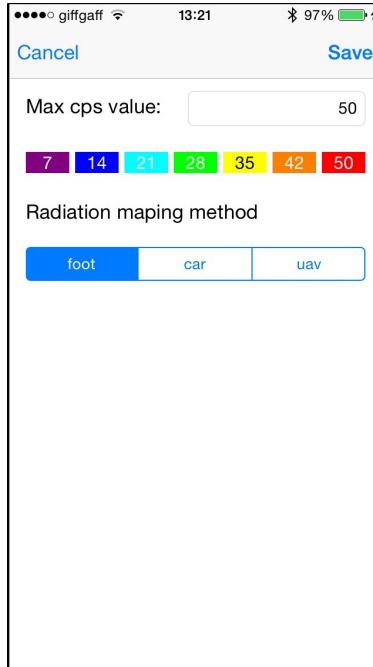


*Fig.E.10 The map settings screen of the radiation mapping application*

In the map settings screen the user can adjust various visualisation parameters (fig.E.10). Firstly, there is the option to select the radiation

mapping which is used to perform the measurements. There are three methods available, measurements taken on foot, by UAV or using a car. According to the selection, the zoom level of the map is changed to allow a reasonable display detail level. Moreover, in this point an attenuation factor can be added since there is a different sensitivity level if the user takes measurements inside of a car or on foot. Secondly, the user can adjust the colour encoding of the measurements. More precisely, the red colour represents measurements close to 500 CPS and purple close 0. In cases where the area is considered safe the colour will remain purple without the ability to represent minor fluctuations of 10 to 20 CPS difference. Thus, in this screen the user is able to define the maximum CPS value and based on this value the CPS range is rescaled accordingly. As a result, with a maximum of 50 CPS the range of each colour will be approximately 7 instead of the initially 71 for the 500 CPS. All in all, when the user returns to the map the measurements are redrawn reflecting the new colour range.

More technical details about the implementation of the application can be found on the “Mobile Applications Configurations” section in the appendices.

---

**Part F**

**UAV**

It will be added

---

## Part G

### Conclusions

It will be added

## Appendix A

# UAV configuration

One of the most important parts of the project was to build a state of the art UAV. There were many individual requirements that the configuration should satisfy. The higher level demands were to use commercial off the shelf (COTS) products in order to save time from implementing again successful existing parts and simplifying the replication due to the practical design. Further than that, open hardware products were chosen so that it would be easy to get support from the related communities and it would also be able to choose from different manufacturers with lower prices. In general, COTS components tend to be inexpensive, upgradable and reconfigurable. Moreover, it is easy to gain experience even before starting to experiment, since many researchers have already used them and published relevant papers. Aside from the general requirements, specific research has been conducted for each individual part in order to use the most appropriate component and how this item can be combined with the others in the most efficient way.

### A.1 Chassis, brushless motors and Electronic Speed Controllers (ESC)

#### A.1.1 General description

The most basic and influencing component in a UAV is its chassis. There is a great range of available options according to the number of motors and their topology. For the current project, a quad copter has been chosen. Some of the advantages of selecting quad copters are the low price, the great manoeuvrability and the enough available power to add accessories since they have only four motors. The option of using a tri-copter has been

discarded due to its limited trust and power capabilities. On the other hand, hex or octo-copters can fly in higher heights and greater flight speeds, are safer if one motor dies, since the rest can pick up the slack and also can handle higher overall payloads. These are considerable advantages but for the specific project these do not affect the objectives and add only unnecessary complexity.

Regarding the motors of the UAV, the most popular type is the brushless motors. Brushless motors are much more efficient than the conventional brushed ones. They have a greater lifetime and they do not require maintenance due to the absence of brushes and commutators. In addition to that, the absence of brushes eliminates the friction and thus they have very high power density (in terms of size and weight), which means longer battery life. In general, brushless motors are very easy to control their speed accurately and adjust it quickly. Nowadays, the prices of the brushless motors are similar to brushed so they are not expensive as they were in the past. Finally, it generates less noise that causes weaker electrical magnetic interference (EMI), which is very important for the interference of the GPS.

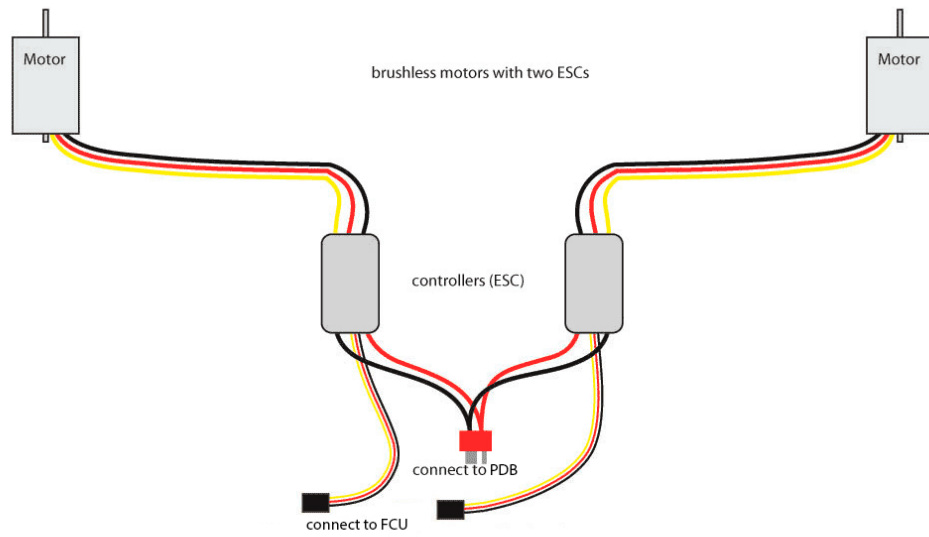


*Fig.A.1 Brushless motors and Electronic Speed Controllers (ESCs) connection to flight management unit and the power distribution board (image modified from one in [www.pteroworks.com](http://www.pteroworks.com))*

The use of brushless motors requires the presence of Electronic Speed controllers (ESC). Electronic speed controllers are responsible for spinning the motors at the speed requested by the flight controller unit (FMU). Each brushless motor is connected with three wires (fig.A.1) to the corresponding ESC. This is because brushless motors are three phase motors having three coils inside. Consequently ESCs activate the coils in sequence and depending on the synchronization they can accelerate or decelerate the motors to the desired speed. The ESCS comprises of the following parts:

- Microcontrollers that activate or deactivate the coils and calculate timing by measuring the feedback in the coils caused by the movement of the magnets.
- 5V voltage regulators to produce a stable supply and a low battery cut-off feature to stop spinning the motor when the lithium polymer battery is drained. This feature protects the battery from suffering permanent damages that occur if it drained below a threshold.

A general schematic of a UAV wiring is shown in the (fig.A.2)

The Interface Analysis Centre (IAC) has a fleet of UAS platforms for radiation mapping such as quad-copters, hex-copters and octo-copters. For the specific project, it provided the chassis of a quad copter having the following components installed:

- Four brushless motors
- Four Electronic Speed Controllers ESCs

#### A.1.2 Vibration damping

The UAV's flight management unit (FMU) sits in the upper part of the central hub. It is equipped with accelerometers in the inertial measurement unit (IMU), which are sensitive to vibrations. In general, in most of the flight modes it is crucial to have a correct position estimate. The calculation of the position estimate is carried out using data from the IMU in combination with

the barometer and GPS. It is clear that vibrations can interfere the operation of these units and lead to unacceptable performance. Generally speaking, the motors and propellers produce a high frequency and low amplitude vibration. The vibration needs to be less than 0.3 g in the X and Y axis and less than 0.5G in the Z axis (Copter.ardupilot.com, 2015).

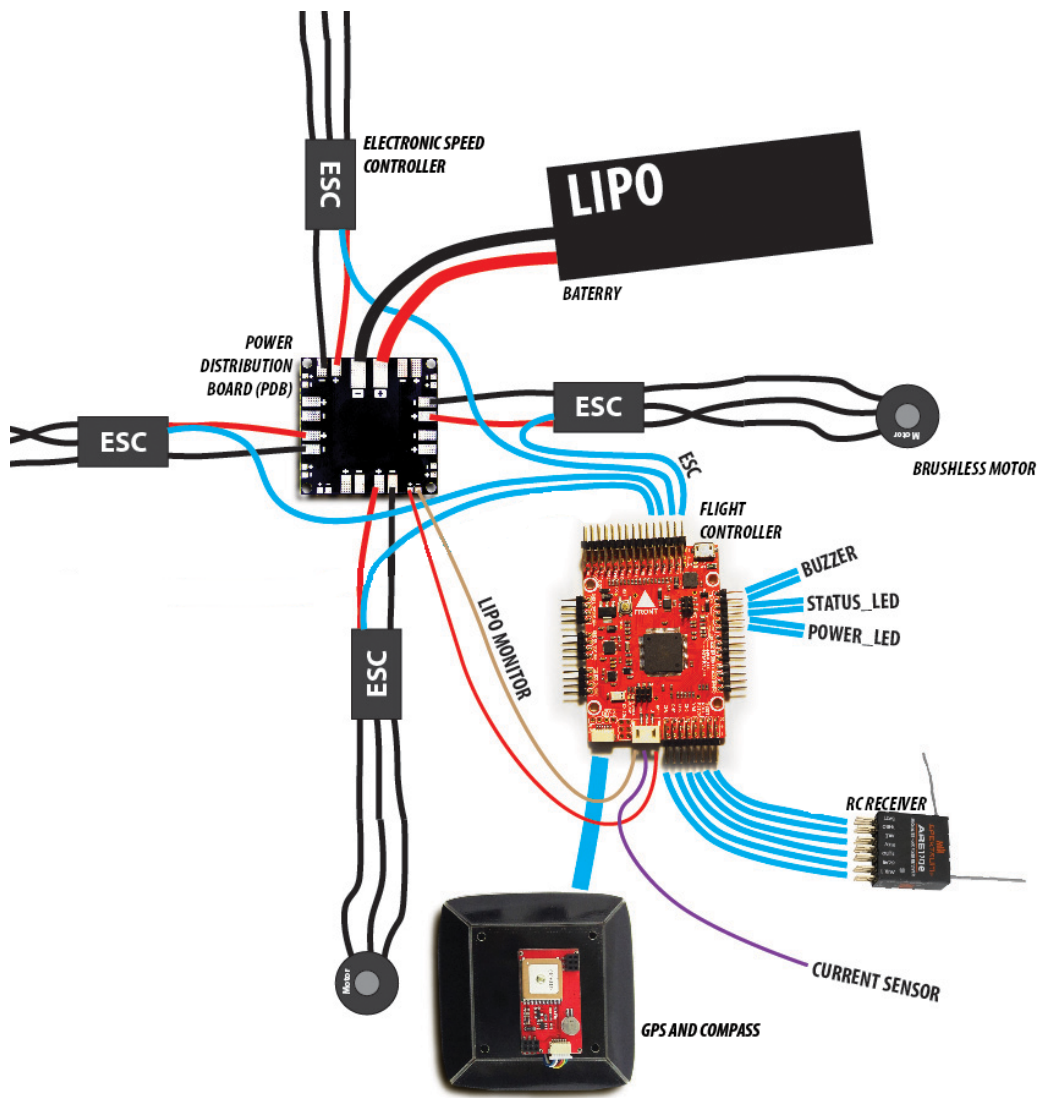


*Fig.A.2 A general schematic of a UAV wiring (image modified from one in [www.diymulticopter.org](http://www.diymulticopter.org))*

The most important factor that affects the vibration is the frame. Frame arms should be as rigid as possible. Carbon fiber armed copters and copters with injection-molded exoskeletons perform much better than cheaper frames, which tend to be flex. It is also very important to assemble secure and flex-

free all the conjunctions like motors to frame arms, frame arms to central hub and accessories to frame. Another factor that plays a role in the vibration is the propellers. They should be fully balanced. The size and the slope are important. Large slow propellers will induce more vibration than small fast ones. In addition, the material from which they are made of affects the vibrations. Carbon fiber-made have the best performance.

Since the UAV has been assembled following the guides for minimizing the sources of vibration, a further optimization step can be implemented. More precisely, the flight controller mounting plate can be installed on the central hub using anti-vibration absorber rubber balls. Inserting inside the rubber balls squeezed PVC foam earplugs can enhance this technique. The earplugs provide an additional damping medium with a different frequency damping range. The earplugs also stiffen the bulb mounts up a bit, preventing excessive free motion from being caused by normal flight maneuvers.

#### A.1.3 Magnetic interference

An additional factor that should be minimized since it degrades the performance and can cause serious problems in various flight modes is the magnetic interference. The DC currents of the UAV cause this interference. The places where DC current exists is in the power distribution board (PDB) and the wires between the ESC and PDB. To combat this effect the following techniques can be adapted:

- Keeping the length of DC current wires as short as possible.
- Placing the external GPS and compass module above the FMU and the PDB in the lowest part of the central hub to ensure the greatest distance between them.
- In cases where it is feasible, twisting the wires between the PDB, ESC and battery and using grounded shielding.
- Finally, using 4-in-1 PDB and ESCs instead of 4 separate ESCS and a PDB, which is the case in our project, so as to produce less

interference since all the circuitry is enclosed in an aluminium case without any free wires running along (fig.A.3).

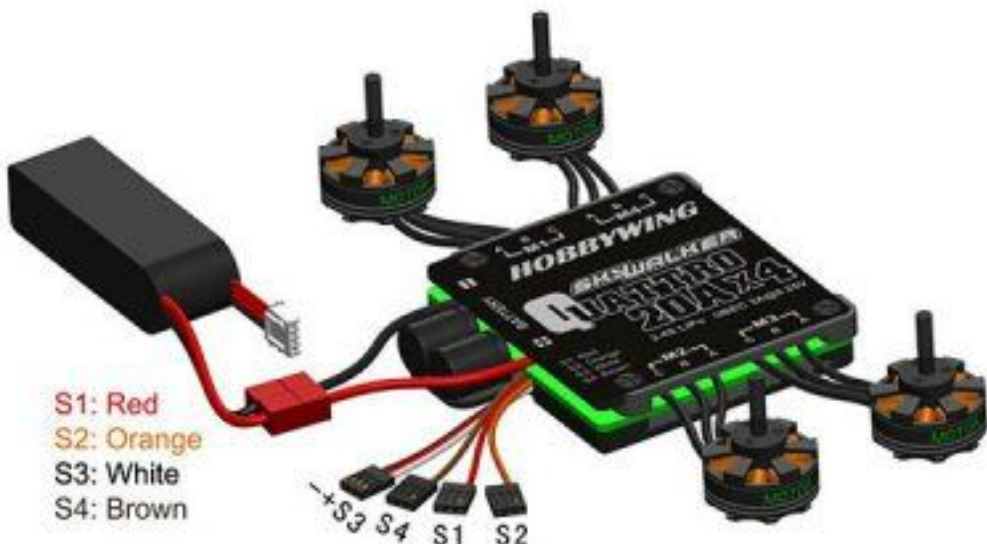


*Fig.A.3 4-in 1 ESC and PDB module for less magnetic interference (image from [copter.ardupilot.com](http://copter.ardupilot.com))*

#### A.1.4 Power module

The project's UAV is powered by Lithium – Polymer (LiPo) batteries. This type of batteries is the preferred power source for the most electric models. The advantages of employing them are the high discharge rates and the high-energy storage/weight ratio. However, they require special handling and charging. The most important matter to consider is the safety. Specific chargers should be used specifically designed to charge LiPo cells with the correct parameter set such as correct voltage and cell count.

In addition to the batteries, in order to provide filtered clean power to the FMU without glitches, a power module has been installed (fig.A.4). Through the 6P cable, it provides stable 5.3V voltage as well as current consumption and battery voltage measurements to the FMU. This module does not provide power to the

ESCs, which are fed directly from the LiPo batteries through the power distribution board (PDB).



*Fig.A.4 Flight control board power module T plug (image from [www.littleblupigs.com](http://www.littleblupigs.com))*

## A.2 Flight controller

The flight controller or flight management unit (FMU) is the nerve center of the UAV. This component is a microcontroller and gathers all the connections from the various accessories. It sends the appropriate commands to the ESC and receives data from the sensors, the GPS and the compass as well as the telemetry link. The flight controller provides a built-in inertial measurement unit (IMU) and a barometer. The IMU, in general, is a component that integrates accelerometers and gyroscopes. It receives data from both and using sensor fusion algorithms it can estimate the current position and attitude of the UAV. The main usage of the barometer is to inform an estimation of height for altitudes above 10m.

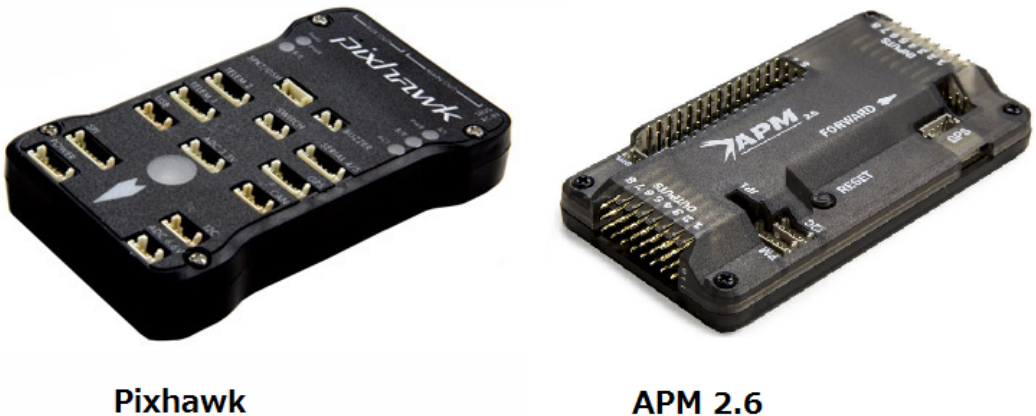


*Fig.A.5 The most popular flight controllers: Pixhawk and APM 2.6 (image from [copter.ardupilot.com](http://copter.ardupilot.com))*

There are two dominant flight controllers in the market (fig.A.5), the APM 2.6 and the Pixhawk. The APM 2.6 is a complete open source autopilot system. It is based on the mega microcontroller based on the Atmel's 8bit ATMEGA2560 chip. It includes a 3-axis gyro and accelerometer (6-DOF MPU-6000) and a barometer (MS5611-01BA03). It is compatible up to the APM:Copter 3.2 version firmware. Generally speaking, it is the most popular and bestselling flight controller with a large supporting community and plenty of online tutorials ranging from simple use to code developing.

On the other hand, the descendant of the APM is the Pixhawk board. The need of having a board that can offer more processing power and more available memory lead the ETH's PX4 team to design it. Pixhawk is an advanced autopilot system designed by the PX4 open-hardware project. A 32-bit ARM Cortex M4 processor running NuttX real time operating system (RTOS) powers it. It provides abundant connectivity options for additional peripherals (UART, I2C, CAN). It also has a MicroSD card slot for data logs.

Essentially, the difference between the two flight controllers is that the APM is old, well tested, and fully featured, but at the end of its development cycle. The Pixhawk board is new, is more powerful, but it has not been as fully tested, and it has a lot of promise for the future. For the current project

although the time frame of developing an application was very restricted, the need of flight controller that can support various advanced sensors and provide capabilities to implement obstacle avoidance techniques restrict the available choices. APM has been satisfying the need for a tried and tested configuration, with a large support and availability of many tutorials since there was no prior experience, yet the Pixhawk has been chosen in order to accommodate the project's enhanced requirements. The Pixhawk is more complex with a restricted knowledge base and a single point of support. It is a new project and quite immature compared to APM but it is the only tool if one wants to carry out professional projects.

### A.3 Telemetry

Telemetry is a popular accessory added in UAVs that provides an air-to-ground data link between the autopilot and your ground station laptop or tablet. Although it is possible to control the UAV via the telemetry stream, it is safe to use an additional remote control (RC) for that, due to the superior reliability of that dedicated radio link and controller.

The telemetry equipment supports two transmission frequencies bands, the 433MHz and 915MHz radio links. The former is selected (fig.A.6) for the current project, mainly for the following reasons:

- The 433MHz is legal in Europe
- The 915MHz interference with the GSM bands, so in regions where mobile antennas exist (more in urban areas) it is more likely to have worse communication.



Fig.A.6 433MHz radio telemetry kit (image from [www.rctimer.com](http://www.rctimer.com))

The project's quad copter is equipped with an open source implementation of the Xbee replacement radio set. It is fully compatible with the 3DR radio system which is the market standard yet significantly cheaper. It has a range of approximately 1 mile using transmit power up to 20dBm. It uses the MAVLink communication protocol (Micro Air Vehicle), which is a very lightweight, header-only message marshaling library. It supports both frequency hopping spread spectrum (FHSS) and adaptive time division multiplexing (TDM).

#### A.4 GPS and compass module

This component includes a GPS and a compass (fig.A.7). The GPS component is the u-blox 6-position engine, a low power consumption high performance GPS adapted to the miniature form factor (NEO-6 series, 2011). It uses the NMEA protocol with baud rate equal to 9600 and 5Hz update rate. The other component is the HMC5883L compass. It is a popular magnetometer with 1-

2 degree compass heading accuracy. It is considerably fast reaching 160Hz maximum output rate (3-Axis Digital Compass IC HMC5883L, 2010).



*Fig.A.7 Neo 6M GPS and MAG v1.2 module (image from [www.rctimer.com](http://www.rctimer.com))*

## A.5 On-board computer

On-board or companion computers, are single board computers that add the real intelligence to the UAV or generally in a robotic system. Admittedly, the addition of on-board computer adds to the restricted payload of a UAV but there is no other way to develop a sense of autonomy to the vehicle. It is noteworthy that the flight controllers (APM or Pixhawk) are not capable of executing complex computer vision or SLAM (Simultaneous Localization and Mapping) algorithms.

From a technical point of view, the actual operation of companion computer is that it can be used to interface and communicate with the flight controller using the MAVLink protocol. Aside from the inter-communication of the subsystems of the vehicle, this protocol is also utilized for the communication between the ground control station and unmanned vehicle. In my case, the companion computer gets all the MAVLink data which are produced by the

autopilot, GPS and the sensors' readings, and can use them to make intelligent decisions during a flight.

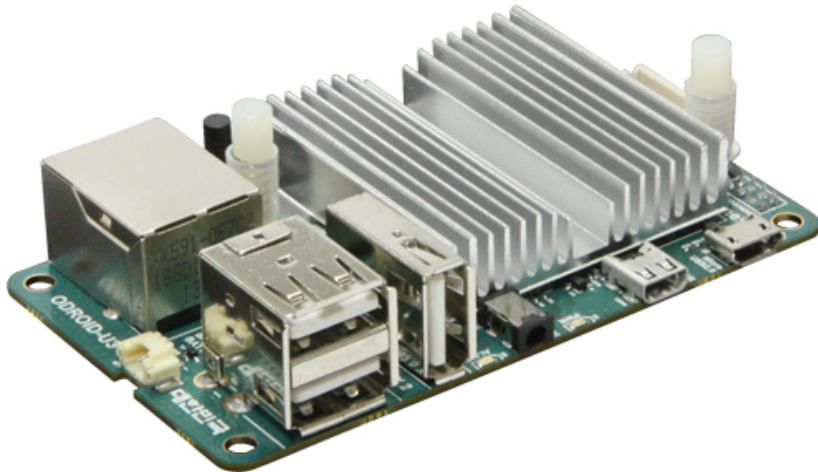


*Fig.A.8 Odroid-U3 companion computer for robotics applications (image from [www.hardkernel.com](http://www.hardkernel.com))*

For the project's UAV, the Odroid U3 mini-computer was employed (fig.A.8). The selection of the specific model was based on the recommendation of the PX4 development community. More precisely, the requirement was to use a mini-computer having the computational power to support a slim Linux version running ROS. Odroid U3 is powered by a 1.7GHz Quad-Core processor and a 2GB RAM. It supports MicroSD and eMMC storage. The latter is 4 times faster than the Micro SD, which allows executing computer vision and robotics algorithms. It hosts 3 high-speed USB2.0 ports and 100Mbps LAN. Odroid U3 on-board computer has also a serial UART port in order to provide system console interface for platform development and debugging. All in all, it is a card-size (83 x 48 mm), light (48g including the heat sink) yet powerful minicomputer, which ideally complies with the robotics control requirements.

## Appendix B

### Sensors Circuits

In this chapter I present all the circuits I utilized to experiment with the sensors. It includes the schematics, the tables with the pins connections as well as comments about specific aspects and behaviours I experienced.

#### B.1 Ultrasonic sensor

Devantech SRF02 features both I2C and Serial Interfaces. For the experiments, the later was used. The serial interface is a standard TTL level UART format at 9600 baud and can be connected directly to the serial ports on any microcontroller. In my case the microcontroller was an Arduino Uno and the exact circuitry is shown in figure (fig.B.1).

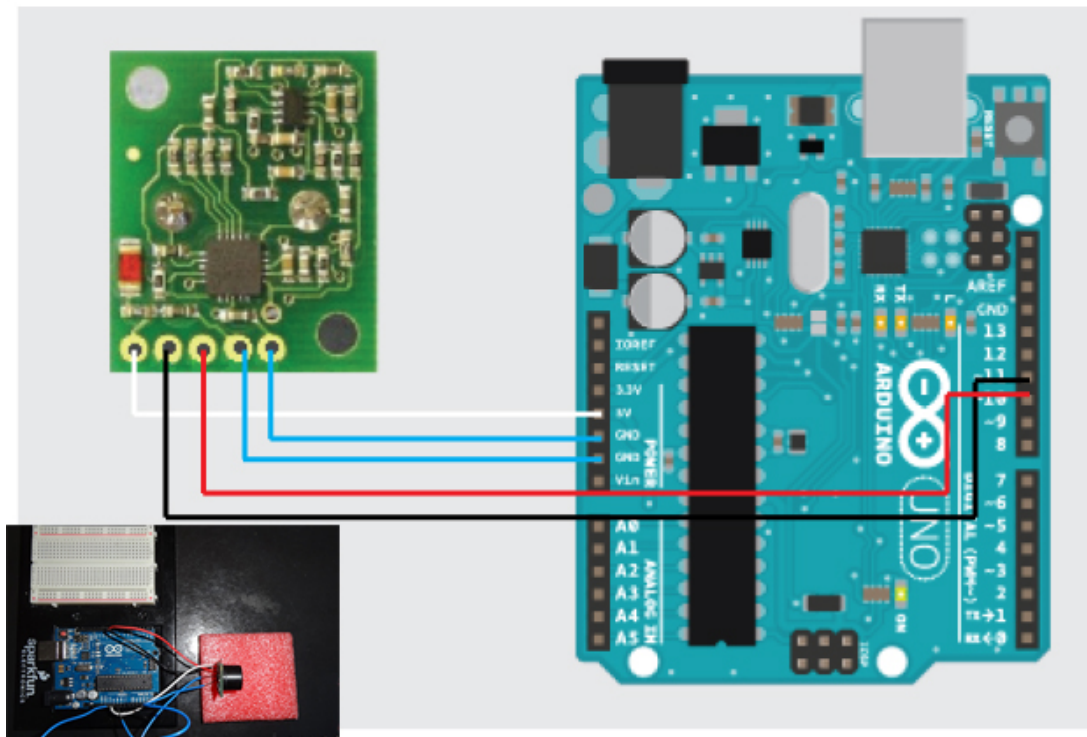


Fig.B.1 SRF02 interfaced with an Arduino Uno

The circuit connections are described in the following table (tbl.B.1):

*Table B.1  
(Connection between SRF02 and Arduino Uno)*

<b>SRF02</b>	<b>Arduino Uno</b>
5V Vcc	5V
Rx	11 digital (Tx)
Tx	10 digital (Rx)
Mode	GND
Ground	GND

To select Serial Connection the mode pin should be connected to ground. The Arduino sketch that was used for the measurements is included in the appendices and the online repository ([goo.gl/buq1hn](http://goo.gl/buq1hn)).

## B.2 Infrared sensor

Sharp GP2Y0A02YK0F infrared sensor has an analog output that varies from 2.8V at 15cm to 0.4V at 150cm with a supply voltage between 4.5V and 5.5V. In order to experiment with the IR sensor, the most convenient way was to use the analog port of an Arduino Uno microcontroller instead of using multi-meter and calculator. The interface between the sensor and the microcontroller is shown in figure (fig.B.2).

The explanation of the circuit connections is depicted in the table (tbl.B.2). The required Matlab file for the conversion and the Arduino sketch are included in the appendices and the online repository ([goo.gl/oHyf0l](http://goo.gl/oHyf0l)).

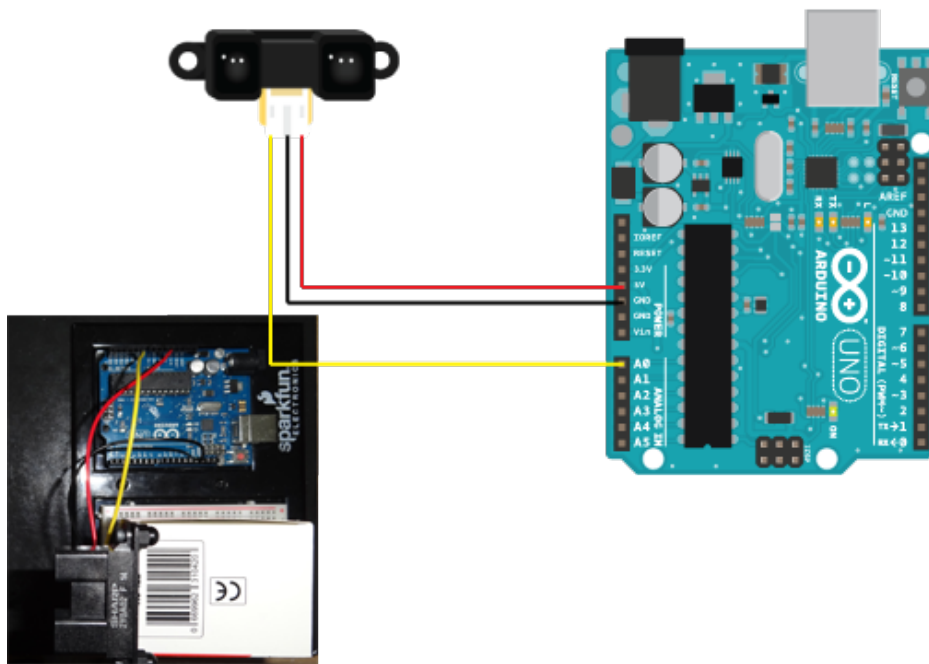


*Fig.B.2 GP2Y0A02YK0F interfaced with an Arduino Uno*

*Table B.2*

*(Connection between GP2Y0A02YK0F and Arduino Uno)*

<b>GP2Y0A02YK0F</b>	<b>Arduino Uno</b>
5V V <sub>cc</sub>	5V
V <sub>o</sub>	A0 analog
Ground	GND

### B.3 Optical sensor

Px4flow smart camera supports various interfaces. The available connections include I2C, micro USB and two USART serial communication ports. For the project's experiments I utilized the first two inputs. For the I2C interface, there was no provided cable on the delivered package. To overcome this lack, I assembled a custom cable using the required Hirose DF13 4 positions plug.

Before starting any use of the px4flow, there are two required procedures that have to be performed. Both tasks were performed using the QGroundControl program ([goo.gl/71fQ2M](http://goo.gl/71fQ2M)).

- The device should be updated to the latest firmware.
- When using the Video Downlink widget from QGroundControl, the focus should be adjusted by loosening the locking screw and turning the lens at an object at 3m distance.

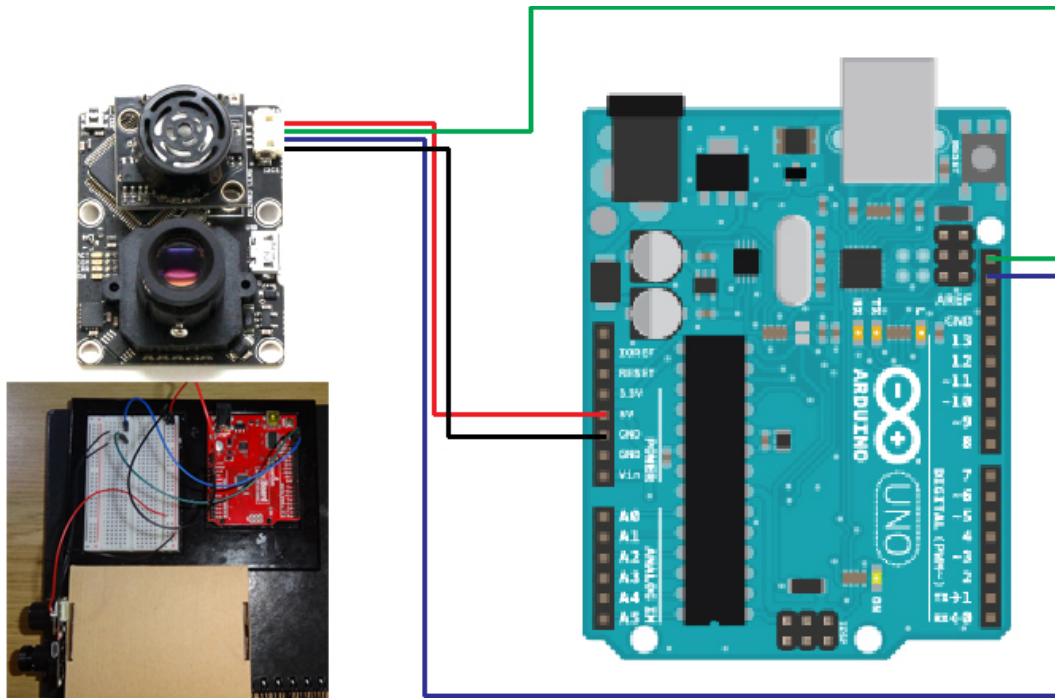


*Fig.B.3 Px4flow interfaced with an Arduino Uno*

The diagram of the circuit is shown in figure (fig.B.3). Moreover, the following table (tbl.B.3) illustrates the required connections to use the sensor in the I2C mode.

*Table B.3  
(Connection between px4flow and Arduino Uno)*

Px4flow	Arduino Uno
5V V <sub>cc</sub>	5V
SCL	SCL
SDA	SDA
Ground	GND

The required sketch is included in the appendices and the online repository ([goo.gl/MGtnhO](http://goo.gl/MGtnhO)).

In addition to previous setup, it is possible to utilize px4flow using ROS drivers. For this case, the device is connected via a USB cable to a computer running ROS (fig.B.4). In order to obtain data from the device, it requires installing the *px-ros-pkg* stack ([goo.gl/bvo1cf](http://goo.gl/bvo1cf)) in a working catkin workspace. After that, following the guide from the px4flow node documentation ([goo.gl/n8IMX9](http://goo.gl/n8IMX9)) it is very easy to have access to the video from the camera as well as to the *opt\_flow* topic. The *OpticalFlow.msg* type messages that are published in this topic include information such as the ground distance, the flow in x and y direction, the velocity in x and y direction and the quality of the optical flow estimate. The experiment was performed using ROS Hydro installed on Ubuntu 12.04 LTS. In order to access the device using the proposed launch file, the proper access permissions should be set for the device, for instance (*sudo chmod a+r /dev/ttyACM0*). In addition, the exact device, for example *ttyACM0*, should be declared in the *px4flow\_parameters.yaml* file that stores the global settings of the corresponding launch file.

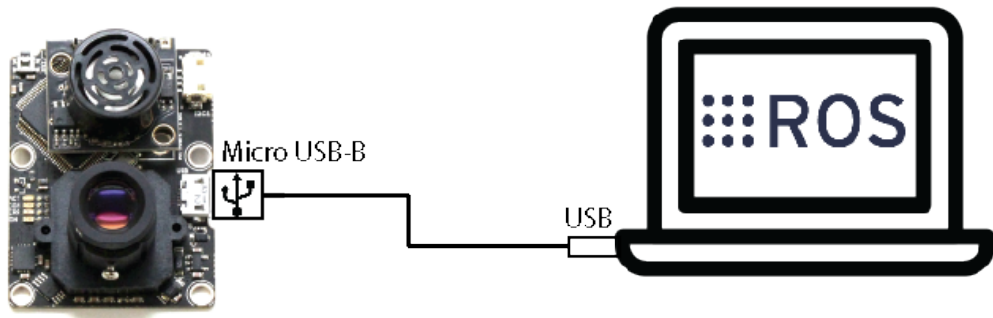


Fig.B.4 Px4flow interfaced ROS

#### B.4 Laser sensor

LIDAR-lite laser sensor supports two communication methods, I2C interface and PWM (Pulsed Width Modulation). For the experiments, the former was

employed. As with the previous sensors, an Arduino Uno was used to interface with the sensor. More precisely, the sketch utilizes the “Arduino I2C Master Library” from the DSS Circuits (Truchsess, 2015), which is a more sophisticated I2C library than what the default Wire library Arduino IDE offers.

The diagram of the circuit is shown in the figure (fig.B.5). Furthermore, the following table (tbl.B.4) illustrates the required connections in order to use the sensor in the I2C mode.

*Table B.4*  
(Connection between LIDAR-Lite and Arduino Uno)

LIDAR-Lite	Arduino Uno
5V V <sub>cc</sub>	5V
PWR EN	(unused)
MODE	(unused)
SCL	SCL
SDA	SDA
Ground	GND

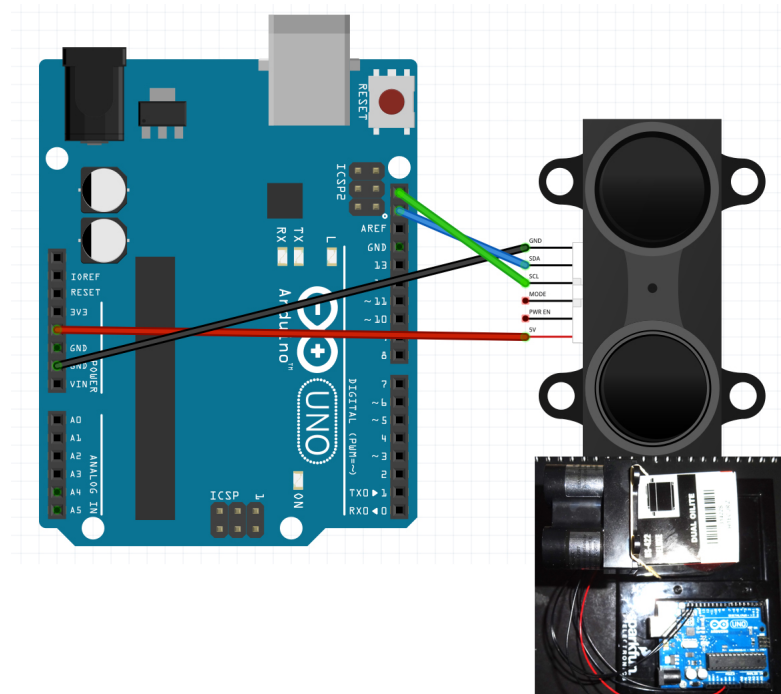


*Fig.B.5 LIDAR-Lite interfaced with an Arduino Uno*

The required sketch is included in the appendices and the online repository ([goo.gl/DSToIp](http://goo.gl/DSToIp)).

## B.5 Laser applications

For the mapping and proximity application the same setup was used. Particularly, both applications required the combination of the laser sensor with an Arduino Uno microcontroller and a servomotor (fig.B.6). For the interface between the laser sensor and the Arduino Uno, the I2C library, which was developed by the DSS circuit, was utilised. At the same time, I experimented with taking a distance reading using Pulse-Width Modulation (PWM), which does not require I2C communication. Although it is a simpler approach, it lacks of precision. Using this approach there is no available method to calibrate the sensor. On the other hand, using the I2C approach there is an easy zeroing procedure where the user should only set the value of a specific register (*CalibrationOffsetValue*) with the required offset.

The motion of the servo was implemented using the Servo library. For the mapping task I used the convenient methods *read* and *write*. The first command reads the current angle of the servo while the second writes a value to the servo, controlling the shaft accordingly. Using the provided servo, this will set the angle of the shaft (in degrees), moving the shaft to that orientation. For the proximity application, which was more demanding in terms of accuracy, speed and synchronisation of the movement, the *writeMicroseconds* command was used. It writes a value in microseconds (uS) to the servo, controlling the shaft accordingly. For the provided servo, this will set the angle of the shaft. Further on that, using that method the servo was calibrated exactly to the proper (uS) so as to correspond to the required angles. Thus, the 555uS corresponds to 0 degrees, the 1500uS to 90° and the 2390us to 180° for this specific servo.

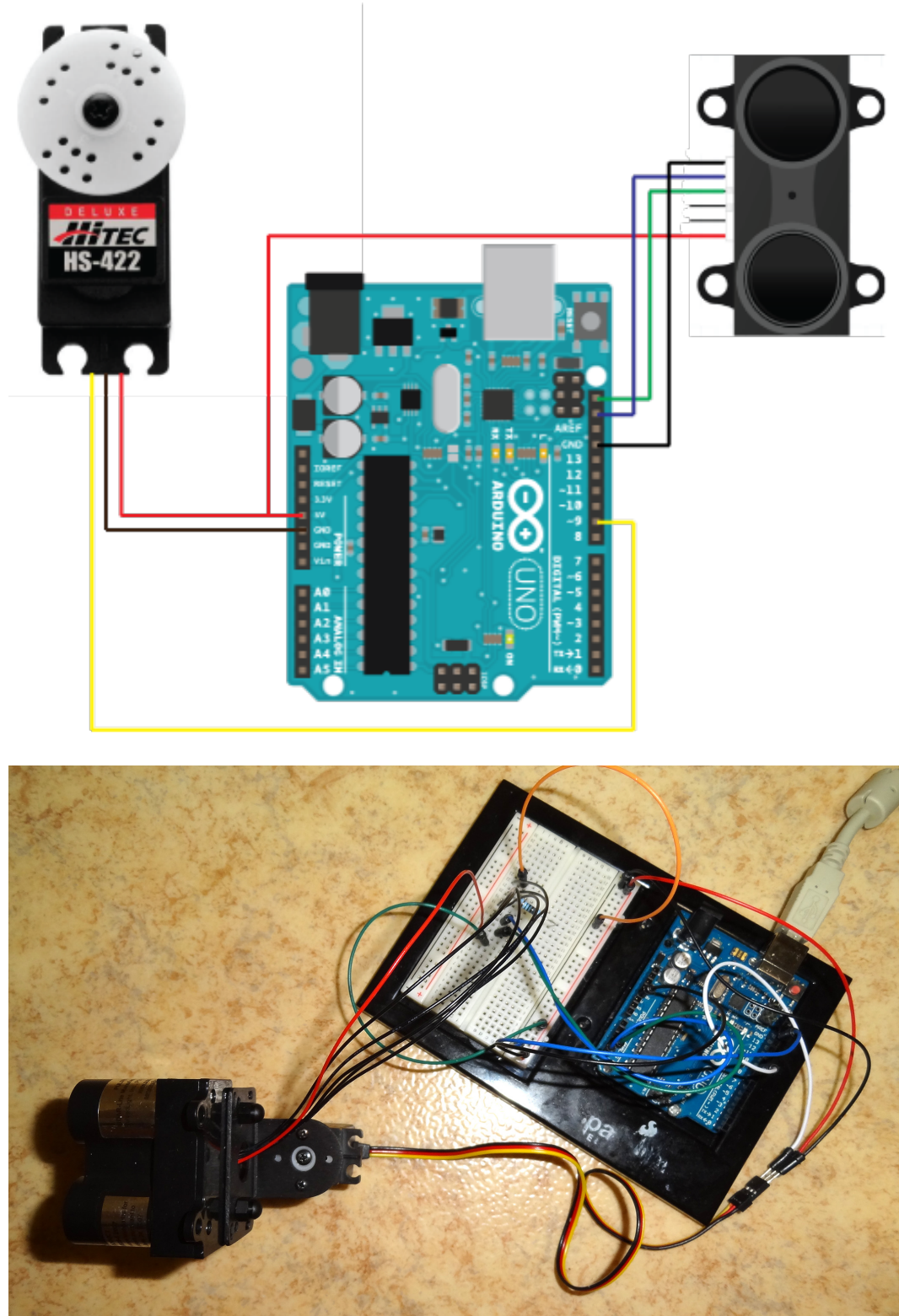


*Fig.B.6 LIDAR-Lite, servo HS-422 deluxe connected to an Arduino Uno. The schematic of the circuit and a photo of the real implementation.*

The connections required between the individual components for the proposed circuit are clarified in the following table (tbl.B.5)

*Table B.5**(Connection between LIDAR-Lite, servo HS-422 and Arduino Uno)*

<b>LIDAR-lite</b>	<b>Arduino Uno</b>
Pwr en	(unused)
Mode	(unused)
SCL	SCL
SDA	SDA
GND	GND

<b>HS-422 Deluxe</b>	<b>Arduino Uno</b>
Signal	9 Digital PWM
5V V <sub>cc</sub>	5V
GND	GND

The code, which has been developed for the presented applications, is included in the appendices section and the online repository ([goo.gl/99Nxqj](http://goo.gl/99Nxqj)).

For the mapping application the user should first execute the Arduino sketch and afterwards the related Matlab file. There is also the requirement to add in the Matlab's path the *ransac\_homography* library ([goo.gl/5yR8IX](http://goo.gl/5yR8IX)).

For the proximity application the ROS and Ubuntu version depends on which board is used. Therefore, Arduino Nano is compatible with ROS Hydro and Ubuntu 12.04 LTS while the Arduino Uno is compatible with ROS Indigo and Ubuntu 14.04. It is observed that in the case of Arduino Nano (fig.B.7), it is better to provide external power supply at least to the servo since the system, if based only on the Nano feed, is unstable. In order to upload the code in the board the appropriate access permission should be set for this device. For instance, in Ubuntu the user need to type: *sudo chmod a+r /dev/ttyUSB0*, if the board is connected at *ttyUSB0*. After that, and assuming that the *roscore* is run, the user employ the *rosserial* package by giving a command like: *rosrun rosserial\_python serial\_node.py /dev/ttUSB0*.

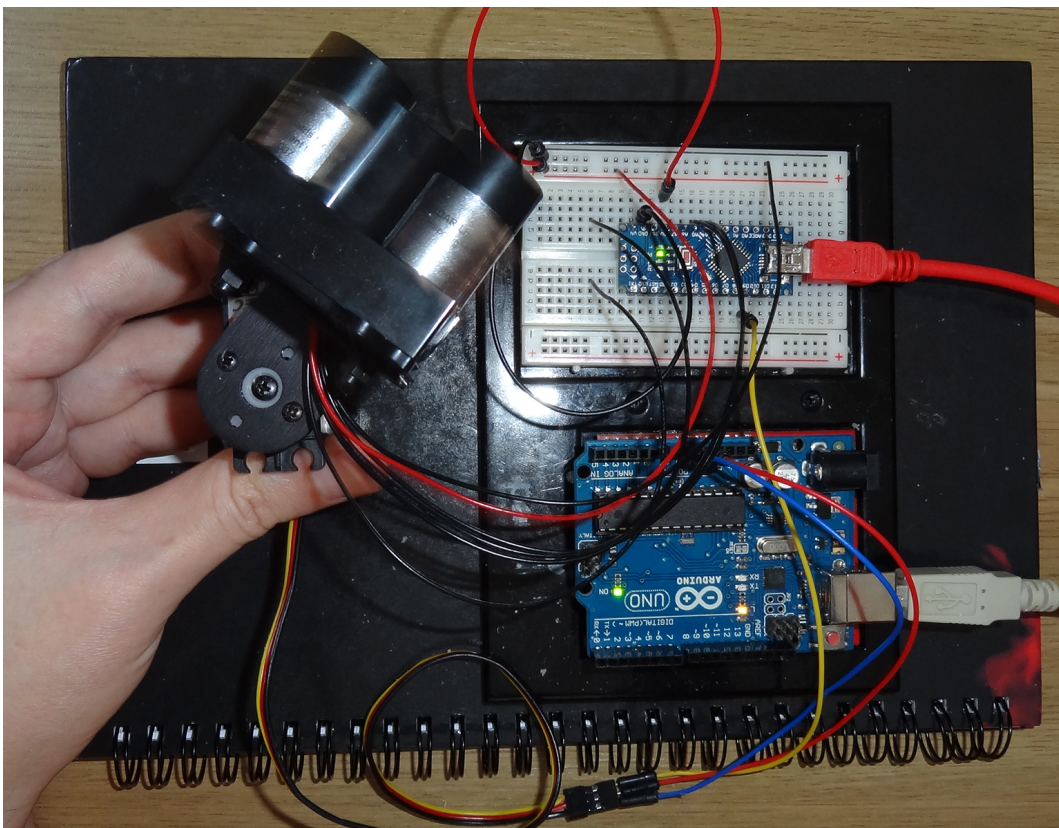


*Fig.B.7 LIDAR-Lite, servo HS-422 deluxe connected to an Arduino Nano. Arduino Uno provides only power supply to servomotor.*

# Appendix C

## Simulation

### Topics

#### C.1 ROS

The Robot Operating System (ROS) is a set of software libraries and tools that make it possible for the users to build robot applications. It is an open source project created by Willow Garage and maintained by the Open Source Robotics Foundation (OSRF). It is sponsored and supported from a wide range of well-known organisations and corporations such as NASA, DARPA, NSF and Bosch, Qualcomm and Mathworks.

The ultimate goal of using this framework is to enable rapid prototyping in robotics. Similarly the web 2.0 could be cited. By using tools like apache, MySQL and python in a Linux environment, it was made possible to move from static web pages to dynamic or user-generated content and the growth of social media. Likewise this example, there is a need for a group of tools, compatible to each other that will boost the development in robotics field. Fortunately these days this can be realized, by exploiting the work of many individual developers' communities; there are many sophisticated and well supported tools like ROS as a framework, Gazebo for 3D simulations, Stage for 2D simulation, OpenCV for computer vision and many others more specialized in specific domains. All these packages are open sourced and structured in way that can be utilized easily by other platforms such as iOS and android.

ROS offers many advantages to the developers and based on these it has become a popular tool used in labs, classrooms and companies around the world. There is a 62% increase in the number of papers citing the ROS

overview paper (Quigley et al., 2009) from August 2103 to July 2014 according to the community metrics report (Conley and Foote, 2014). Some of the strong points that make ROS a dominant solution in robotics are the following:

- It is an easy to use, cross-language (C++, python, Lisp) inter-process communication system that is fairly versatile. It is based on TCP-IP as well as shared memory communications.
- It allows easy integration of a wide range of tools such as visualization of robot kinematics and sensor data, path planning and perception algorithms. In addition, it includes a wide range of low-level drivers for commonly used sensors.
- It is a fully scalable platform that can support anything from simple ARM CPUs to Xeon clusters.
- There is a large international online community that offers support in possible problems and requests, registering a total of 18.144 questions in the duration of one year (Aug.13 – Jul.14). Something that indicates the growing popularity of ROS is the fact that this number of questions is 38% higher compared to the previous year, according to the community metrics report (Conley and Foote, 2014).

Aside from the loud advantages that ROS has, there are also inevitable drawbacks. From my perspective, it has a very steep learning curve; it is not easy for new users to grasp. The users should spend considerable time to install the packages in Linux machines and solve any dependency incompatibilities between the different versions and computer configurations. As a result at the beginning of the process a lot of effort is spent for the setup rather than the design and understanding of the algorithms. Despite it not being clearly stated on the software, having good C++ skills is a strong advantage. Moreover, there are only a few books available to learn it, although the ros.org website offers many tutorials. As a result there are not many teaching alternatives to experimenting with a working ROS installation and starting from the classic turtle simulation, then

moving towards more complex structures like manipulators and mobile robots. At the end of the day, it is all about effort and time.

## C.2 Gazebo

Gazebo is a very popular tool in robotics simulation. Gazebo is a 3D simulator, while ROS serves as the interface for the robot. Combining both results in a powerful robot simulator. It allows rapid algorithm testing, robot design and regression testing using realistic scenarios. It can be used for both indoor and outdoor scenarios. In addition, it supports simulation of population of robots. Some of the great characteristics of Gazebo are the way by which it facilitates the integration physics engines and its high quality graphics. Furthermore, it offers convenient programmatic and graphical interfaces. Using Gazebo the users have access to a wide range of ready-made robot models and sensors with noise. Having said that, it is also possible for the users to use a specific language called SDF to build their own models and sensors too. Finally, by using Gazebo, users have access to multiple high-performance physics engines, which can easily simulate effects on illumination, gravity, inertia and other physic entities.

All in all, Gazebo is a great tool that every roboticist should have available in their toolbox. It speeds up the testing in difficult or dangerous scenarios without any harm to the robot. Most of the time it is faster to run a simulator instead of starting the entire procedure on a real robot. From my personal experience of using this tool, I concluded that it is that sometimes unstable and gives errors while other times it executes flawlessly without any change. It is computational-resources ‘greedy’ and highly affected by the graphics card’s characteristics and capabilities. It is probably inadvisable to execute Gazebo in machines with low resources.

### C.3 Terminology

There is a solid structure that a ROS system should follow independently of the programming language or the nature of the application. This allows us to have a simple standard code structure and to follow a schematic way of work.

Henceforth, there is a concise presentation of the ROS ecosystem (fig.C.1). References taken from (Bohren, 2015) and (ROS.org, 2015)

#### ROS Core

*ROS core* is a collection of nodes and programs that are pre-requisites of a ROS-based system. More precisely, it consists of three programs that are necessary for the ROS runtime. These programs are:

- *ROS master* which manages the communication connections. It provides name service in ROS.
- *Parameter Server* which stores persistent configuration parameters and other user-defined data.
- *Rosout* which is a network-based standard output for human readable messages.

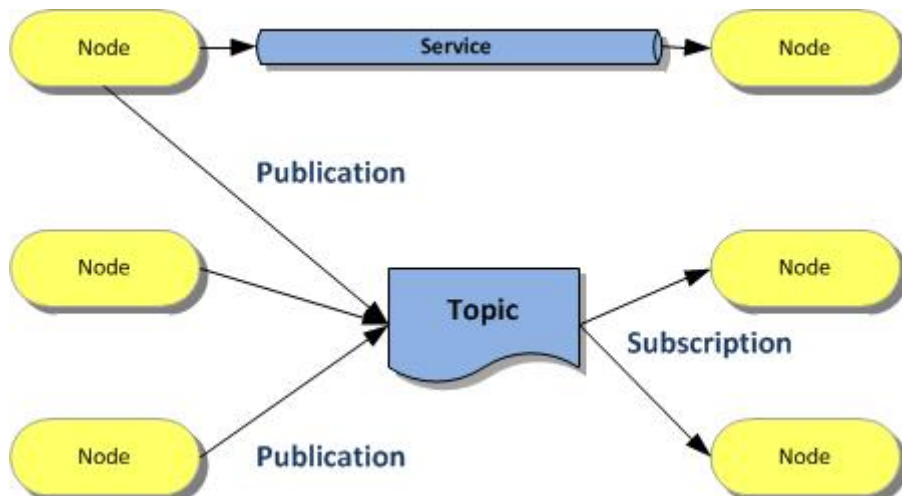


Fig.C.1 ROS structure of the basic elements (image from [generationrobots.developpez.com](http://generationrobots.developpez.com))

## Nodes

*Nodes* are executable files within ROS packages. They represent processes in a ROS network. Nodes use ROS client library to communicate with each other. They can publish or subscribe to a *Topic* and provide or use a *Service*.

## Parameters

During runtime there are data related to the configuration and initialisation stored in the Parameter Server called *parameters*.

## Topics

*Topics* can be perceived as data streams, asynchronous many-to-many ? between nodes. It should be used for continuous data streams like sensor data or robot state.

## Messages

As computer languages have supported data types, ROS supports *messages* used when subscribing or publishing to a topic.

## Services

ROS nodes can exchange data not only using topics but also using *services*. Essentially, they are synchronous one-to-many network-based functions. *Services* should be used for remote procedure calls that terminate quickly. For instance, a *service* can be utilized for querying the state of a node or doing a quick calculation such as inverse kinematics (IK). Not using them for longer running processes is recommended. Furthermore, *services* cannot support processes that might be required to preempt if exceptional situations occur.

## Actions

In cases where the service takes a long time to execute, the users might want the ability to cancel the request during execution or get periodic feedback about how the request is progressing. *Actions* provide the means to build specific servers that execute long-running goals that can be preempted. Moreover, it also provides client interface in order to send the related

requests. Thus, if a server is executing two action goals simultaneously, for each client a separate state instance can be kept since the goal is uniquely identified by its id.

#### C.4 ROS development approach

In the “Simulation” Part of the dissertation I have clarified the reason why the ROS framework is going to be employed with the integration of the Gazebo 3D simulator for the project’s simulation. On top of them, the Hector quadrotor will form the basis for my UAV with various sensors, customised as required. Even if the users have reached this stage of decision-making, the way in which they are going to work is not predefined. This is owed mainly to the way that ROS is built, giving the users complete freedom to implement nodes as long as they can conform to the communication protocols.

My first attempt to start developing ROS system nodes for designing simple robotics algorithms was to use Matlab’s robotics system toolbox. This is new feature of Matlab (R2015a). Robotics Toolbox provides an interface between MATLAB and Simulink and ROS that enables applications testing and verification on ROS-enabled robots and robot simulators such as Gazebo. It supports C++ code generation. Thus, it enables the generation of a ROS node from a Simulink model and deployment to a ROS network. This is a great addition to the strict ROS terminal based interface. Matlab suite and scripting language is developer friendly and it can boost the research and productivity in higher levels.

The way that Matlab and ROS work is based mainly on the TCP/IP communication (fig.C.2). Although Matlab can autonomously execute ROS master and host the entire ROS ecosystem, most of the time users need to experiment with third-party ROS packages. To host these needs, it is assumed that Matlab is installed in a windows or mac host computer. To

execute external ROS master, Matlab directs the users to download an Ubuntu virtual machine. After that, the users can normally execute any package in ROS master in the virtual machine and have access to topics and services from the Matlab in the host computer.

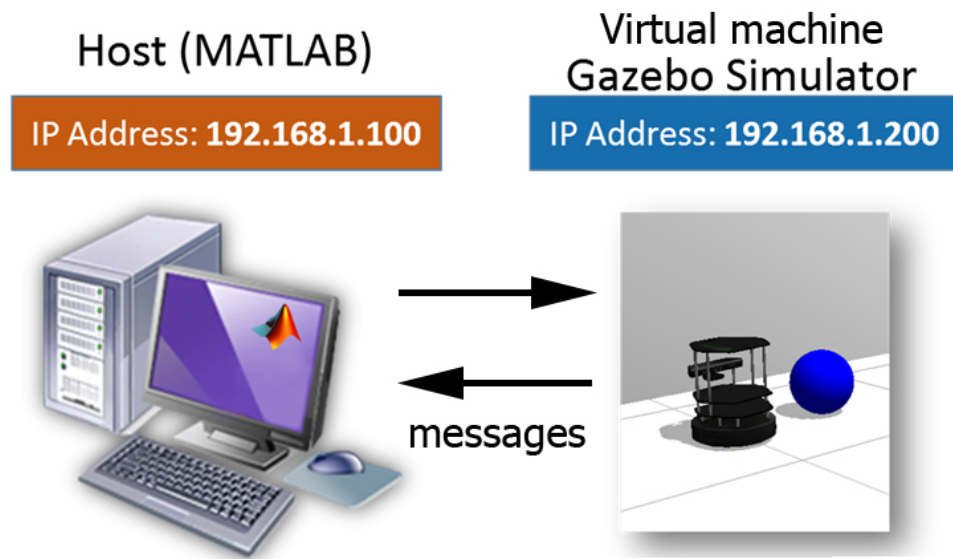


*Fig.C.2 Interface between Matlab and ROS (image modified from [www.mathworks.com](http://www.mathworks.com))*

The proposed way of work is convenient when there is a need to process data obtained from ROS nodes, transmitted using the topics. However, it is not straightforward to deploy more complex algorithms. From my experience in working with it, although I followed successfully all the learning material from the Matlab knowledge base, using the classic *turtlesim* simulation, when I attempted to get data from the Hector simulator I encountered problems. More precisely, Matlab couldn't receive laser scanning from hector quadrotor. In addition, the set up of working in two different places at the same time makes the workflow more complicated. In my opinion, the interface between Matlab and ROS is a very strong combination, which can exploit the advantages of both successful platforms. Nevertheless, the implementation was just released and it needs time to mature with bug fixes and optimization.

For my project, I wanted a simpler approach. I preferred a setup implemented with fewer stages in order to eliminate potential point of failures. The solution to that was to work directly on a ROS installation in Ubuntu using the terminal and a simple text editor. In my first attempt I utilized python language, for some people the free counterpart of Matlab. Python is a high level programming language, with enhanced readability. It is an interpreted language rather than compiled like C++. This means that in ROS the users merely have to develop scripts without caring about the settings in the *CMakeList.txt* file which configures the compilation. This is by itself a great advantage since these settings require a degree of experience to make them work correctly and efficiently.

The use of Python in ROS is officially supported and facilitates complex developments making the robotics rapid prototyping a reality. The syntax allows programmers to express concepts in fewer lines of code that it would be possible in languages such as C++. However, this level of abstraction and simplicity comes at a cost. From my experience, although the scripts were interpreted without any errors, the applications did not work. This is because there were errors in my code that were not reported from the lenient python interpreter.

The native ROS development language is C++. Using this language the users can develop everything they want in the ROS ecosystem. It requires having good programing skills in object oriented programming in C++. To compile the code the users should manually edit the settings in the *CMakeList.txt* file and *package.xml* file of the package. It is particularly hard at the beginning and even a simple task could take considerable time to accomplish. When the users acquire the needed experience, everything is simpler. On the other hand, the compiler is very strict compared to the python interpreter. If the users manage to compile the application successfully it is guaranteed that is going to work, unless it has logical errors. In addition, the compile error messages are self-explanatory and direct the users to the specific error. Finally, the syntax might not be so friendly like higher-level languages but it

is concise and integrates powerful structures and tools. In short, C++ on a ROS installation was the development method that I adapted since it was the most straightforward and simpler, in terms of configuration, approach I could apply.

## C.5 UAV manipulation input devices

By and large, the control of the UAV can be implemented by designing a publisher that transmits messages of type *geometry\_msgs/Twist* in the *cmd\_vel* topic. A recommended way to teleoperate the UAV is to use a joystick. The hector quad-rotor comes with a node that is configured to utilize the xbox controller for teleoperation. In order to achieve continuous movement, which is disabled for safety reasons, a specific parameter, *autorepeat\_rate*, should be enabled and set to the required rate. The edited launch file can be found in ([goo.gl/b63Ugr](http://goo.gl/b63Ugr)). Further than that, the throttle should also be adjusted to move the UAV smoothly. The required changes in the teleoperation node to achieve this can be found in ([goo.gl/K173HW](http://goo.gl/K173HW)).

There is also a simpler way to control the UAV using just the keyboard. To use the keyboard for the UAV manipulation the users should install an appropriate package that includes the required nodes. One option is to use the ROS package (*pr2\_apps*) developed by Willow Garage for the PR2 robot. Once the package has installed successfully, by executing the *teleop\_keyboard.launch* file the users can control the translation on the x and y axis, the yaw angle and the speed.

## C.6 System configuration

The proper setup of the working environment in ROS and Gazebo is a very hard task. Factors that need to be considered when the system is configured are the following:

- Operating system

It is recommended to use Linux. Actually, Linux is the only OS that is officially supported in ROS. The installation debian packages (unix archives) for ROS are available for Ubuntu Linux.

- ROS version

Following a developing cycle similar to Ubuntu, ROS releases new versions every 6 months to one year. At the time of the project implementation, the latest was Jade (May 2015). However, because of compatibilities issues a hydro version was used. This version was released in September 2013. Making this decision I was restricted to install Ubuntu 12 LTS (Long Term Support) as operating system in order to gain maximum compatibility.

- Gazebo version

Since ROS Hydro, Gazebo is considered a system package instead of a ROS package. The practical meaning is that one major version of gazebo is selected at the beginning of the ROS release cycle and remains the same during the whole life of the ROS distribution. In my case ROS Hydro is compatible with Gazebo version 1.9.

- Hardware

Hardware is also a parameter in simulation system. In case that the ROS is combined with Gazebo, there is a need for at least 4GB RAM. Gazebo requires a working graphics card with OpenGL 3D accelerated driver to perform various rendering and image simulation tasks correctly. For the current project, an extensive use of virtual machines was engaged. Particularly, I utilize both VMware Fusion and VirtualBox software supervisors. Moreover, there are available virtual machines with pre-installed ROS distributions, which could be easier for the beginners. All in

all, both virtualisation methods performed well, supporting the ROS ecosystem.

To summarize, my setup configuration based on virtual machines having Ubuntu 12.04 and 14.04 as operating system using ROS Hydro and Indigo respectively.

# Appendix D

## Mobile Applications

### Configurations

## D.1 UAV Teleoperation application

My scenario is based on the Apple's iOS device since I have a previous experience on coding for this ecosystem. The prototype application is visually structured for the layout of iPhone 5 (4 inches diagonal, 1136x440, 326ppi). The targeted version iOS version is 8.

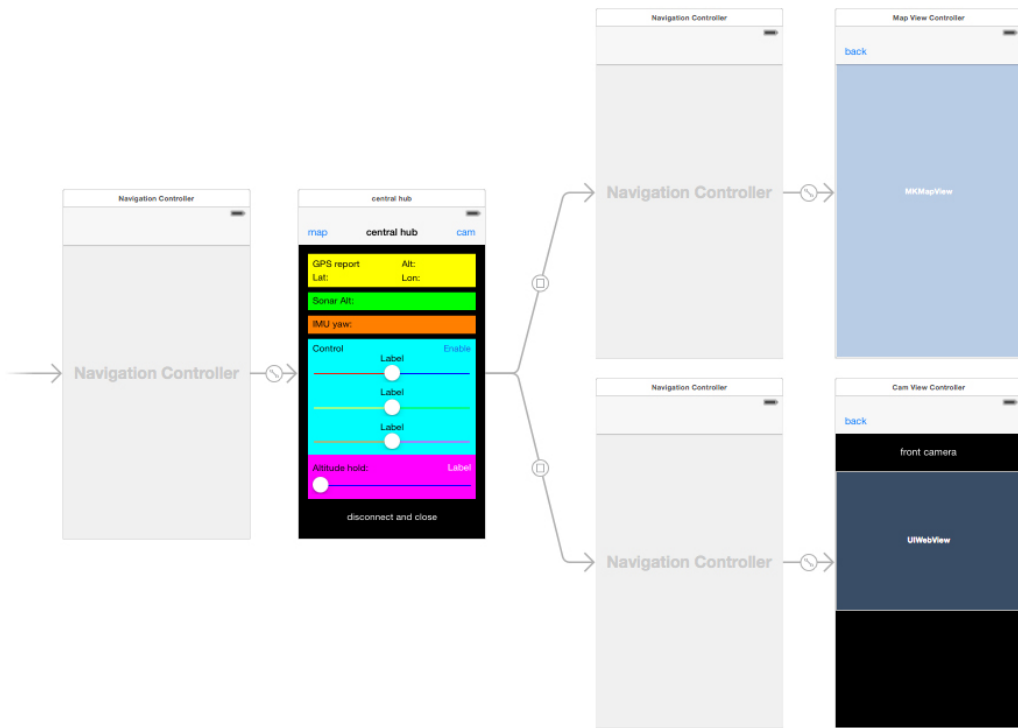


*Fig.D.1 The storyboard of the teleoperation application*

The implementation of the application was based on three *UIViewController*s embedded in navigation controllers (fig.D.1). The navigation between the

screens was accomplished using segues. In the projects' workspace, three external libraries have been imported, namely:

- SocketRocket
- RBManager
- MKMapView

As long as the control tab is enabled, the control messages are published in a continuous rate of 10Hz using an *NSTimer* object.

On the other side ROS was executed in a VMWare Virtual Machine. The ROS distribution was Indigo and the operating system Ubuntu 14.04 LTS. The simulation was based on Hector quad-rotor ROS stack. The host computer was connected with the iPhone via a Wi-Fi access point. The network topology is shown in figure (fig.D.2).

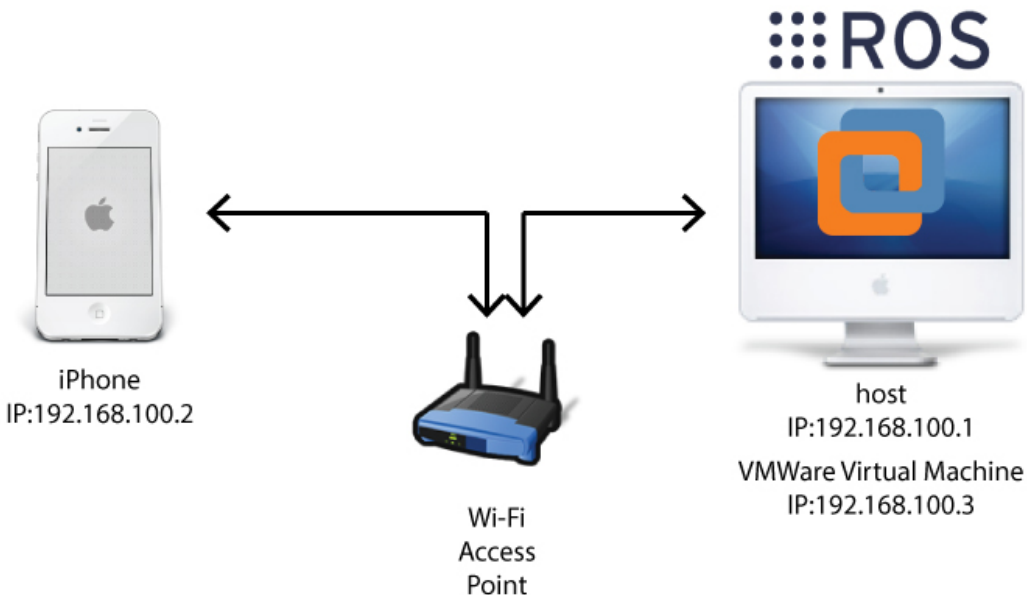


*Fig.D.2 The network topology of the development environment*

For a successful working scenario the *my\_hector* package, which was developed for the assisted obstacle avoidance flight mode, had to be installed. Particularly, the hover node had to be executed to allow the altitude hold mode (*rosrun my\_hector hover*). In addition, the *Rosbridge* and the *MJPEG*

server also had to be turned on and to be running using the following commands:

- *roslaunch rosbridge\_server rosbridge\_websocket.launch*
- *rosrun mjpeg\_server mjpeg\_server*

The iOS source files of the project are available online in the project's github repository ([goo.gl/TKlkE5](https://goo.gl/TKlkE5))

## D.2 Radiation mapping application

Similarly to the previous one, the radiation mapping application was developed based on the iPhone 5 screen dimensions. Consequently, the layout and the size of the elements are adapted to this device. The minimum supported iOS version is the 7<sup>th</sup>.

The implemented application consists of three *UIViewControllers* embedded in navigation controllers (fig.D.3). The main data structure that holds the mapping data is an *NSArray*. The elements, which the mapping array stores, are objects that belong to the custom class *Measurement*. The advantages of using an array are: the potential future integration of a save and load mechanism as well as the easy handling of data as a set in the map visualization (redraw/clear).

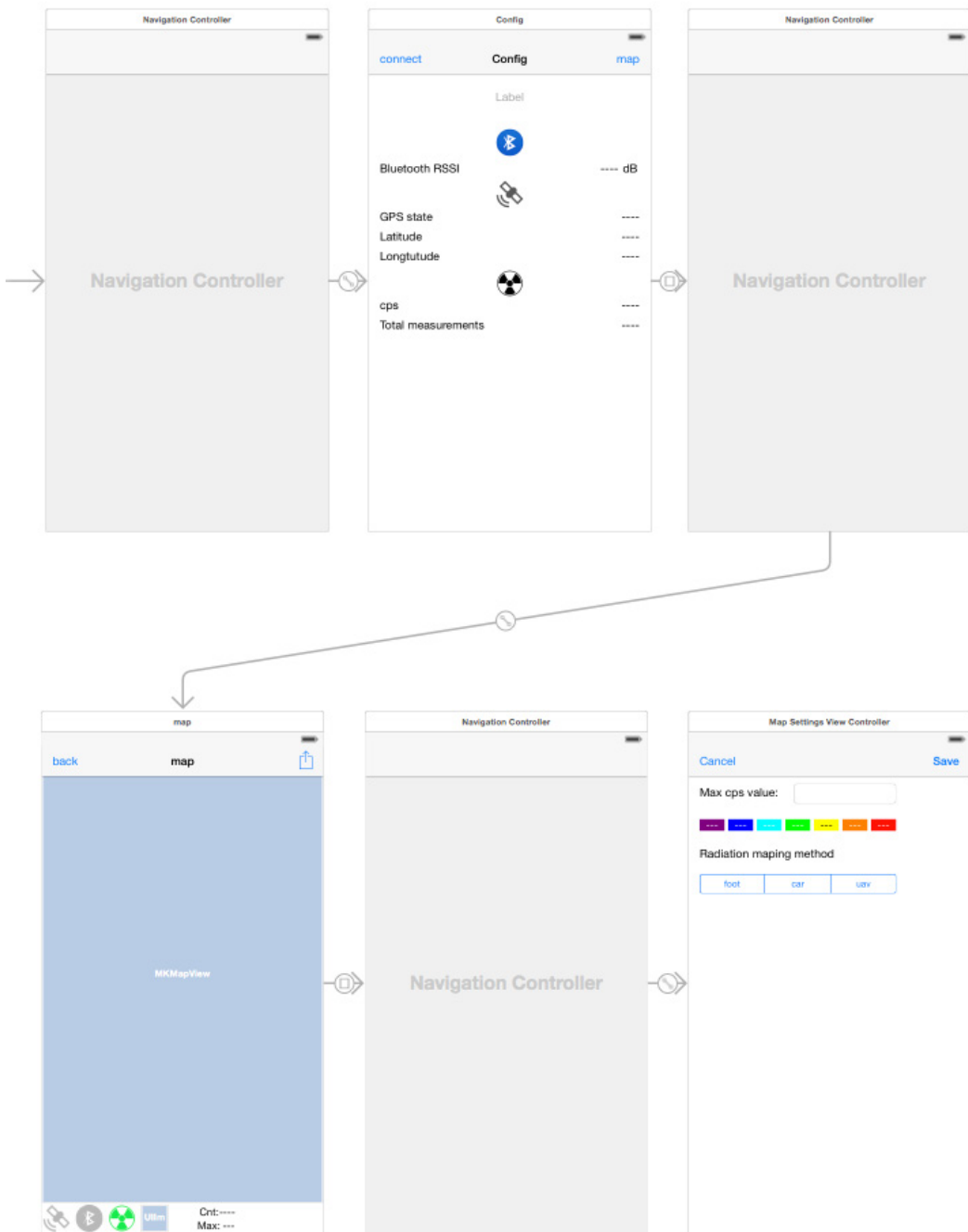


Fig.D.3 The storyboard of the radiation mapping application

The first screen is called “Configuration”. The related `UIViewController` is mainly responsible to handle the Bluetooth connection. It includes the entire set of the related methods, which are provided by the BLE library. When the user clicks the “Connect” button, using the appropriate sequence of methods’ execution, the Bluetooth connection is activated if a compatible device is enabled within the range. Afterwards, having established the connection, the

application receives the messages, which are transmitted from the measurement unit. The *UIViewController* has all the required tools to parse the payload of the messages. More precisely, at the beginning, two data structures are defined in order to handle binary floating-point numbers (32bit) and binary integer numbers (16bit). When the specific bit of the status byte gets enabled, the parsing of the raw bytes begins. The payload of the message contains information about the number of connected satellites, the longitude, the latitude and the CPS value. The last three elements are stored in a newly created *Measurement* object and then, in turn, this object is stored in the mapping array.

The next screen is the map. It can be switched on, on that screen, only if the GPS is locked. One noteworthy mechanism that has been implemented is the share of the same BLE manager with the previous *UIViewController*. Particularly at the transition, the same BLE manager is passed to the map screen. This is desirable because map screen needs to receive messages and status information for the summary section. Before the transition is made, the reception of new messages is disabled in the previous screen and enabled in the new screen and vice versa for the reverse switch. In case of having individual BLE managers means that in the new screen the Bluetooth connection would have to be established again, which is unacceptable. Not only do the two screens share the BLE managers but they also share the mapping array. Consequently, this array is unique in the application and is passed to each active *UIViewController*.

Another important characteristic in the implementation of the map screen is the approach that enables the individual color of each point. The standard method of using *MKCircle* overlays does not support the selection of color for each point. It is possible to select only the color for the entire overlay. To extend the provided class, I used class inheritance and I sub-classed the *MKCircle* to create *MyCircle*. This approach allowed me to use the same standard visualization mechanism and at the same time satisfy the enhanced requirements.

The last noteworthy task implemented in this screen was the adaptive zoom level on the map. According to the value that the user selects in the next screen, the zoom level and the size of the circle, which represent the measurement, change. To reflect the change, all the measurements that are contained in the mapping array need to be redrawn. This is feasible using the developed helper methods.

In the third screen the user is provided with the option to select the maximum range of the CPS values color range and the mapping methods. The functionality is simple and when the user clicks the save button, the selected values return to the map screen and update the related features accordingly.

All in all, the navigation between the *UIViewControllers* is implemented using segues. The exchange of the data between them is accomplished using delegate methods.

On the other side the measurement unit consists of an Arduino Mega ADK as the base microcontroller and three shields (fig.D.4). The installed shields are namely:

- RedBear's lab BLE Shield
- Wireless SD Shield
- Adafruit Ultimate GPS

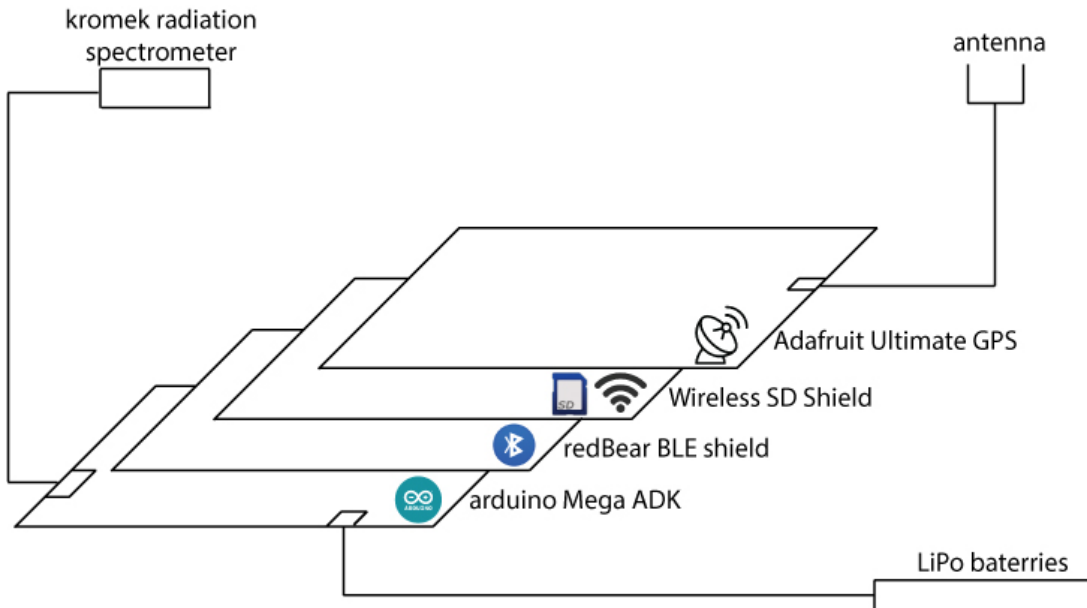


*Fig.D.4 The hardware profile of the measurement unit*

The Arduino sketch includes many external libraries in order to successfully support the operation of all the individual interfaces. The required libraries are:

- Adafruit GPS Library
- BLE
- RBL nRF8001
- TinyGPS
- USB Host Shield v2.0

One of the advanced features implemented in this Sketch is the break of the native data types to bytes in order to compose the payload of the message. The approach is very similar to what is implemented in the iOS side. Likewise, two data structures are defined in the beginning of the script. The first supports binary 32bits floats and the second binary 16bit integers. The data, using this mechanism, are broken to bytes and sent sequentially by employing the BLE shield.

It is important to cite that the initial IAC sketch was compatible with the Arduino 1.0.x IDE and not with the most recent 1.5.x and 1.6.x. versions. In order to avoid the required time to build the sketch from scratch, since it was

not working with the newer versions, I adapted the 1.0.x version by downgrading the BLE and the RBL nRF8001 libraries. This way I maintained the compatibility, in order to have a working set of code.

The iOS and Arduino source files of the project are available online in the project's github repository ([goo.gl/565h4M](http://goo.gl/565h4M)).

## References

3-Axis Digital Compass IC HMC5883L. (2010). 1st ed. [ebook] Available at: [http://www.adafruit.com/datasheets/HMC5883L\\_3-Axis\\_Digital\\_Compass\\_IC.pdf](http://www.adafruit.com/datasheets/HMC5883L_3-Axis_Digital_Compass_IC.pdf) [Accessed 9 Jul. 2015].

A.R. Al-Omari, M., A. Jaradat, M. and Jarrah, M. (2013). Integrated Simulation Platform for Indoor Quadrotor Applications. In: Proceedings of the 9th International Symposium on Mechatronics and its Applications (ISMA13). Amman, Jordan.

Bohren, J. (2015). ROS Crash-Course, Part I Introduction to ROS distribution, build system and infrastructure.

Bristol.ac.uk, (2015). Bristol University | School of Physics | About. [online] Available at: <http://www.bristol.ac.uk/physics/research/iac/about/> [Accessed 16 Jul. 2015].

Caa.co.uk, (2015). Unmanned Aircraft and Aircraft Systems | Aircraft | Operations and Safety. [online] Available at: <http://www.caa.co.uk/default.aspx?catid=1995&pagetype=90&> [Accessed 16 Jul. 2015].

Chen, M., Edwards, D., Boehmer, E., Eller, N., Slack, J., Speck, C., Brown, S., Williams, H., Wilson, S., Gillum, C., Lewin, G., Sherriff, M. and Garner, G. (2013). Designing a spatially aware and autonomous quadcopter. pp.213-218.

Conley, K. and Foote, T. (2014). ROS community metrics. [online] ROS. Available at: <http://download.ros.org/downloads/metrics/metrics-report-2014-07.pdf> [Accessed 30 Jul. 2015].

Copter.ardupilot.com, (2015). Vibration Damping | Copter. [online] Available at: <http://copter.ardupilot.com/wiki/initial-setup/assembly-instructions/vibration-damping/> [Accessed 8 Jul. 2015].

Crick, C., Jay, G., Osentoski, S., Pitzer, B. and Jenkins, O. (2011). Rosbridge: ROS for non-ros users. In: International Symposium on Robotics Research (ISRR 2011),.

Cyberbotics.com, (2015). Webots: robot simulator - Overview. [online] Available at: <https://www.cyberbotics.com/overview> [Accessed 30 Jul. 2015].

Developer.apple.com, (2015). UIWebView Class Reference. [online] Available at:  
[https://developer.apple.com/library/ios/documentation/UIKit/Reference/UIWebView\\_Class/](https://developer.apple.com/library/ios/documentation/UIKit/Reference/UIWebView_Class/) [Accessed 10 Aug. 2015].

Faa.gov, (2015). Unmanned Aircraft Systems (UAS) Regulations & Policies. [online] Available at: [https://www.faa.gov/uas/regulations\\_policies/](https://www.faa.gov/uas/regulations_policies/) [Accessed 16 Jul. 2015].

Fischler, M. and Bolles, R. (1981). Random sample consensus: a paradigm for model fitting with applications to image analysis and automated cartography. Communications of the ACM, 24(6), pp.381-395.

Fowers, S., Lee, D., Tippetts, B., Lillywhite, K., Dennis, A. and Archibald, J. (2007). Vision Aided Stabilization and the Development of a Quad-Rotor Micro UAV. pp.143-148.

Goodhoofd, W. (2014). wesgood/RBManager. [online] GitHub. Available at: <https://github.com/wesgood/RBManager> [Accessed 10 Aug. 2015].

GP2Y0A02YK0F. (2006). [online] Sharp. Available at:  
[https://www.sparkfun.com/datasheets/Sensors/Infrared/gp2y0a02yk\\_e.pdf](https://www.sparkfun.com/datasheets/Sensors/Infrared/gp2y0a02yk_e.pdf)  
[Accessed 18 Jul. 2015].

Hartman, D., Landis, K., Mehrer, M., Moreno, S. and Kim, J. (2014). dch33/Quad-Sim. [online] GitHub. Available at:  
<https://github.com/dch33/Quad-Sim> [Accessed 18 Jun. 2015].

Herissé, B., Hamel, T., Mahony, R. and Russotto, F. (2012). Landing a VTOL Unmanned Aerial Vehicle on a Moving Platform Using Optical Flow. *Robotics, IEEE Transactions on*, 28(1), pp.77-89.

Honegger, D., Meier, L., Tanskanen, P. and Pollefeyns, M. (2013). An open source and open hardware embedded metric optical flow CMOS camera for indoor and outdoor applications. pp.1736-1741.

Hrabar, S. (2011). Reactive obstacle avoidance for Rotorcraft UAVs. pp.4967-4974.

Imitec Limited, (2014). Advanced Airborne Radiation Monitoring System.

Imitec, (2014). Sellafiend Trial. [video] Available at:  
<https://vimeo.com/97758715> [Accessed 16 Jul. 2015].

INEA consulting, (2015). Global commercial and civil UAV market guide 2014-2015. [online] Available at: [http://www.slideshare.net/terrai/global-commercialandciviluavmarketguide20142015?qid=44e5ff39-fd9f-4529-836a-72704177a3cc&v=default&b=&from\\_search=1](http://www.slideshare.net/terrai/global-commercialandciviluavmarketguide20142015?qid=44e5ff39-fd9f-4529-836a-72704177a3cc&v=default&b=&from_search=1) [Accessed 16 Jul. 2015].

Jenkins, D. and Vasigh, B. (2013). 1st ed. [ebook] AUVSI. Available at:  
<https://higherlogicdownload.s3.amazonaws.com/AUVSI/958c920a-7f9b-4ad2-9807->

f9a4e95d1ef1/UploadedImages/New\_Economic%20Report%202013%20Full.pdf [Accessed 16 Jul. 2015].

Lewis, M. (2015). Introducing SocketRocket: A WebSocket library for Objective-C. [online] Corner.squareup.com. Available at: <https://corner.squareup.com/2012/02/socketrocket-websockets.html> [Accessed 10 Aug. 2015].

Mellander, H. (1995). The role of mobile gamma spectrometry in the Swedish emergency response programme for nuclear accidents- experience and future plans. In: Application of Uranium Exploration Data and Techniques in Environmental Studies.,

Mendes, J. and Ventura, R. (2012). Safe teleoperation of a quadrotor using FastSLAM. pp.1-6.

MEXT, (2015). Results of the Fourth Airborne Monitoring Survey by Ministry of Education, Culture, Sports & Technology (MEXT). [online] Available at: [http://radioactivity.nsr.go.jp/en/contents/4000/3179/24/1270\\_1216.pdf](http://radioactivity.nsr.go.jp/en/contents/4000/3179/24/1270_1216.pdf) [Accessed 13 Jul. 2015].

Meyer, J., Sendobry, A., Kohlbrecher, S., Klingauf, U. and Stryk, O. (2012). Comprehensive Simulation of Quadrotor UAVs using ROS and Gazebo. p.

NEO-6 series. (2011). 1st ed. [ebook] p.Versatile u-blox 6 GPS models. Available at: [https://www.u-blox.com/images/downloads/Product\\_Docs/NEO-6\\_ProductSummary\\_\(GPS.G6-HW-09003\).pdf](https://www.u-blox.com/images/downloads/Product_Docs/NEO-6_ProductSummary_(GPS.G6-HW-09003).pdf) [Accessed 9 Jul. 2015].

Pitzer, B. (2011). mjpeg server. 1st ed. [ebook] Bosch Research Std. Available at: <http://www.ros.org/wiki/mjpeg%20server> [Accessed 10 Aug. 2015].

Pixhawk.org, (2015). PX4 ROS SITL Setup - PX4 Autopilot Project. [online] Available at: <https://pixhawk.org/dev/ros/sitl> [Accessed 31 Jul. 2015].

Protecting Privacy From Aerial Surveillance. (2011). 1st ed. [ebook] ACLU. Available at:  
<https://www.aclu.org/files/assets/protectingprivacyfromaerialsurveillance.pdf> [Accessed 16 Jul. 2015].

Quigley, M., Conley, K., Gerkey, B., Faust, J., Foote, T., Leibs, J., Wheeler, R. and Ng, A. (2009). ROS: an open-source Robot Operating System. p.5.

Richards, A. (2015). State Space Modelling and Simulation. 1st ed. Robotics Systems notes.

Robot-electronics.co.uk, (2015). Ultrasonic Rangers SRF04. [online] Available at: [http://www.robot-electronics.co.uk/htm/sonar\\_faq.htm](http://www.robot-electronics.co.uk/htm/sonar_faq.htm) [Accessed 17 Jul. 2015].

Romero, H., Salazar, S. and Lozano, R. (2009). Real-Time Stabilization of an Eight-Rotor UAV Using Optical Flow. *Robotics, IEEE Transactions on*, 25(4), pp.809-817.

Ros.org, (2015). ROS.org | About ROS. [online] Available at:  
<http://www.ros.org/about-ros/> [Accessed 17 Jun. 2015].

Royal Aeronautical Society, (2013). UAV: A new industrial system?. [online] Available at:  
<http://aerosociety.com/Assets/Docs/Publications/DiscussionPapers/UASDiscussionPaper.pdf> [Accessed 16 Jul. 2015].

Sanderson, D., Allyson, J., Tyler, A. and Scott, E. (1995). Environmental applications of airborne gamma spectrometry.

Schwarz, G., Rybach, L. and Klingele, E. (1995). Data processing and mapping in airborne radioactivity surveys. In: Application of uranium exploration data and techniques in environmental studies, IAEA-TECDOC-827, IAEA, 61-70.

Scott, T. (2014). UAV radiation mapping survey of a Japanese school. [video] Available at: <https://vimeo.com/95921788> [Accessed 16 Jul. 2015].

Technology Brief. (2015). LIDAR-Lite Documentation. [online] PulsedLight. Available at:  
<http://kb.pulsedlight3d.com/support/solutions/articles/5000552320-lidar-lite-technology-brief> [Accessed 19 Jun. 2015].

The Economist, (2011). Drones and the man. [online] Available at:  
<http://www.economist.com/node/21524876&%5BAccessed&27th&> [Accessed 16 Jul. 2015].

Truchsess, W. (2015). Arduino I2C Master Library. [online] Dsscircuits.com. Available at: <http://www.dsscircuits.com/index.php/articles/66-arduino-i2c-master-library> [Accessed 20 Jul. 2015].

Uk.mathworks.com, (2015). Robotics System Toolbox Documentation. [online] Available at:  
<http://uk.mathworks.com/help/robotics/index.html?refresh=true> [Accessed 18 Jun. 2015].

Unmanned Aerial Vehicles in Humanitarian Response. (2014). 1st ed. [ebook] OCHA. Available at:  
<https://docs.unocha.org/sites/dms/Documents/Unmanned%20Aerial%20Vehicles%20in%20Humanitarian%20Response%20OCHA%20July%202014.pdf> [Accessed 16 Jul. 2015].

Wang, S., Zhen, Z., Zheng, F. and Wang, X. (2014). Design of autonomous flight control system for small-scale UAV. pp.1885-1888.

Wilson, R. (2014). Ethical issues with use of Drone aircraft. pp.1-4.